博士論文

Elucidation of the Role of CXCR4 Signaling in Hematopoietic Stem Cell Repopulation

(造血幹細胞と CXCR4 シグナル: 骨髄再構築過程における役割の解明)

賴 貞儀

Contents

List of Abbreviation **1**

Abstract **2**

Chapter I. Introduction **3**

1.1. Hematopoietic stem cells 3

1.2. Hematopoietic stem cell transplantation 5

1.3. Hematopoietic reconstitution 5

1.4. Problems of hematopoietic stem cell transplantation 6

1.5. Chemokine and C-X-C chemokine receptor 6

1.6. C-X-C chemokine receptor 4 in hematopoietic system 7

1.7. Uncertainty over the roles played by CXCR4 in transplanted hematopoietic stem cells 9

Chapter II. Materials and methods **11**

2.1. Mice 11

2.2. Mouse HSCs and HSPCs 11

2.3. Purification of mouse HSCs and HSPCs 11

2.4. Construction of system permitting gain-of-function studies on the role of Cxcr4 in murine HSPCs 12

2.5. Retrovirus transduction of murine HSCs and HSPCs 12

2.6. Cell lines 13

2.7. Quantitative reverse transcription-polymerase chain reaction 13

2.8. Assessment of cell surface Cxcr4 expression 13

2.9. Migration assay 14

2.10. Cell proliferation assay 14

2.11. Intracellular Ca2+ flux assay 14

2.12. Single-cell colony assays in liquid culture 15

2.13. Assessment of seeding efficiency in stromal cell co-culture 15

2.14. Immunoblot analysis of intracellular phosphorylation kinetics of Erk protein 15

2.15. Intracellular phosphorylation kinetics of signaling molecules 16

2.16. HSPC homing assay 16

2.17. Early HSPC repopulation kinetics in recipient BM 17

2.18. Competitive repopulation assays 17
2.19. Long-term donor chimerism analysis in hematopoietic cell populations 18
2.20. Assessment of AMD3100-induced mobilization effect on donor chimerism 18
2.21. Statistical analysis 19

Chapter III. Results 20

3.1. Stepwise Gain-of-Function Effects of Exogenous Cxcr4 on Transduced HS(P)Cs, with Greater Response for the ΔC-Type Receptor 20
3.2. Enhanced in Vitro Proliferative Response of HS(P)Cs under Particular Circumstances by Gain-of-Function Modification in Cxcr4 Signaling 21
3.3. Augmented Cxcr4 Signaling in Murine HS(P)Cs/HSPCs Does Not Enhance BM Homing/Lodging, but Improves Subsequent BM Repopulation 22
3.4. Continuous Overexpression of Exogenous Cxcr4 Receptors in HS(P)Cs Leads to Poor Peripheral Reconstitution 23
3.5. Enhanced Donor Cell Chimerism Occurs in BM Cells Throughout Developmental Stages of HS(P)Cs Expressing Gain-of-Function Cxcr4 Receptors 24
3.6. Loss-of-Function Studies Support the Proposed Roles of Cxcr4 in Murine HSPCs in Transplantation 25
3.7. Alteration in Phosphorylation Kinetics of Erk in Response to SDF-1 in HS(P)Cs Expressing ΔC-Cxcr4 26

Chapter IV. Discussion 27

4.1. Role of Cxcr4 signaling in an initial homing process of transplanted HSC/HSPCs 27
4.2. Role of Cxcr4 signaling in early repopulation process of transplanted HSC/HSPCs 28
4.3. Role of Cxcr4 signaling in an in vivo expansion of transplanted HSC/HSPCs 28
4.4. Implication of Cxcr4 signaling for HSC/HSPCs transplantation medicine 29

Chapter V. Conclusions 31

Figures and Figure Legends 32

Tables 81

References 84

Copyright Statement 90

Acknowledgements 91

Abbreviations

HSPCs	hematopoietic stem /progenitor cells
HSCs	hematopoietic stem cells
HPCs	hematopoietic progenitor cells
HSCT	hematopoietic stem cell transplantation
LT-HSCs	long-term hematopoietic stem cells
ST-HSCs	short-term hematopoietic stem cells
CXCR4	C-X-C chemokine receptor type 4
SDF-1	stromal cell derived factor 1
WHIM	Warts, Hypogammaglobulinemia, Infections, and Myelokathexis
NOD/SCID	Nonobese diabetic/severe combined immunodeficiency
BM	bone marrow
PB	peripheral blood
Erk	Extracellular signal-regulated kinases
CD	cluster of differentiation
GVHD	graft-versus –host-disease
HLA	human leukocyte antigen
Hox	Homebox protein
INK4	inhibitor of cyclin-dependent kinase 4
GCPR	G-protein-coupled receptor
KO	knock out
WT	wild type
LM	littermate
CLP	common lymphoid progenitor
CMP	common myeloid progenitor
GMP	granulocyte/macrophage progenitor
ProB	progenitor B cells
PreB	pre-mature B cells
MaB	mature B cells
PriNeu	primitive neutrophils
MaNeu	mature neutrophils
B	B cells
Mye	myeloid cells

Abstract

Hematopoietic cell transplantation has proven beneficial for various intractable diseases, but it remains unclear how hematopoietic stem/progenitor cells (HSPCs) home to the bone marrow (BM) microenvironment, initiate hematopoietic reconstitution, and maintain life-long hematopoiesis. The use of newly elucidated molecular determinants for overall HSPC engraftment should benefit patients. Here we report that modification of C-X-C chemokine receptor type 4 (Cxcr4) signaling in murine HSPCs does not significantly affect initial homing/lodging events, but leads to alteration in subsequent BM repopulation kinetics, with observations confirmed by both gain- and loss-of-function approaches. By using C-terminal truncated Cxcr4 as a gain-of-function effector, we demonstrated that signal augmentation likely led to favorable in vivo repopulation of primitive cell populations in BM. These improved features were correlated with enhanced seeding efficiencies in stromal cell co-cultures and altered ligand-mediated phosphorylation kinetics of Extracellular signal-regulated kinases (Erk) observed in Cxcr4 signal-augmented HSPCs in vitro. Unexpectedly, however, sustained signal enhancement even with wild-type Cxcr4 overexpression resulted in impaired peripheral blood (PB) reconstitution, most likely by preventing release of donor hematopoietic cells from the marrow environment. We thus conclude that timely regulation of Cxcr4/CXCR4 signaling is key in providing donor HSPCs with enhanced repopulation potential following transplantation, whilst preserving the ability to release HSPC progeny into PB for improved transplantation outcomes.

Chapter I. Introduction

1.1. Hematopoietic stem cells

Blood cells constitute the major population that is responsible for maintenance of the immune system to prevent us from various infections. The stem cells that form blood and immune cells are called hematopoietic stem cells (HSCs). These are a rare and unique population of cells capable of multi-lineage hematopoietic cell differentiation and daily replenishment of mature blood cells including platelets, red blood cells, lymphocytes and myeloid cells. The HSCs replicate themselves (self-renew) to sustain lifelong hematopoiesis. The balance between self-renewal and differentiation is thought to be tightly regulated by requisite factors within the bone marrow (BM) microenvironment (niche) where HSCs reside [1-3]. However, the whole picture of this regulation has not been fully elucidated.

The discovery of blood-forming cells comes from studies of individuals who had experienced the atomic bomb in 1945. Given that they had been exposed to low-dose irradiation, their subsequent deaths were attributed to a number of reasons with insufficient production of leukocytes to fight against infection and/or inadequate numbers of platelets to stop bleeding being the major ones. Researches with mice were subsequently carried out to recapture this phenomenon. Studies indicated that lethally irradiated mice could be rescued if single bone or spleen were protected or if they received BM cells from a healthy donor. Later in assessing the radiation sensitivity of BM cells, Till and McCulloch discovered the two hallmark characteristics of HSCs: self renewal ability and multi blood lineage differentiation potential [4].

There are two types of HSCs: long-term HSCs (LT-HSCs) and short-term HSCs (ST-HSCs). LT-HSCs are capable of self-renewal, thereby contributing to continuous blood production and the sustainment of life-long hematopoiesis. ST-HSCs are derived from LT-HSCs and have the ability to repopulate and proliferate for a limited period of time in the BM. In addition, there are other classes of precursor cells or immature cells with limited self-renewal capacity [5], which may overall be categorized as hematopoietic progenitor cells (HPCs). It is important to distinguish LT-HSCs from ST-HSCs and HPCs because only LT-HSCs possess the two hallmark characteristics as mentioned earlier, which are believed to be critical for successful outcomes when viewed in a setting of clinical transplantation [6].

The purification of mouse HSCs was first achieved using a panel of cell surface markers, and confirmed for their reconstitution potential in transplantation experiments by Irving Weissman's group in 1988 [7]. Later, Osawa *et al*. achieved the higher purity by using CD34 as a negative marker [$CD34^{neg/low}$, $CD117^{pos}$, Sca-1^{pos}, lineage $(Lin)^{neg}$ (34^{-}KSL)] to a level that allowed reconstitution of all hematopoietic lineages by transplanting only a single HSC [8]. Other groups have subsequently defined the murine HSC population by different marker combinations such as $CD117^{high}$, CD90.1^{low}, $Lin^{neg/low}$, Sca-1^{pos} [9], CD90.1^{low}, Lin^{neg}, Sca-1^{pos} Rhodamine123^{low} [10], and CD150 ^{pos}, $CD48^{neg}$, $CD244^{neg}$ [11]. Similar attempts have also been made to define human HSCs by using CD34, CD38, CD90, and other markers. It has been proposed that a Lin^{neg}, $CD34^{pos}$, $CD38^{neg}$, $CD90^{pos}$, $CD45RA^{neg}$ population [12], and more recently, a Lin^{neg}, $CD34^{pos}$, $CD38^{neg}$, $CD90^{pos}$, $CD45RA^{neg}$, Rho^{low}, $CD49f^{pos}$ population [13] constitutes the most primitive human HSCs. However, highly purified human HSCs can only be defined in experimental settings, *i.e*., by using xeno-transplantation models. In contrast, hematopoietic stem cell transplantation (HSCT) usually utilizes simple enrichment for CD34-positive cells, if necessary, mostly because of practical reasons [14, 15]. Needless to say, $CD34^{pos}$ cells should contain not only LT-HSCs but also other progenitor cells that are already lineage-committed, thus lacking the capacity for long-term hematopoietic reconstitution. So far, only limited numbers of clinical trials have been reported to use more purified human HSCs for transplantation [15, 16]. At present, it thus remains to be further investigated if the highest purity of human HSCs are actually obtainable and their functionality is eventually evaluable in a combination of basic and clinical studies.[15, 16]

When conducting the research by using HSCs as the test materials, one should note the different status of HSCs: they may exist in different stages of development (*e.g*., embryonic vs. adult hematopoiesis), derive from different mouse strains [17], come from different species [18], and may stay in different activation status [19]. Although the immunophenotyping by flow cytometry analysis remains a powerful tool for purification of HSCs as mentioned, expression of cell surface markers are prone to alteration depending on the surrounding cues, one thus needs particular caution when to examine them in inflammatory environment, such as BM after myeloablative conditioning. As for human settings, the source of HSCs should have an impact on transplantation medicine; cells containing HSCs can be harvested from BM, peripheral blood (PB), or umbilical cord blood.

1.2. Hematopoietic stem cell transplantation

The first HSCT was conducted more than 50 years ago. Due to the unique regenerative characteristics of HSCs, they have been used as a source of transplants for treating a variety of diseases such as leukemia, congenital hematological/immunological disorders, metabolic diseases, and autoimmune diseases to restore normal hematopoietic and immune function in the patients [20] [21]. There are two types of HSCT depending on the origin of the cells: autologous transplantation, in which the cells are taken from individual's own bodies, and allogeneic transplantation, in which the cells are donated from healthy donors either unrelated or related to the patients [20]. These two are summarized below.

Autologous transplantation: More than 30,000 autologous transplantations are carried out annually worldwide with almost two thirds performed for the patients with multiple myeloma or non-Hodgkin's lymphoma [20]. Given that the donor and recipient are the same in this therapeutic scheme, the risk of graft-versus-host-disease (GVHD) is very low, or virtually absent. Typical autologous HSCT for hematological malignancies requires the harvest and the cryopreservation of the patient's own HSC-sources. Prior to the actual transplantation procedure, the patients with malignancies receive chemotherapy with or without radiotherapy to have the malignant cells eradicated, resulting in partial or complete destruction of host hematopoiesis. This "conditioning" procedure gives space for engraftment to and facilitates the growth of transplanted cells. The stored HSCs are then returned to patients' own body, which will eventually replenish the irradiated BM compartment with the restoration of normal hematopoiesis.

Allogeneic transplantation: Allogeneic HSCT on the other hand requires human leukocyte antigen (HLA) typing, since the HSCs are from genetically-different individuals. The HLA type should be matched between a donor and a recipient at more than 3 loci of the HLA gene. However even with a perfect match, immunosuppression will be usually required to prevent or suppress GVHD [21]. More than 15,000 allogeneic transplantations are performed annually worldwide with nearly half of those for acute leukemias [20].

1.3. Hematopoietic reconstitution

Hematopoietic reconstitution is the process that occurs following HSCT [22]. It is the dynamic process that may be simply divided into three steps: 1) a homing/lodging step where

infused donor HSCs transmigrate into and seed the bone marrow cavity; 2) a BM repopulation step where HSCs differentiate into progenitor cells with multi-lineage differentiation potential and simultaneously replicate themselves to ensure the lifelong maintenance of hematopoiesis; 3) a peripheral reconstitution step where mature cells are released from BM. The systemic production of mature cells is achieved as a consequence. Once steady-state hematopoiesis gets established, long-term sustainment of the normal homeostasis can be expected in the immune and hematopoietic systems. On the other hand, failure in any of these steps could impair transplantation outcomes [23].

1.4. Problems of hematopoietic stem cell transplantation

There are inherent risks associated with HSCT, with the most serious one being treatment-related mortality resulting from various complications, including mucositis, sinusoidal obstruction syndrome characterized by painful hepatomegaly and jaundice, lung injury, and GVHD [20]. These complications often limit the use of HSCT only to patients suffering from diseases with life-threatening risks.

In light of the transplantation related mortality, the low engraftment efficiency in HSCT can be critical, one thus needs to overcome it. Insufficient numbers of stem cells and the loss of HSC stemness are amongst the challenges that potentially result in the reduction of life-long functional cells after HSCT [24, 25]. It is thought that HSC functions are tightly regulated within the BM niche [2, 3]. Researchers have been quite active in trying to identify the factors and signaling pathways involved in this regulation, which mimics the existing regulatory mechanisms that occurs in the stem cell niche. This is to allow the possible augmentation of certain signals that will help to preserve HSC functions both in *ex vivo* and *in vivo*. For example, attempts have been made to provide supportive growth factors, stromal cell derived ligands such as Notch ligand Delta 1 or to target pathways used by HSCs such as the Hox family or the INK4 family [21, 25, 26]. However, the truly effective expansion methods applicable for human HSCs in transplantation setting still remain to be established.

1.5. Chemokine and C-X-C chemokine receptor

The chemokines are a small family of secreted proteins and they are regarded as special types of cytokines that have many functions but they are best known for their ability to induce cell migration. The name is derived from their ability to induce chemotaxis in target cells.

Proteins are classified as chemokines based on shared structural characteristic and four cysteine residues in the conserved location. Members of the chemokines can be divided into 4 groups, C, CC, CXC, and CX3C chemokines depending on the spacing between first 2 cysteines. Chemokines can also be divided into two types according to their expression pattern. Those induced during inflammation are called inflammatory chemokines and those expressed constitutively in specific tissue or cells are called homeostatic chemokines. The homeostatic chemokines have roles on lymphoid organogenesis, general organogenesis, and key roles in stem cell migration in the body [27].

The chemokine receptors are expressed on the surface of various types of cells. There are 19 different chemokine receptors and 48 superfamily of ligands described in mammals. These receptors are G-protein coupled receptors (GPCR) that have the seven transmembrane structures coupled to a G-protein for signal transduction. Activation of chemokine receptors triggers an influx of Ca^{2+} and leads to cell responses such as chemotactic movement of the cells to a desired location within the organism. Chemokine receptors are divided into four different families according to the subfamilies of chemokines that they bind [27-29].

1.6. C-X-C chemokine receptor 4 in hematopoietic system

CXC chemokine receptor type 4 (CXCR4) was first cloned from human leukocytes in 1994 and gained much attention after being identified as the co-receptor for HIV infection. It is also known as fusin or cluster of differentiation 184 (CD184) [30-32]. CXC chemokine ligand (CXCL) 12, also known as stromal cell-derived factor 1 (SDF-1) or as pre-B-cell growth-stimulating factor (PBSF), is the primary physiologic ligand for CXCR4. SDF-1 and CXCR4 are believed to constitute a unique ligand-receptor pair unlike other chemokines that uses different chemokine receptors in promiscuous manner. Recently, extracellular ubiquitin was demonstrated as the natural ligand of CXCR4 [33].

In 2003, mutations in the *CXCR4* gene were identified in patients with WHIM (Warts, Hypogammaglobulinemia, recurrent bacterial Infection and Myelokathexis) syndrome. This is considered to be the first, and still the only example of a human disease caused by defects of a chemokine receptor [34]. WHIM is the acronym derived from the major 4 features of disorders mentioned above. WHIM syndrome is a rare autosomal dominant immunodeficiency characterized also by neutropenia, which is one characteristic phenotype of the patients. The model mouse has recently been developed [35]. Several distinct mutation

sites within *CXCR4* have been identified in patients, all of them cause the truncation of intracellular carboxy terminus (C-terminal) domain of the receptor. The mutation R334X is the most common of all [36]. SDF-1 binding to CXCR4 triggers a cascade of processes that include conformational change of the receptor and uncoupling from G-proteins [37]. The negative feedback loop also gets activated at the same time through the C-terminus cytoplasmic tail of CXCR4. Due to defects in the C-terminal domain, the negative feedback control was concealed and thus increasing the stability of the receptor on cell surface. Leukocytes from WHIM patients reportedly show prolonged activation and demonstrate enhanced chemotactic responses to SDF-1 [38]. Administration of G-CSF or plerixafor, the latter of which is known to be an inhibitor for the CXCR4 receptor, had been used to attenuate the phenotypic neutropenia observed in WHIM patients [39]. Besides, this CXCR4 antagonist has been used as a mobilizer of human $CD34^+$ cells in the clinical setting, thus demonstrating the importance of this signaling in the retention of HSC/HPC in human bodies [27].

CXCR4 receptors are expressed by hematopoietic cells and have been reported to serve as an important player in the HSC niche [40, 41]. The SDF-1/CXCR4 axis began to draw attention in the field of transplantation medicine, as SDF-1 was found to be a growth-stimulating factor for B cell precursor clones. In addition, the treatment of human $CD34^+$ cells with antibodies to CXCR4 was demonstrated to prevent human cell engraftment to NOD/SCID mice [42, 43], suggesting the crucial role of this signaling in transplanted cells. Further information will be provided in the next section 1.7.

Homozygous *Cxcr4* null mice die in early embryonic development and show defects in B-cell lymphopoiesis, myelopoiesis, the central nerve system and cardiac septum formation. Similar phenotypes were also observed in *Sdf-1* null mice. There observations further strengthen the idea that these two molecules most likely constitute the monogamous ligand-receptor pair [44-46]. Studies utilizing conditional knockout mice have offered some clarification on the role of CXCR4 in adult hematopoiesis. Induced deletion of Cxcr4 resulted in a severe reduction of HSC numbers and the loss of the quiescent state in primitive progenitor cells within the bone marrow [40, 47, 48]. These studies provided important information regarding the roles of CXCR4 signaling in steady-state hematopoiesis.

1.7. Uncertainty over the roles played by CXCR4 in transplanted hematopoietic stem cells

The studies mentioned above also used conditionally knocked out BM cells in transplantation experiments to test the reconstitution potential of Cxcr4-defective HSCs. All of these studies made similar conclusions that the CXCR4-null HSCs were devoid of long-term reconstitution ability from the observation that the recipients of CXCR4-null BM cells showed poor peripheral reconstitution. General understanding of SDF1/CXCR4 axis is that this signaling is essential for HSC homing into the BM [49]. However, there is no single report that has ever tested the roles of the Cxcr4 receptor in mouse HSCs assessing the whole kinetics throughout marrow reconstitution process using "highly purified HSCs" as the transplantation source. The same is true not only in loss-of-function studies, but also in gain-of-function studies in that no report has ever addressed how the overexpression of the CXCR4 in purified HSCs affects the *in vivo* kinetics of hematopoietic reconstitution in mouse models.

For human HSCs/HPCs, the importance of the SDF1/CXCR4 axis in transplantation was first identified in a publication, which reported a reduction of $CD34^+$ cell engraftment in NOD/SCID mice caused by blocking CXCR4 signaling before transplantation [43]. Following this observation, overexpression of CXCR4 in human $CD34^+$ cells was attempted to see whether this treatment favorably enhanced their migration and therefore engraftment of human cells in NOD/SCID mice [50-52]. Even though the definitive proof of enhanced HSC activity was not demonstrated in this study due to the current limitation in human HSC research, enhanced engraftment in BM was observed suggesting the modification of CXCR4 signaling might benefits transplantation outcomes.

Collectively, the above references strongly suggest that CXCR4 may possess a number of crucial roles in the homing, retention and engraftment of HSCs/HPCs. However, successful hematopoietic reconstitution is a dynamic process resulting from a series of sequential events following transplantation. It therefore remains unclear which steps specifically is CXCR4 attributable for and subsequently how it influences the fate of purified transplanted donor HSCs. To address this question, I investigated the roles of CXCR4 signaling in the repopulation kinetics of transplanted HSCs *in vivo* by using both gain-of-function (overexpression) and loss-of-function (KO or desensitization) approaches. In

semi-quantitative analysis of gain-of-function effects, I used not only wild-type (WT) Cxcr4-overexpressing cells but also cells expressing Cxcr4 with a specific C-terminal deletion (ΔC) homologous to that found in patients with WHIM syndrome. This truncation is regarded as a gain-of-function mutation, because it increases cell-surface stability of CXCR4 without impairing CXCR4 signaling capabilities [35, 38, 51, 53, 54]. By using this combinational approach, I assessed each of the multiple steps in donor cell reconstitution in mice that received Cxcr4-modified HSC/HSPCs and dissected stage-specific roles that Cxcr4 signaling plays in transplanted cells.

Chapter II. Materials and methods

2.1. Mice

C57BL/6 (B6)-Ly5.1 mice came from Sankyo Labo Service. B6-Ly5.2 mice were from Japan SLC. Mice were used between 8 and 12 weeks after birth, unless otherwise indicated. *Cxcr4*-conditional knockout mice were generated by crossing two strains, one harboring *loxP* sites flanking exon 2 of *Cxcr4* (*Cxcr4*$^{flox/flox}$) [55] and the other capable of expressing *Cre* recombinase under the control of an IFN-inducible *Mx* promoter [56]. Expression of *Cre* was induced by intraperitoneal injection of 250 μg polyinosinic-polycytidylic acid (pIpC, Sigma-Aldrich) 5 times at 2-day intervals. Mice harboring only the *Cxcr4*$^{flox/flox}$ allele, without an *Mx-Cre* cassette, were used as littermate controls (LM). Two weeks after final pIpC administration mice were sacrificed and used. A C57BL/6J (B6) mouse strain stably expressing Kusabira Orange (KuO) was generated from retrovirally transduced 129 embryonic stem cells [57, 58], using procedures analogous, except for the retroviral vector used, to those used for the generation of B6 mice constitutively expressing enhanced green fluorescent protein (EGFP) [59, 60]. These mice were used after sufficient cycles (>12) of backcrossing to a B6 strain.

2.2. Mouse HSCs and HSPCs

Purified murine CD34$^{neg/low}$ c-Kit^{+}Sca-1^{+}Lineage marker-negative (CD34^{-}KSL) cells were used as the HSC source [8, 61]. Where indicated, c-Kit^{+}Sca-1^{+}Lineage marker-negative (KSL) cells (referred to as HSPCs) were used. Considering the status of cells, *i.e.*, either fresh or post-expansion, we defined CD34^{-}KSL cells as fresh HSCs or cultured HS(P)Cs and defined KSL cells as fresh HSPCs or cultured HSPCs. Cell sorting was performed on a MoFlo cytometer (Beckman Coulter) or a FACSAria II (BD Bioscience). The Institutional Animal Care and Use Committee, University of Tokyo, approved all animal experiments.

2.3. Purification of mouse HSCs and HSPCs

BM cells obtained from 8- to 12-week-old mice were stained with allophycocyanin (APC)-conjugated anti-c-Kit antibodies (BD Biosciences) and c-Kit^{+} cells were enriched using anti-APC magnetic beads and columns (Miltenyi Biotec). These cells were then stained with a lineage-marker cocktail consisting of biotinylated anti-Gr-1, -Ter119, -B220, -CD4, -CD8, and -IL7R (interleukin-7 receptor) monoclonal antibodies (mAb) (BD Bioscience),

fluorescein isothiocyanate (FITC)-conjugated anti-CD34, APC-conjugated anti-c-Kit, PE-conjugated Sca-1 mAbs, and streptavidin-Alexa 780, and were subjected to cell sorting. Lineage-marker-negative, c-Kit$^+$, Sca-1$^+$ cells are defined as HSPCs (KSL cells), whereas highly purified long-term HSCs are defined as a CD34-negative/dull fraction within KSL cells [61]. Information regarding the mAbs is shown in Table 1. Typical features of purified HSCs are shown in the context of our serum-free expansion culture (Fig. 8).

2.4. Construction of system permitting gain-of-function studies on the role of Cxcr4 in murine HSPCs

We constructed a retroviral-system for gain-of-function studies using a combination of the GCDNsam backbone vector [62] and 293GPG cells [63]. The pGCDNsam-IRES-EGFP (DNsam-I/E) was used unmodified as a control vector (Mock). Murine WT-Cxcr4 cDNA was used to construct DNsam-WT-Cxcr4-I/E. We constructed from it DNsam-DC-Cxcr4-I/E, harboring mutant cDNA that encodes C-terminal truncated murine Cxcr4, which mimics the type of mutation most frequent in WHIM syndrome [34, 53] (Fig. 1 and Fig. 2). Production of highly concentrated, VSV-G-pseudotyped retroviruses is described [60]. As human and mouse CXCR4/Cxcr4 share almost identical amino acid sequences in the C-terminal tail (Fig. 2), the mutant Cxcr4 was predicted to imitate the biological characteristics of the human counterpart [53] [34].

2.5. Retrovirus transduction of murine HSCs and HSPCs

Murine HSCs or HSPCs were sorted into U-bottom 96-well plates precoated with human fibronectin fragments (RetroNectin, TAKARA BIO), with each well containing alpha-minimal essential medium (α-MEM) supplemented with 1% FBS, 50 ng/ml mouse stem cell factor (mSCF), 100 ng/ml mouse thrombopoietin (mTPO) (Peprotech), and 50 μM 2-mercaptoethanol (2-ME; Sigma Chemical). One day later, cells were transduced with retroviral particles at a multiplicity of infection of ~600 for 24 hours. After transduction, medium was replaced with S-clone SF-O3 (Sanko Junyaku) supplemented with 1% BSA, 50 ng/ml mSCF, 100 ng/ml mTPO, and 50 μM 2-ME. On day 4 of culture after transduction, cells expressing EGFP at high intensity (EGFP$^+$ cells) were sorted and used for subsequent assays. Transduction efficiency ranged between 61.3% and 94.4% (Table 2A). Representative plots analyzed by flow cytometry are shown in Fig. 3A.

2.6. Cell lines

CEM cells are immortalized human T-lymphoblastoid cells (a generous gift from Dr. Arinobu Tojo, University of Tokyo). 32D cells are a murine hematopoietic progenitor cell line (a generous gift from Dr. Seishi Ogawa, Kyoto University). Both cell lines were maintained in RPMI 1640 medium (SIGMA) containing 10% fetal bovine serum (FBS), 2 mM L-glutamine, 100 U/ml penicillin, and 0.1 mg/ml streptomycin (all Invitrogen), with supplementation of 3~5 ng/ml murine IL-3 (Peprotech) only for 32D cells. Exponentially growing 32D cells were transduced with each viral supernatant in the presence of 10 μg/ml protamine sulfate, sorted for EGFP-positive cells, and subjected to downstream assays.

2.7. Quantitative reverse transcription-polymerase chain reaction

Total RNA was extracted from transduced HS(P)Cs 7-10 days after $EGFP^+$ cell-sorting using the RNeasy Micro Kit (Qiagen). First-strand cDNA was synthesized using a High-Capacity cDNA Reverse Transcription Kit (Applied Biosystems). Transcripts of both glyceraldehyde 3-phosphate dehydrogenase (GAPDH) and Cxcr4 were quantified by quantitative reverse transcription-polymerase chain reaction (RT-PCR). Each sample was run in triplicate using a ViiA™ 7 real-time PCR system (Applied Biosystems). For GAPDH assessment, TaqMan Rodent GAPDH Control Reagents were utilized, whereas for Cxcr4 transcripts the Universal ProbeLibrary system (Roche Diagnosis) was used (probe ID #38). The data obtained from the condition that PCR running efficiency was between 80% to 120% and R value of standard curve was greater than 0.98. Forward Cxcr4 primer: 5'-tggaaccgatcagtgtgagt-3'; reverse Cxcr4 primer: 5'-gggcaggaagatcctattga-3'.

2.8. Assessment of cell surface Cxcr4 expression

Cell surface expression of Cxcr4 was analyzed by flow cytometry. Overexpression of the receptor after transduction was confirmed in cultured HS(P)Cs (Fig. 4), cultured HSPCs (Fig. 7), and 32D cells (Fig. 5). To assess ligand-mediated receptor internalization, test cells were either left unstimulated or stimulated with 100 or 500 ng/ml murine SDF-1 (Peprotech) for 30 minutes. They then were stained with phycoerythrin-conjugated anti-mouse (for murine receptors, clone 2B11) or anti-human (for CEM cells, clone 12G5) CXCR4 mAb (eBioscience) and analyzed with a FACSCanto II. Percent reduction of surface Cxcr4 levels

was calculated using mean fluorescence intensity (MFI) values in stimulated cells and in unstimulated cells ([unstimulated - stimulated] / unstimulated).

2.9. Migration assay

To analyze chemotactic responses, sorted EGFP$^+$ cultured HS(P)Cs were expanded for 7 days in S-clone (SF-O3, Sankyo Junyaku) with 1% bovine serum albumin (BSA, Sigma-Aldrich), 20 ng/ml mSCF, 20 ng/ml mTPO, and 50 μM 2-ME (ST-basal medium), and 3 x 10^4 cells re-suspend in the 1%BSA/S-clone medium were added to upper chambers of a 96-well transwell apparatus (Costar; pore size 5 μm) containing varying concentrations of SDF-1 in its lower chambers[64]. The cells that transmigrated in the indicated minutes were counted by flow cytometry using Flow-Count Fluorosphere beads (Beckman Coulter). Forty to fifty ml of Fluorosphere beads were added and data acquiring was stopped as beads count reached 5,000 per sample during FACS analysis.

2.10. Cell proliferation assay

Cell proliferation was assessed in liquid culture with 96-well U-bottom plates containing ST-basal medium with varying concentrations of SDF-1. Fresh HSCs (CD34-neg/low KSL cells) and multipotent progenitors (CD34-positive KSL cells) were used at 50 cells/well. After culture for 7 days cells were counted by flow cytometry. As shown in Fig. 9, addition of SDF-1 at "a desensitizing concentration in many cases (500 ng/ml)" stimulated basal proliferation without substantial differentiation. Of note is that even at 1,000 ng/ml SDF-1 still stimulated proliferation in HSCs, whereas it evoked a blunted response in multipotent progenitors (Fig. 9).

2.11. Intracellular Ca^{2+} flux assay

Ca^{2+} influx response was assessed [65] in a series of 32D cell lines that were 1) untransduced, or transduced with retroviral vectors and thus expressing either 2) EGFP alone (Mock), 3) excess amounts of wild-type Cxcr4 (WT), or 4) ΔC-type receptor (ΔC). Exponentially growing cells were collected (~2 x 10^6 cells), washed in PBS, then incubated for 30 minutes at 37ºC with the fluorescent calcium indicator Rhod-2 (2.5 μM) in loading buffer containing 1.25 mM probenecid and 0.04% Pluronic F-127. After washing in recording medium, cells were resuspended in 500 μl of pre-warmed recording medium. Rhod-2 fluorescence was continuously measured using a FACSCalibur for 150 seconds. Ten μl of

each stimulant was added to the cells 20 seconds after record initiation. EGFP and Rhod-2 fluorescence values were recorded with a proper compensation setting. Ca^{2+} influx kinetics in response either to ionomycin or to varying doses of SDF-1 was represented as Rhod-2 MFI using FlowJo software (Tree Star). The reagents described above, including "loading buffer" and "recording medium", are from Dojindo Molecular Technologies.

2.12. Single-cell colony assays in liquid culture

Our colony assay in liquid medium is described [61, 66]. In brief, test cells were sorted clonally into 96-well plates containing S-clone supplemented with 10% fetal bovine serum (FBS), 1% BSA, 10 ng/ml mSCF, 10 ng/ml mTPO, 10 ng/ml mouse interleukin-3 (mIL-3), 1 U/ml human erythropoietin (hEPO; both Peprotech), and 50 μM 2-ME, with varying concentrations of SDF-1. Colonies were evaluated at days 11 and 14 for gain-of-function and loss-of-function studies respectively.

2.13. Assessment of Seeding Efficiency in Stromal Cell Co-culture

The ability to repopulate an irradiated stromal cell layer was tested in sorted $EGFP^+$ HS(P)Cs or fresh HSCs using the *in vitro* co-culture assay [67] that we developed from cobblestone-like area formation assays [68, 69], and is similar to a system recently shown to be useful to assess HSCs' clonogenic ability in stromal co-cultures at a clonal level [70]. Test cells were sorted onto irradiated (50 Gy) C3H10T1/2 stromal cell layers pre-established in 6-well plates containing a-MEM medium with 10% FBS, 1%PSG, and 10 ng/ml mSCF, 10 ng/ml mTPO, 10 ng/ml mouse interleukin-3 (mIL-3), 1 U/ml human erythropoietin (hEPO; both Peprotech). The culture medium was replaced twice a day. Formed cobblestone-like areas were counted between days 10 and 14. Specific ability to form cobblestone-like areas in the presence of C3H 10T1/2 cell layers was assessed in test cells as reported [67].

2.14. Immunoblot analysis of intracellular phosphorylation kinetics of Erk protein

Aliquots of the same series of 32D cells (1×10^5 cells per point), except for untransduced cells, were cytokine- and serum-starved for 12 hours and then were re-stimulated with 100 ng/ml SDF-1. Whole-cell lysate samples were subjected to immunoblot analysis using anti-p44/42 MAPK (Erk1/2) and anti-phospho-p44/42 MAPK (Erk1/2)(Thr202/Tyr204) rabbit mAb, followed by signal detection using horseradish peroxidase-conjugated goat

anti-rabbit IgG (Cell Signaling Technology), according to manufacturer's instructions (Fig. 33).

2.15. Intracellular phosphorylation kinetics of signaling molecules

Sorted EGFP$^+$ cultured HS(P)Cs were expanded for 7 days in S-clone (SF-O3, Sankyo Junyaku) with 1% bovine serum albumin (BSA, Sigma-Aldrich), 20 ng/ml mSCF, 20 ng/ml mTPO, and 50 μM 2-ME (ST-basal medium), cytokine-starved for 6 hours, then re-stimulated with 100 ng/ml or 500 ng/ml SDF-1. At the indicated times, cells were fixed and permeabilized and were stained with anti-phospho-p44/42 MAPK (Erk1/2)(Thr202/Tyr204), anti-phospho-Akt (Thr308), or isotype-control rabbit mAb (Cell Signaling Technology), followed by Alexa Fluor 647-goat anti-rabbit IgG (Invitrogen), according to manufacturer's instructions. (Fig. 33 and Fig. 34)

2.16. HSPC Homing Assay

For the gain-of-function study, EGFP$^+$ cultured HSPCs (test cells) were co-transplanted into irradiated recipients with either fresh KSL or total BM cells from KuO-Tg mice (reference cells) numbered as shown. B6-KSL cells were transduced and sorted as EGFP$^+$ with procedures like those used for HSC transduction.

These cultured HSPCs (test cells; 50,000 cells) were co-transplanted into lethally-irradiated recipients with 17,000 fresh KSL cells (reference cells) isolated from transgenic B6 mice constitutively expressing KuO fluorescent protein (KuO$^+$ cells). Twenty-four hours later, both EGFP$^+$- and KuO$^+$-cells were counted in the same harvested BM samples (collected from 2 pelvic bones, 2 femurs, and 2 tibias of each individual recipient mouse) using flow cytometry analysis (Fig.18). Homing events were represented by the ratio of EGFP$^+$ cells (test cells) to KuO$^+$ cells (reference cells) and compared between samples. To maximize assay sensitivity, we acquired as many events as possible with a FACSCanto II. HSPC homing at earlier time points (4, 15, and 24 hours) was consecutively assessed in an experiment conducted in the same way as that above except for the use of 17,000 test cells together with 10^6 whole BM cells isolated from KuO$^+$ Tg mice (Fig.19).

To desensitize HSPCs to SDF-1, fresh KuO-expressing (KuO$^+$) KSL cells preincubated with AMD3100 [37-39] (test cells) were co-transplanted into irradiated recipients with total BM cells from EGFP-Tg mice (reference cells)(schematic representation, Fig. 29A). At the

times indicated, both $EGFP^+$- and KuO^+- cells were counted in the same BM samples using flow cytometry analysis. Homing events were represented by the ratio of test cells to reference cells (Fig. 29).

2.17. Early HSPC Repopulation Kinetics in Recipient BM

An assay system to estimate HSPC repopulation kinetics early after transplantation is described [67]. In this study, we estimated early (16 and 24 hours) and late homing (day 2) and subsequent repopulation (days 4 and 6) of infused test cells by examining colony-forming cells (CFCs) detectable in BM of irradiated recipients. $EGFP^+$ cultured HS(P)Cs or fresh HSCs were transplanted alone into lethally-irradiated recipient mice. Cells obtained at indicated times from recipient femurs, tibias, and pelvic bones were subjected to colony-forming assays and scored. To evaluate CFCs, we used methylcellulose medium either obtained from Stem Cell Technologies (maximum sensitivity) or made at our laboratory using SF-03 (for routine use), containing 30% FBS, 10 ng/ml mouse SCF, 10 ng/ml human TPO, 10 ng/ml mouse IL-3, and 2 units/ml hEPO in 35-mm dishes. Cells were incubated for 11 days at 37ºC in a humidified atmosphere with 5% CO_2 for gain-of function assay and for 14 days for loss-of-function assay.

2.18. Competitive Repopulation Assays

To assess both short-term (2-3 weeks) and long-term (> 16 weeks) reconstitution ability in test cells, a competitive repopulation assay was used [61]. For long-term analysis in a gain-of-function setting, 700 $EGFP^+$ cultured HS(P)Cs or 100 fresh HSCs obtained from Cxcr4-KO mice were used per recipient mouse. For short-term analysis, we used 100 $EGFP^+$ cultured HS(P)Cs or 200 fresh HSCs per recipient. Whole BM cells from Ly5.1/5.2 F1 mice were used as competitors at 2×10^5 cells per recipient. For secondary transplantation, pooled BM cells from primary recipients were transplanted into lethally-irradiated recipients at 4×10^5 cells per recipient. Donor cell chimerism of multiple hematopoietic lineages was evaluated by flow cytometry. Generally, a high percentage of donor cells (~70-90%) retained EGFP positivity long-term in recipients, most likely due to inherent resistance to gene silencing of the DNsam retroviral backbone vector [57, 59, 60] used in this study (Table 2B and Fig. 3B).

2.19. Long-term donor chimerism analysis in hematopoietic cell populations

Phenotypic cell-surface markers used to define each hematopoietic subset are summarized below. Antibody descriptions in detail are listed in Table 1.

LT-HSC (long-term hematopoietic stem cells):

lineage (Gr1, Mac1, Ter119, CD4, CD8, B220, IL7R)$^-$CD34$^-$c-kit$^+$Sca1$^+$

ST-HSC (long-term hematopoietic stem cells):

lineage (Gr1, Mac1, Ter119, CD4, CD8)$^-$CD34$^+$c-kit$^+$Sca1$^+$

CLP (common lymphocyte progenitors):

lineage (Gr1, Mac1, Ter119, CD4, CD8, B220, CD3, CD5)$^-$IL7R$^+$ Flk2$^+$Sca1^{dull}cKit^{dull}

CMP (common myeloid progenitors):

lineage (Gr1, Ter119, CD4, CD8, B220, IL7R, IgM, CD3, CD19, Sca1)$^-$ckit$^+$CD34$^+$FcgR$^-$

GMP (granulocyte/macrophage progenitors):

lineage (Gr1, Ter119, CD4, CD8, B220, IL7R, IgM, CD3, CD19, Sca1)$^-$ckit$^+$CD34$^+$FcgR$^+$

ProB (progenitor B cells): CD43$^+$IgM$^-$B220$^+$

PreB (premature B cells): CD43$^-$IgM$^-$B220$^+$

MaB (mature B cells): CD43$^-$IgM$^+$B220$^+$

PriNeu (primitive neutrophils): Gr1^{dull}Mac1^{dull}

MaNeu (mature neutrophils): Gr1$^+$Mac1$^+$

B (peripheral blood B cells): CD4$^-$CD8$^-$Gr1$^-$Mac1$^-$B220$^+$

Mye (peripheral blood myeloid-lineage cells): CD4$^-$CD8$^-$Gr1$^+$Mac1$^+$B220$^-$

2.20. Assessment of AMD3100-induced mobilization effect on donor chimerism

Lethally irradiated recipient mice were transplanted with 300 EGFP$^+$ cells along with 2 x 10^5 competitor cells (as described in "Competitive repopulation assays") in a gain-of-function setting. Baseline donor cell chimerism in total leukocytes was analyzed by flow cytometry 11 weeks after transplantation ("pre-mobilization" values) and the mice were left untouched for stabilization. One week later, each mouse received a single dose of intraperitoneal AMD3100 (10 mg/kg). PB donor chimerism was analyzed one hour after AMD3100 injection ("post-mobilization" values). See Fig. 26.

2.21. Statistical Analysis

All data are expressed as means ± SD. Comparisons between two groups were subjected to Student's unpaired *t* test using *Prism 4* software (GraphPad), and comparisons of more than two groups were performed by Dunnett's multiple comparison (*vs*. control) unless otherwise annotated. *P* for trend was tested using polynomial contrast in general linear models. A level of $P < .05$ was considered significant.

Chapter III. Results

3.1. Stepwise Gain-of-Function Effects of Exogenous Cxcr4 on Transduced HS(P)Cs, with Greater Response for the ΔC-Type Receptor

The system that allows to study the gain-of-function effect in HSCs and HSPCs was constructed. As the retroviral gene delivery technology was used, the transduction efficiency was assessed. After transduction, the percentage of cells expressing EGFP, a marker of transgene expression, was similar between groups (Fig. 3A). Next, the expression level of Cxcr4 was examined. In comparison to control group (Mock), overexpression of Cxcr4 receptors, either in wild-type configuration or in their C-terminus truncated form, was confirmed in transduced HS(P)Cs (Fig. 4A and Fig. 6), transduced HSPCs (Fig. 7), and in the murine hematopoietic cell line 32D (Fig. 5A). The detailed flow cytometry analysis revealed correlation between the expression levels of Cxcr4 receptors and the EGFP marker in cells overexpressing exogenous Cxcr4 receptors (Fig. 4B and 5B). These data demonstrated that the established retroviral system was readily able to confer the overexpression of Cxcr4 receptors to transduced cells.

In general, the presence of its ligand is known to initiate two major events, intracellular signaling responses and rapid internalization of the receptor in cells expressing a chemokine receptor [71]. Upon SDF-1 stimulation, surface Cxcr4 receptor is recycled via an endocytosis process for which an intact cytoplasmic C-terminal domain is required. Defective internalization of ΔC-Cxcr4 in response to SDF-1/CXCL12 has been reported in previous studies [35, 50, 53, 54, 72, 73], and it was also clearly observed in this study for ΔC-Cxcr4-32D cells with 100 ng/ml of SDF-1 (Fig. 12A). With this low concentration of SDF-1, however, as the degree of receptor internalization in both Mock- and WT-Cxcr4-HS(P)Cs cells was far less than that observed in transduced 32D cells and human T cell line CEM (Fig. 12B), blunting of the response of ΔC-Cxcr4 was therefore not evident (Fig. 11A). Nevertheless, HS(P)Cs overexpressing ΔC-Cxcr4 showed a blurred response in receptor internalization with a higher concentration of SDF-1 (500 ng/ml, Fig. 11B).

Gain-of-function effects were confirmed in WT- and ΔC-Cxcr4-transduced cells in comparison with Mock-cells by a chemotaxis assay and a Ca^{2+} influx assay; a stepwise enhancement in transwell migration to SDF-1/CXCL12 was evident with greater response for ΔC-Cxcr4-cells than that for other cell types (Fig. 13), consistent with an enhanced

chemotactic response in human cells expressing WHIM-type CXCR4 [27, 53, 54, 64, 74, 75]. With 30 minutes' incubation, the difference between groups remained relatively small, but it became evident with longer incubation time, 90 minutes (Fig. 13B). The stepwise nature of gain-of-function for WT- and ΔC-Cxcr4 was further confirmed with a Ca^{2+} influx assay using 32D cells (Fig. 10).

3.2. Enhanced *in Vitro* Proliferative Response of HS(P)Cs under Particular Circumstances by Gain-of-Function Modification in Cxcr4 Signaling

I next examined the characteristics of these cultured HS(P)Cs using a series of *in vitro* assays. At first, clonogenic ability and differentiation characteristics were compared in *in vitro* single-cell liquid culture. As shown in Fig. 14, modification of Cxcr4 did not alter frequencies of HS(P)Cs capable of colony formation, with colony types also unaffected (no SDF-1). Addition of SDF-1 produced no remarkable influence on these cultures (SDF-1 50 and 500 ng/ml). These results suggest minimal influences of Cxcr4 receptor modification on HS(P)Cs' clonogenic ability in stroma-free liquid culture and on their differentiation properties. We next tested proliferative characteristics of bulk populations in liquid culture. As described in materials and methods, our basal culture system is distinct from others in allowing self-renewal of murine HSCs both at a single cell level [58, 76] and at a population level [77] with the minimum cytokines (SCF and TPO) needed in a serum-free setting. In this so-called "HSC-self-renewal compatible" culture, we found fresh HSCs highly resistant to desensitization to Sdf-1 (Fig. 9). When cultured HS(P)Cs were tested in this system (input cells = 50 cells/well), massive expansion was observed for all cell types in the absence of SDF-1/CXCL12 (Fig. 15B, SCF+TPO alone = SDF-1: 0 ng/ml). Cell proliferation was unexpectedly enhanced in the presence of SDF-1/CXCL12 especially at the highest concentration (500 ng/ml), which was considered "desensitizing" for most cell types [35, 78, 79]. Interestingly, the additive effects of exogenous Cxcr4 receptors on HS(P)C proliferation became evident only in the presence of 500 ng/ml SDF-1; as shown in Fig. 15B, stepwise (*i.e.*, WT < ΔC-Cxcr4) enhancement in response was observed in comparison with control samples (Untransduced and Mock). Similar to the result of a chemotaxis assay, the cell expansion was generally observed in all three groups suggesting the positive effect of SDF-1/Cxcr4 signaling in HS(P)Cs' proliferation (Fig. 15A). This feature was supported by cell cycle analysis, the ΔC-Cxcr4-HS(P)Cs showed more cells at S phase than other groups (Fig. 16).

We then tested whether overexpression of exogenous Cxcr4 affected HSPCs' ability to colonize and to repopulate C3H10T1/2 feeder cell layers in an *in vitro* co-culture assay [67]. In this assay, test cells can be scored for *in vitro* clonogenic ability in the presence of stromal cells by counting characteristic cobblestone-like areas that form underneath the feeder layers. I first confirmed both the presence of Sdf-1 in this culture supernatant and the significance of the Sdf-1/Cxcr4 axis for cobblestone-like area formation using the CXCR4 antagonist AMD3100. In this system, the presence of Sdf-1 in culture medium of feeder cells and bone marrow was detected (Fig. 17C). To test the relationship between the SDF-1/Cxcr4 axis and the colonization ability in cells, the Cxcr4 antagonist was added to culture medium through out the assay. As the CXCR4 antagonist concentration increased, the ability of HSCs to form the area was decreased indicating that this signaling is important for HSCs to colonize and repopulate the feeder layers (Fig. 17B). When Cxcr4-modified HS(P)Cs were subjected to this assay, the ability to form cobblestone-like areas proved remarkably enhanced in comparison with that in Mock control cells; enhancement occurred in a stepwise manner, with the greatest response in ΔC-Cxcr4-overexpressing cells (Fig. 17A). Collectively, these findings demonstrated that augmented Cxcr4 signaling alters cellular responses to favor HSPC survival/proliferation, especially in the presence of high concentrations of Sdf-1 and/or of supporting feeder layers that produce this ligand.

3.3. Augmented Cxcr4 Signaling in Murine HS(P)Cs/HSPCs Does Not Enhance BM Homing/Lodging, but Improves Subsequent BM Repopulation

I then examined how augmentation in Cxcr4 signaling affected the *in vivo* behavior of transplanted HS(P)Cs at different times during BM reconstitution. In preliminary experiments where BM homing efficiency of purified HSCs was assessed with a direct quatification method, we could detect only marginal numbers of events in recipient BM by flow cytometry, and found difficult the reliable quantitation of cells that home in marrow after infusion of $CD34^{-}$KSL cells, even with extremely high numbers (up to ~15,000 cells per mouse; data not shown). We thus decided to use KSL cells as the starting material to assess rare events of BM homing/lodging. As the earliest process, BM homing efficiency was assessed using $EGFP^{+}$ cultured HS(P)C populations (Figs. 18 and 19). As shown, I found no enhancement in BM homing of HSPCs at the indicated times (4-24 hours) by gain-of-function Cxcr4 modification (Fig. 18 and 19). This was also true when we used $EGFP^{+}$ cultured HS(P)Cs as the sole

transplants and assessed BM homing by counting number of CFCs recovered from each recipient at 16 and 24 hours (Fig. 20). The earlier time points (4 and 8 hours) was also examined for transduced/cultured HS(P)Cs, but there were no CFCs detectable in the recipient BM in this assay (data not shown). I next examined subsequent BM repopulation kinetics by extending the times of analysis, similarly as previously reported [67]: in this setting, CFCs measurable in BM are supposed to reflect not only homing, but also subsequent cell division shortly after homing. As shown in Fig. 19C, augmentation of Cxcr4 signaling in HS(P)Cs did not lead to increased numbers of CFCs in recipient BM at days 2 and 4. Collectively, these results demonstrate that augmentation in murine Cxcr4 signaling does not affect the earliest events after HSPC transplantation, including BM homing/lodging by HSPCs.

I further tracked *in vivo* BM repopulation by donor HS(P)Cs beyond the above time points. As recipients of HS(P)Cs alone barely survived lethal-dose irradiation beyond day 7, test HS(P)Cs were transplanted with competitor cells, with their relative contributions to BM repopulation determined at days 14 and 21 (Fig. 21). Of note is that stepwise increases in donor chimerism were visible in BM at these time points (P for trend = 0.038) with ΔC-Cxcr4-cells showing the highest donor cell contribution (*vs*. Mock, P = 0.035). The advantage in BM repopulation for Cxcr4-augmented HS(P)Cs was also noticeable in cohorts of long-term recipients (Fig. 21C, P for trend = 0.042), again with ΔC effects being the highest (*vs*. Mock, P = 0.038). From these observations, we conclude that the Sdf-1/Cxcr4 axis plays a role in productive BM repopulation by transplanted HSPCs after the second phase (weeks 2-3) that follows transplantation.

3.4. Continuous Overexpression of Exogenous Cxcr4 Receptors in HS(P)Cs Leads to Poor Peripheral Reconstitution

The possible correlation between Cxcr4 signal intensity in HS(P)Cs and their short-term BM reconstitution efficiency made me wonder how long-term transplantation outcome would fare in gain-of-function experiments. In competitive repopulation assays, ΔC-Cxcr4-transduced HS(P)Cs contributed poorly to PB chimerism at 4 weeks (Fig. 25B) and 16 weeks (Fig. 25C), consistent with the major features of WHIM syndrome, lymphocytopenia and neutropenia [34, 36, 51, 74]. That overexpression of WT-Cxcr4 in HS(P)Cs also did not improve PB reconstitution (Fig. 25, WT) was unexpected, as beneficial

effects of similar treatment are reported for human $CD34^+$ cells [50, 52]. To figure out that this low donor chimerism in PB was due to excessive Cxcr4 signaling in HS(P)Cs or not, Cxcr4 antagonist (AMD3100) was systematically injected into long-term recipients. Significantly increased PB donor chimerism was observed in WT- and ΔC-Cxcr4 groups, suggesting that blunted peripheral mobilization of donor cells played a causal role in poor PB reconstitution in these mice (Fig. 26).

3.5. Enhanced Donor Cell Chimerism Occurs in BM Cells Throughout Developmental Stages of HS(P)Cs Expressing Gain-of-Function Cxcr4 Receptors

Of note is that the recipients of ΔC-Cxcr4-transduced HS(P)Cs showed obvious long-term donor cell chimerism in BM (Fig. 21C); this may accompany favorable *in vivo* expansion of transplanted HSCs, or may simply indicate accumulation of certain cell types at a particular differentiation stage, thus reflecting conditions that in some respect are abnormal. To distinguish these possibilities, we scrutinized recipient BM for donor cell chimerism in multiple cell compartments, including the long-term HSC fraction (LT-HSC; Fig. 23). As shown in Fig. 22, individual recipients of Mock-treated HS(P)Cs did not display significant alterations in donor cell chimerism among these populations, suggesting little influence on hematopoiesis by Mock-transduction of HS(P)Cs. In contrast, donor cell chimerism differed clearly between PB leukocytes (open histograms) and BM compartments (colored histograms) in each recipient that received Cxcr4 signal-enhanced HS(P)Cs (Fig. 22, WT and ΔC). General enhancement of chimerism in the BM compartments, including LT-HSC, was striking, with no difference between fractions, which suggested that Cxcr4 signal-dependent donor cell expansion might occur even at a stem cell level. When donor cell chimerism was similarly assessed along two major paths of lineage development, *i.e.*, B cells and neutrophils, results were consistent with the idea that Cxcr4 signal augmentation induced no gross alterations, such as maturation arrest, in hematopoietic development, but likely caused exaggerated BM retention of donor cells (Fig. 22). Since Cxcr4 signaling had been implicated in B cell differentiation, comparison between control (Mock) and Cxcr4-modified groups were conducted. As shown in Fig 24, no obvious changes in the percentages of either Pro B cells or immature/mature B cell populations between groups. Furthermore, similar B cell differentiation pattern between competitor and test cells was observed within the same recipient BM (Fig. 24). The increase of "phenotypically-defined" LT-HSCs might not

necessarily imply, however, that functional HSC numbers were amplified. We could demonstrate persistence within primary recipient BM of reconstituting cells that were capable of establishing donor chimerism upon serial transplantation (Fig. 27, PB). No advantage over Mock-treated cells, however, was observed for WT- and ΔC-Cxcr4-expressing cells in repopulation of secondary recipient BM (Fig. 27, BM), unlike the case with primary recipients (Fig. 21C) (see Discussion, below).

3.6. Loss-of-Function Studies Support the Proposed Roles of Cxcr4 in Murine HSPCs in Transplantation

To understand Cxcr4's roles in murine HSPCs better in transplantation, the loss-of-function analyses in experimental settings like those used for the gain-of-function studies were conducted. To this end, I mostly used purified HSCs obtained from *Cxcr4* conditional KO mice [55] and littermate (LM) control mice after induction (Fig.1). First, the absence of Cxcr4 receptors did not affect HSCs' colony-forming ability in liquid medium or their multilineage potentials (Fig. 28A). When cell proliferation was tested in liquid culture, I found loss of SDF-1-responsiveness in KO-HSCs (Fig. 28B, KO) whereas control LM-HSCs showed a response similar to that observed in both fresh B6 HSCs (Figs. 8A and Fig. 9) and cultured HS(P)Cs (Fig. 15). Consistent with the loss of SDF-1-response phenotypes, the ability of Cxcr4-deficient HSCs to form cobblestone-like area formation was shown to be severely impaired (Fig. 28C). The defect in Cxcr4-KO-HSCs found in this assay may be regarded as a mirror-image of the results in gain-of-function experiments (Fig. 17A), thus further supporting the importance of Cxcr4 receptors in HSC/HSPC colonization and proliferation in the presence of feeder cell environments that produce Sdf-1/Cxcl12.

We then examined how the absence of Cxcr4 signaling in HSCs affected *in vivo* kinetics of donor cell repopulation. Early BM homing was assessed using fresh HSPCs with or without receptor desensitization using the Cxcr4 antagonist AMD3100 following established preincubation methods [72, 80, 81](Fig. 29A). As assessed at 15 hours, I did not detect a decrease in BM homing of HSPCs that had been rendered unresponsive to Sdf-1/Cxcl12, even with additional systemic administration of AMD3100 (Fig. 29B). Supporting this observation, assessment of subsequent repopulation in BM on days 4 and 6 demonstrated that in the absence of Cxcr4 expression (KO) transplanted HSCs yielded numbers of CFCs comparable with those observed for wild type HSCs (LM; Fig. 30). Genotyping PCR demonstrated that

most randomly picked-up CFCs had the Cxcr4 locus completely knocked out (31 in 33, 93.9%), thus indicating that the "highly purified HSCs" that we injected alone into lethally-irradiated recipients were capable of BM homing *in vivo* and colony formation *ex vivo* in the absence of functional Cxcr4 expression. KO-HSCs, contrary to these findings, clearly showed significant impairment in capability of BM repopulation at 2 and 3 weeks after transplantation (Fig. 31B). As expected, KO-HSCs contributed to PB long-term less than did LM control HSCs (Fig. 31C), consistent with previous observations [40, 43, 47].

Our comprehensive approach has pointed out the importance of the Sdf-1/Cxcr4 axis in HSC/HSPCs for productive engraftment and repopulation in recipient BM, especially for a particular phase after transplantation, that is, the early/sub-early repopulation phase (~2-3 weeks), which follows the initial engraftment process (< 1 week).

3.7. Alteration in Phosphorylation Kinetics of Erk in Response to SDF-1 in HS(P)Cs Expressing ΔC-Cxcr4

To obtain mechanistic insights, I examined how overexpression of exogenous Cxcr4 receptors altered downstream signaling events in HS(P)Cs. Phosphorylation kinetics in Erk1/2 and Akt were tested in $EGFP^+$ cultured HS(P)Cs by flow cytometry analysis. While phosphorylated Akt intensity was unaltered before and after stimulation (Fig. 34), clear alterations in phosphorylated Erk1/2 (pErk) signals confirmed that the HS(P)Cs used the MAPK/Erk signaling pathway in response to SDF-1/CXCL12 (Fig. 33). The peak response was seen 3 minutes after stimulation, with the greatest response in ΔC-Cxcr4-expressing cells. Response termination was delayed in ΔC-Cxcr4-expressing cells, with residual pErk-signals still detectable at 15-30 minutes, whereas cells in the other two samples (Mock and WT) quickly returned to baseline status by 15 minutes. Of note is that with even a "desensitizing-high" concentration of SDF-1 (500 ng/ml), ΔC-expressing cells still showed visibly enhanced phosphorylation at peak and delay in its termination. Similar behavior was confirmed by immunoblotting assay using the 32D murine hematopoietic cell line (Fig. 32).

Chapter IV. Discussion

The goal of this study is to use experimental findings to benefit patients undergoing transplantation. To this end, I sought to clarify the stage-specific role of Cxcr4 signaling in transplanted cells during hematopoietic reconstitution. With gain-of-function experiments, augmentation of Cxcr4 signaling appeared relatively unimportant in accelerating the homing/lodging of murine HSC/HSPCs, but efficient in enhancing their subsequent repopulation of BM. This pattern of stage-specificity in Cxcr4's role was also demonstrated in a series of loss-of-function experiments. These results strengthen the generally held idea that CXCR4 signal modification can benefit transplantation outcomes [50, 52], by demonstrating enhancement in donor cell expansion, possibly even at a stem cell level. Also to note, however, is that sustainment of augmented signal led to detrimental effects on transplantation outcomes in this study, even with overexpression of a non-mutant Cxcr4 receptor.

4.1. Role of Cxcr4 signaling in an initial homing process of transplanted HSC/HSPCs

That the SDF-1/CXCR4 axis plays an indispensable role in BM homing by adult HSCs seems widely accepted [49, 82]; this may contrast with my findings. This view, however, rests on pioneering studies that used human HSPCs, mostly in loss-of-function settings [43, 83]. These were followed by gain-of-function studies that demonstrated improved human HSPC engraftment in immunodeficient mice with overexpression of wild-type CXCR4 [50-52]. KO mouse studies have clearly demonstrated the importance of Cxcr4 for robust hematopoietic reconstitution in transplantation but have not specifically addressed BM homing by purified HSCs [40, 47]. This study of the role of Cxcr4 is, so far as I know, the first gain-of-function approach to use murine HSC/HSPCs. Using cultured HSPCs derived from KSL cells, I demonstrated that overexpression of exogenous Cxcr4 receptors did not lead to enhanced BM homing (Figs. 18 and 19). Short-term homing (16-24 hours) and subsequent repopulation kinetics (days 2-4) in BM, assessed by using cultured HS(P)Cs, also did not alter with Cxcr4-overexpression (Figs. 20B and 20C). These results indicate that augmentation of Cxcr4 signaling does not benefit transplanted murine HSC/HSPCs in these early processes.

In loss-of-function experiments, I used purified HSCs freshly isolated from Cxcr4-deficient mice for the assessment of early BM repopulation capability (days 4 and 6;

Fig. 30B). The results supported the idea that the Sdf-1/Cxcr4 axis may be of little importance in this phase of BM repopulation. The impact of Cxcr4 signaling on early BM homing was assessed using fresh, uncultured HSPCs following established desensitizing methods utilizing the Cxcr4 antagonist AMD3100 [72, 80, 81]. The results demonstrated that BM homing (15 hours) of purified HSPCs did not much depend on the Sdf-1/Cxcr4 axis, consistent with previous observations [80]. There may be controversy, however, on this issue, because other workers observed impaired BM homing by HSPCs after AMD3100 treatment [72]. This can probably be attributed to differences in study design, with the most significant one being that I used HSPCs alone as the sole transplant/analyte whereas others assessed homing of HSPCs by injecting donor cells preincubated with AMD3100 as either low-density BM cells [81] or lineage-negative BM cells [72]. The importance of these observations should be emphasized, as in clinical settings unpurified hematopoietic cells are most often used in transplantation. Nevertheless, I believe that my findings also are of importance, because clinical gene therapy trials currently in progress use purified $CD34^+$ HSPCs [84], thus resembling my experimental settings.

4.2. Role of Cxcr4 signaling in early repopulation process of transplanted HSC/HSPCs

In contrast to the above findings, studies of donor cell reconstitution within BM at weeks 2 and 3 clearly accorded a role to Cxcr4 signaling (Figs. 21B and 31B). Although the frequency of donor HSCs in BM could not be determined by immunophenotyping due to transient change of surface markers of HSCs at these early time points, the results obtained by cobblestone-like area formation experiments (Fig. 17A) mirrored *in vivo* donor chimerism at 2-3 weeks (Fig. 21B). This in turn supports the idea that augmentation of Cxcr4 signaling leads to expansion (colonization, proliferation) of HSPCs *in vivo*, where the presence of stromal cells is expected to promote this event.

4.3. Role of Cxcr4 signaling in an in vivo expansion of transplanted HSC/HSPCs

Cxcr4-mediated effects on *in vivo* HSC/HSPC expansion may arise from improved survival/proliferation and/or enhanced retention of HSPCs within BM. Consistent with this idea, studies suggested that CXCR4 relays a survival-promoting signal within HSPCs [49, 85]. Of note is that Cxcr4 signal-mediated enhancement in proliferation was more evident when HSPCs either were in contact with feeder cells (Fig. 17A) or were stimulated with

SDF-1 in high concentrations (500 ng/ml, Fig. 15B). Promotion of cell cycling in HSPCs by SDF-1/CXCL12 may conflict with recent descriptions of a role for Cxcr4 in maintenance of HSC quiescence [40, 47, 48]. However, I think it possible to explain this discrepancy by the difference in culture systems. In fact, in our defined culture system [76, 77], HSCs, either fresh or after stimulation, resisted desensitization to high concentrations of SDF-1 (Figs. 9 and 15). There were readily measurable levels of Sdf-1 in murine BM cavities irrespective of irradiation conditioning (Fig. 17C), one can expect local levels of Sdf-1 to be very high *in vivo*, especially in the functional niche environment. I therefore speculate that in our scenario, high concentrations of Sdf-1 may allow favorable proliferative response in murine HSC/HSPCs when they exist in "self-renewal-comparable" conditions.

Kawai *et al*. demonstrated that transplantation of human HSPCs overexpressing WHIM-mutant receptor resulted in the WHIM phenotype in the mouse environment [51]. More recently, generation of WHIM-type mice was reported with many interesting findings [35]. Mine is the first study of the WHIM-type receptor in the murine system in the context of HSPC transplantation. Most notable is that enhanced BM repopulation was observed in the LT-HSC population, at least as defined by immunophenotyping, upon signal augmentation (Fig. 22). Altered Erk activation kinetics may be responsible for the observed enhancement of repopulation capability in HSC/HSPCs equipped with gain-of-function Cxcr4, but further investigation is needed for more mechanistic insights.

Secondary transplantation, however, did not confirm stem cell expansion in primary BM by definition (Fig. 27, PB); this was partly explained by the properties of "defects in PB release", which should inhere in phenotypically defined HSCs still expressing exogenous Cxcr4. Furthermore, the highest donor chimerism by ΔC-Cxcr4-expressing cells in BM (Fig. 21C) was not phenocopied to the BM of secondary recipients (Fig. 27, BM), probably suggesting impaired repopulating ability in each donor LT-HSC due to long-term non-physiological Cxcr4 signaling events.

4.4. Implication of Cxcr4 signaling for HSC/HSPCs transplantation medicine

When considering implications of this study for clinical transplantation, poor PB contribution by HS(P)Cs overexpressing WT-Cxcr4 is significant; this may contrast with the favorable effects of CXCR4 overexpression on the engraftment/repopulation of human HSPCs [50, 52]. Species differences may account for this discrepancy. Differences in study

design, however, may contribute more importantly. I transplanted only cells expressing EGFP at high levels (thus likely exogenous Cxcr4 receptors as well, see Fig. 4A), which might have led to unfavorable, extreme gain-of-function effects on hematopoietic reconstitution. Alternatively, improved reconstitution reported in the case of CXCR4 overexpression may be attributable to the co-injection of non-HSC/HSPCs, so-called "facilitating cells" [82], mostly missing in our study.

In this work, cultivation of HSCs is required in gain-of-function settings, thus those findings may be applicable to cycling HSC/HPSCs (likely present in the setting of gene therapy) but not to their fresh counterparts. Our culture system [76, 77], however, is capable of maintenance of progenitor phenotypes in most cells after 7 days (Figs. 8B and C) and actually is "self-renewal compatible". It is therefore I believe that this study complements general knowledge concerning the role of CXCR4 in HSPC transplantation [49, 86, 87].

Further investigation is necessary for formal demonstration of whether enhanced HSC self-renewal is feasible, using an experimental system that allows *in vivo* inducible expression of exogenous Cxcr4 in test cells for a certain period of time after transplantation. More practically, it would be intriguing, for clinical application of my findings, to aim at drug discovery by screening for an efficacious and specific small molecule having characteristics of a CXCR4 agonist with limited desensitization. With elucidation of mechanisms underlying CXCR4/Cxcr4 signal-mediated effects, perhaps combined multiple strategic approaches will eventually culminate in greater clinical benefits.

Chapter V. Conclusions

In this study, I have addressed stage-specific roles for Cxcr4 signaling in donor cell repopulation in BM for the first time using purified mouse HSC/HSPCs. With unique combinational approaches that used both loss-of-function and gain-of-function modification of Cxcr4 receptors, I found that Cxcr4 signaling appears unimportant for the homing/lodging of mouse HSC/HSPCs, but vital for their subsequent repopulation of BM. Cxcr4 signal enhancement likely favored BM repopulation by donor cells at a level of primitive cell populations, but was shown to be detrimental to PB reconstitution when sustained too long. Consequently, I think it important to investigate further when and how long signaling via this chemokine receptor is to be modified in order favorably to enhance HSPC engraftment in future transplantation medicine.

A

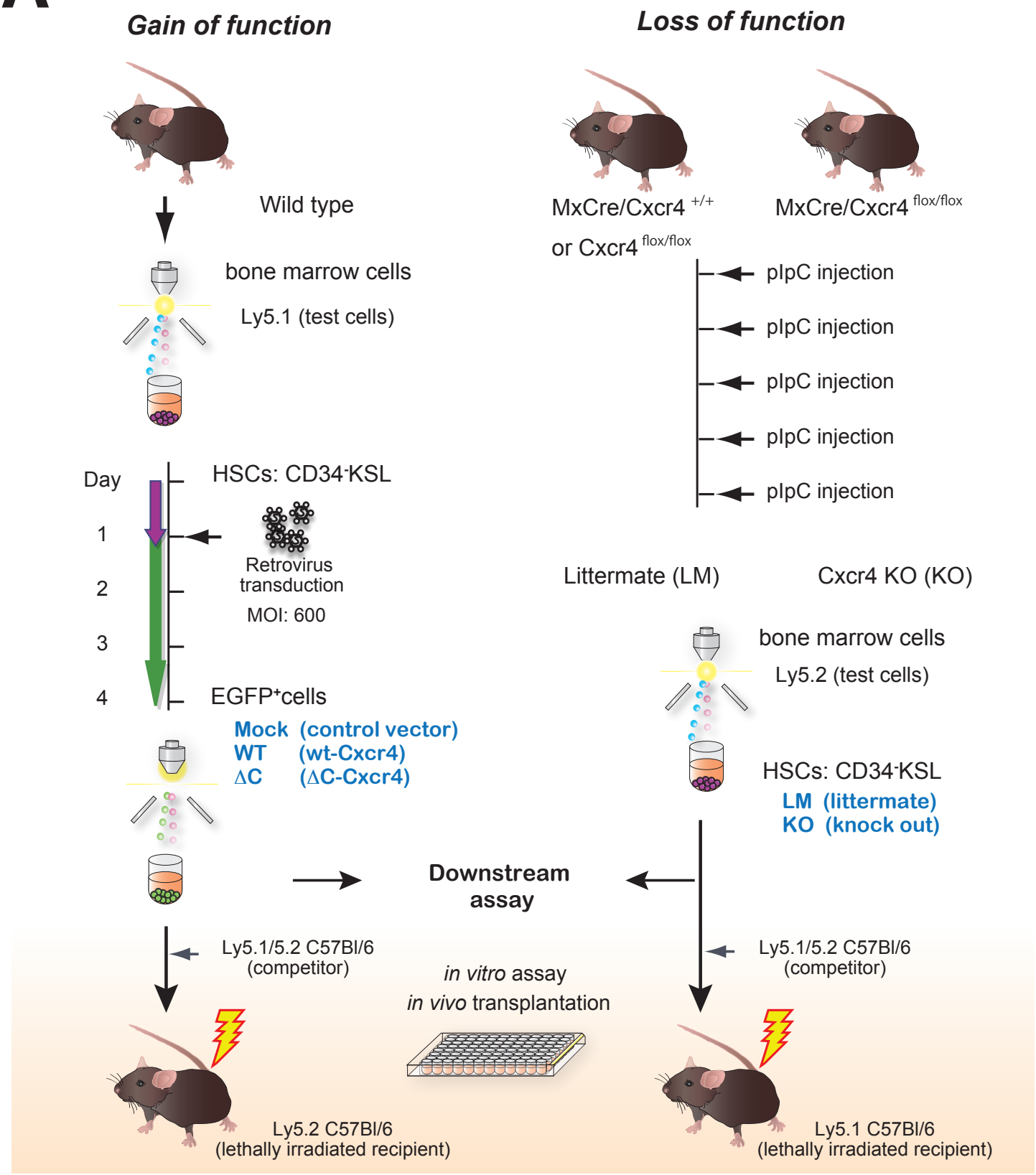
Gain of function
Loss of function
Wild type
bone marrow cells
Ly5.1 (test cells)
MxCre/Cxcr4 +/+
or Cxcr4 flox/flox
MxCre/Cxcr4 flox/flox
pIpC injection
pIpC injection
pIpC injection
pIpC injection
pIpC injection
Day
1
2
3
4
HSCs: CD34-KSL
Retrovirus transduction
MOI: 600
EGFP+cells
Mock (control vector)
WT (wt-Cxcr4)
ΔC (ΔC-Cxcr4)
Littermate (LM)
Cxcr4 KO (KO)
bone marrow cells
Ly5.2 (test cells)
HSCs: CD34-KSL
LM (littermate)
KO (knock out)
Downstream assay
Ly5.1/5.2 C57Bl/6 (competitor)
in vitro assay
in vivo transplantation
Ly5.1/5.2 C57Bl/6 (competitor)
Ly5.2 C57Bl/6 (lethally irradiated recipient)
Ly5.1 C57Bl/6 (lethally irradiated recipient)

B

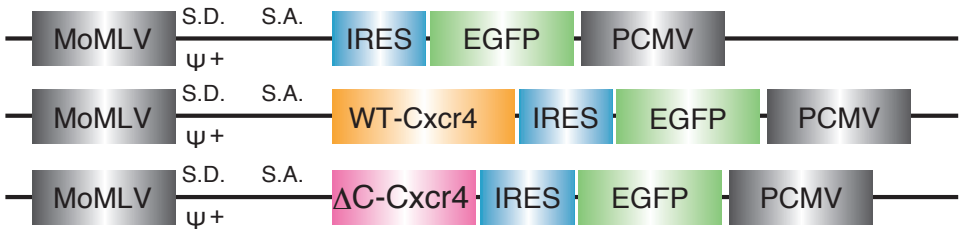
MoMLV
S.D.
S.A.
ψ+
IRES
EGFP
PCMV
MoMLV
S.D.
S.A.
ψ+
WT-Cxcr4
IRES
EGFP
PCMV
MoMLV
S.D.
S.A.
ψ+
ΔC-Cxcr4
IRES
EGFP
PCMV

Figure 2

Human CXCR4

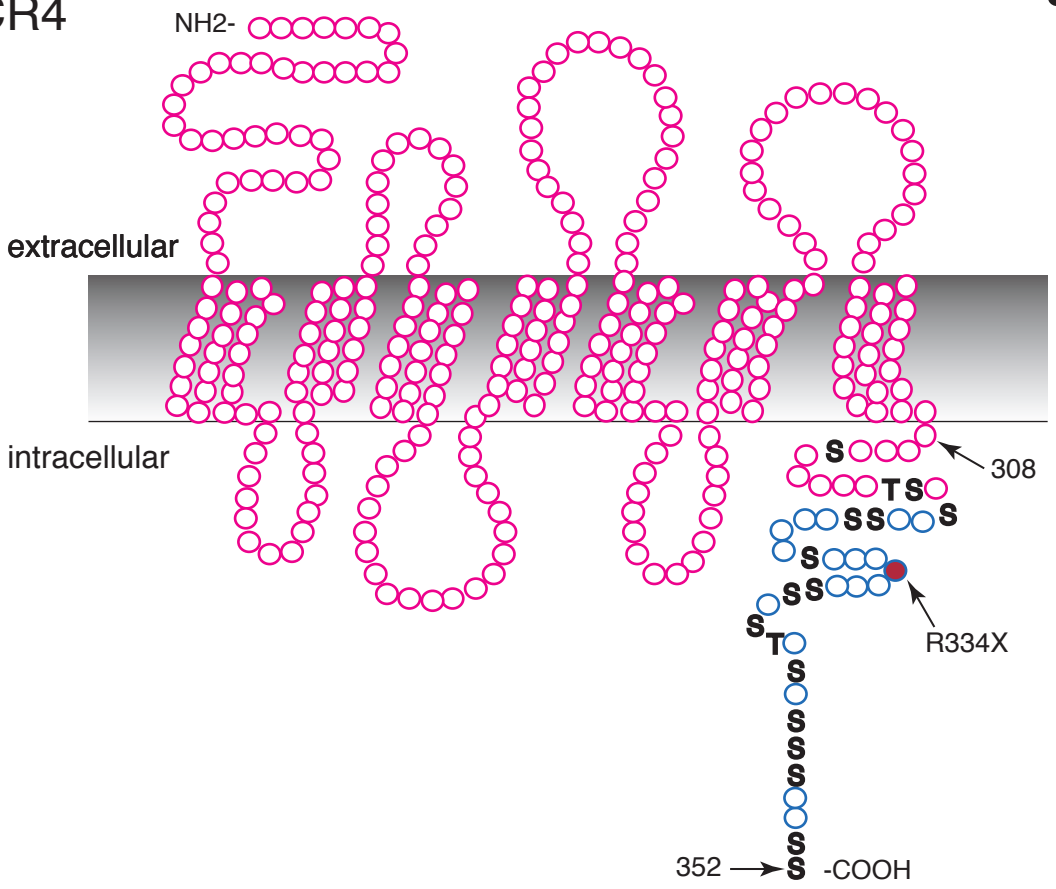

Amino acid sequence of the CXCR4/Cxcr4 C-terminal tail

Human CXCR4

308 334 352

KFKTSAQHALTSVSRGSSLKILSKGKRGGHSSVSTESESSSFHSS

ΔC-mutant CXCR4 (R334X, D19 a.a.)

308 333

KFKTSAQHALTSVSRGSSLKILSKGK

Mouse Cxcr4 (WT)

315 341 359

KFKSSAQHALNSMSRGSSLKILSKGKRGGHSSVSTESESSSFHSS

Mouse ΔC-type Cxcr4 (R341X, D19 a.a.)

315 340

KFKSSAQHALNSMSRGSSLKILSKGK

A

HSC transduction efficiency

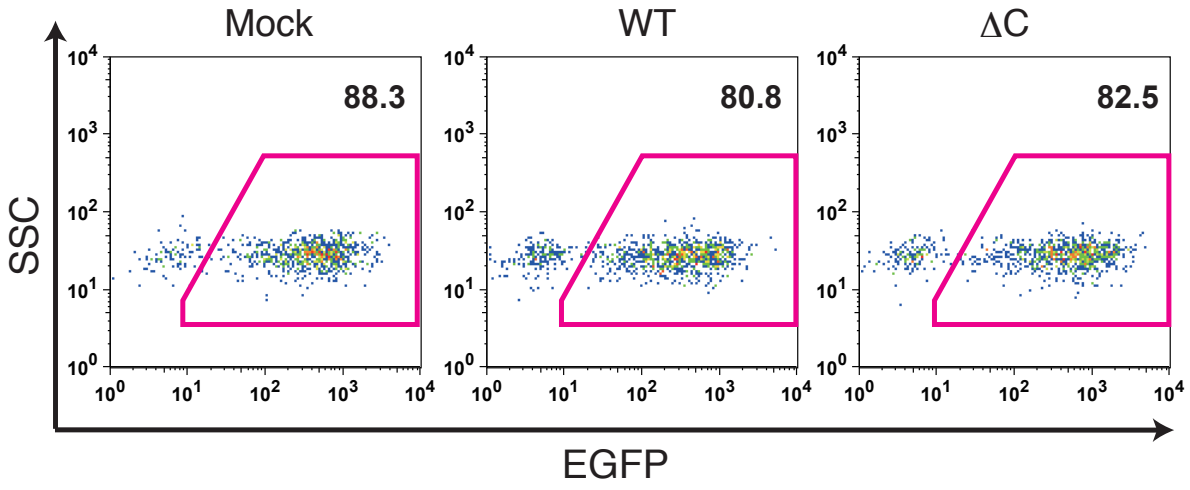

B

Long-term EGFP expression after transplantation

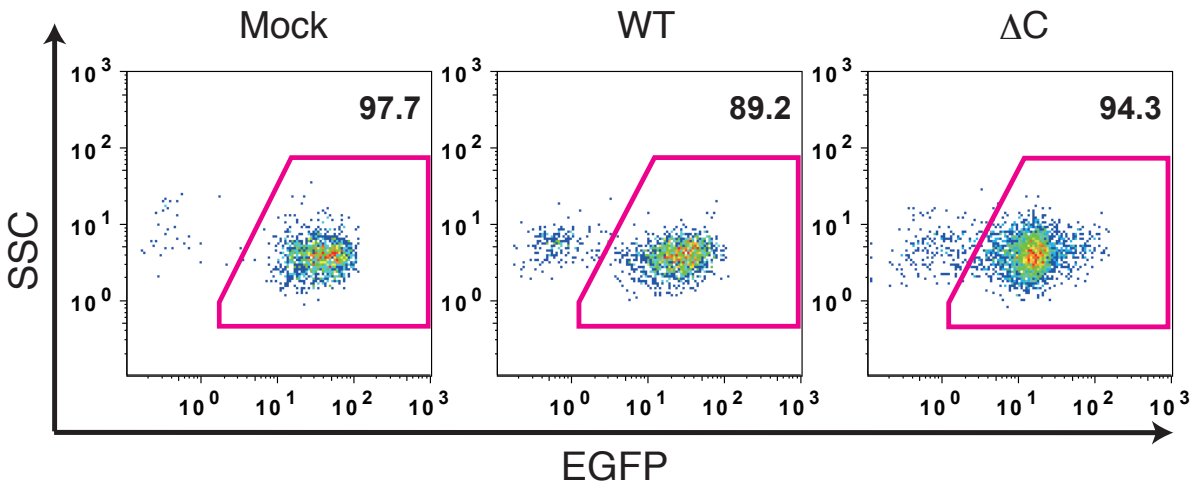

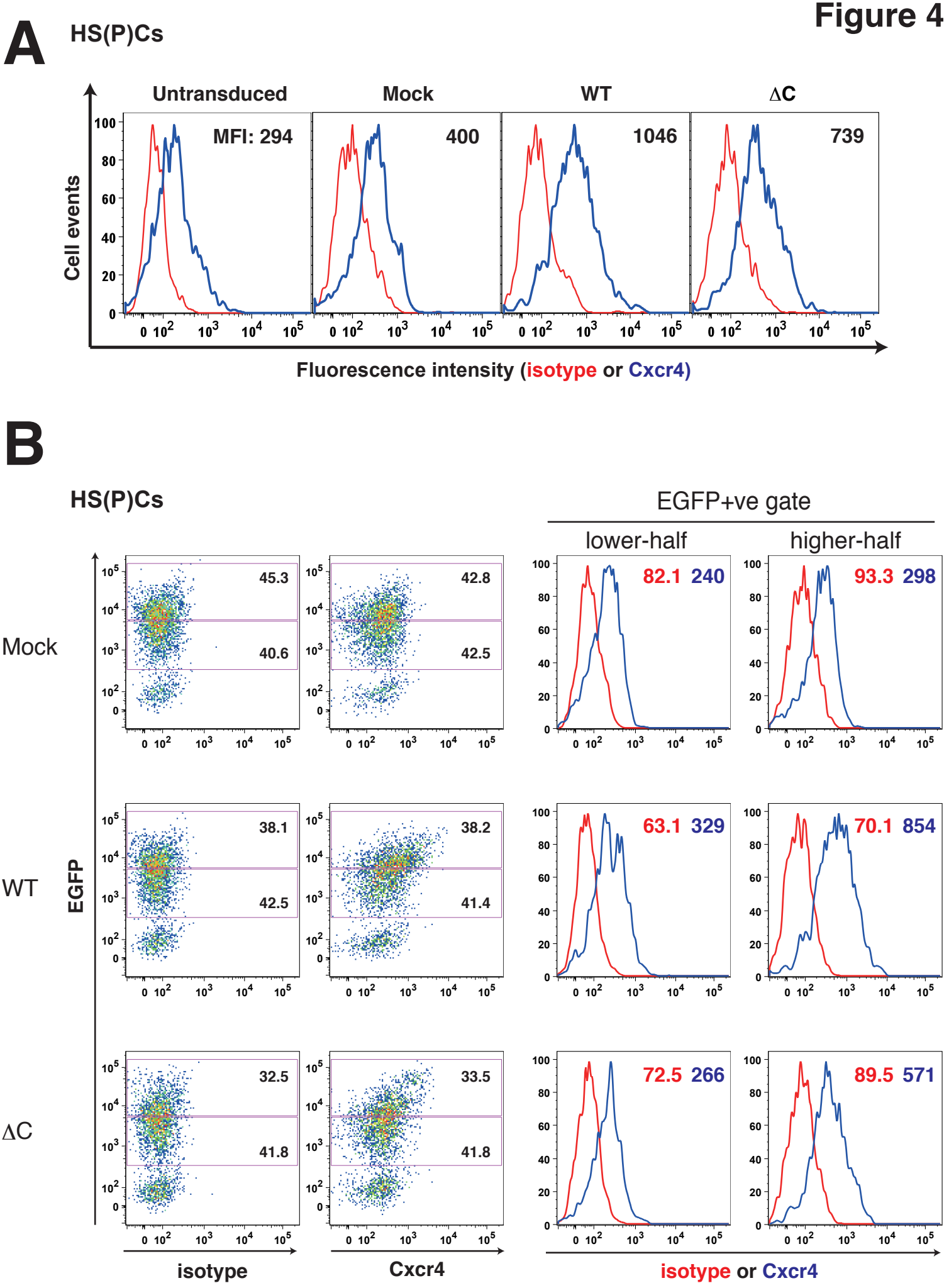
A
HS(P)Cs
Untransduced
Mock
WT
ΔC
MFI: 294
400
1046
739
Cell events
Fluorescence intensity (isotype or Cxcr4)
B
HS(P)Cs
EGFP+ve gate
lower-half
higher-half
Mock
WT
ΔC
EGFP
45.3
40.6
42.8
42.5
82.1 240
93.3 298
38.1
42.5
38.2
41.4
63.1 329
70.1 854
32.5
41.8
33.5
41.8
72.5 266
89.5 571
isotype
Cxcr4
isotype or Cxcr4

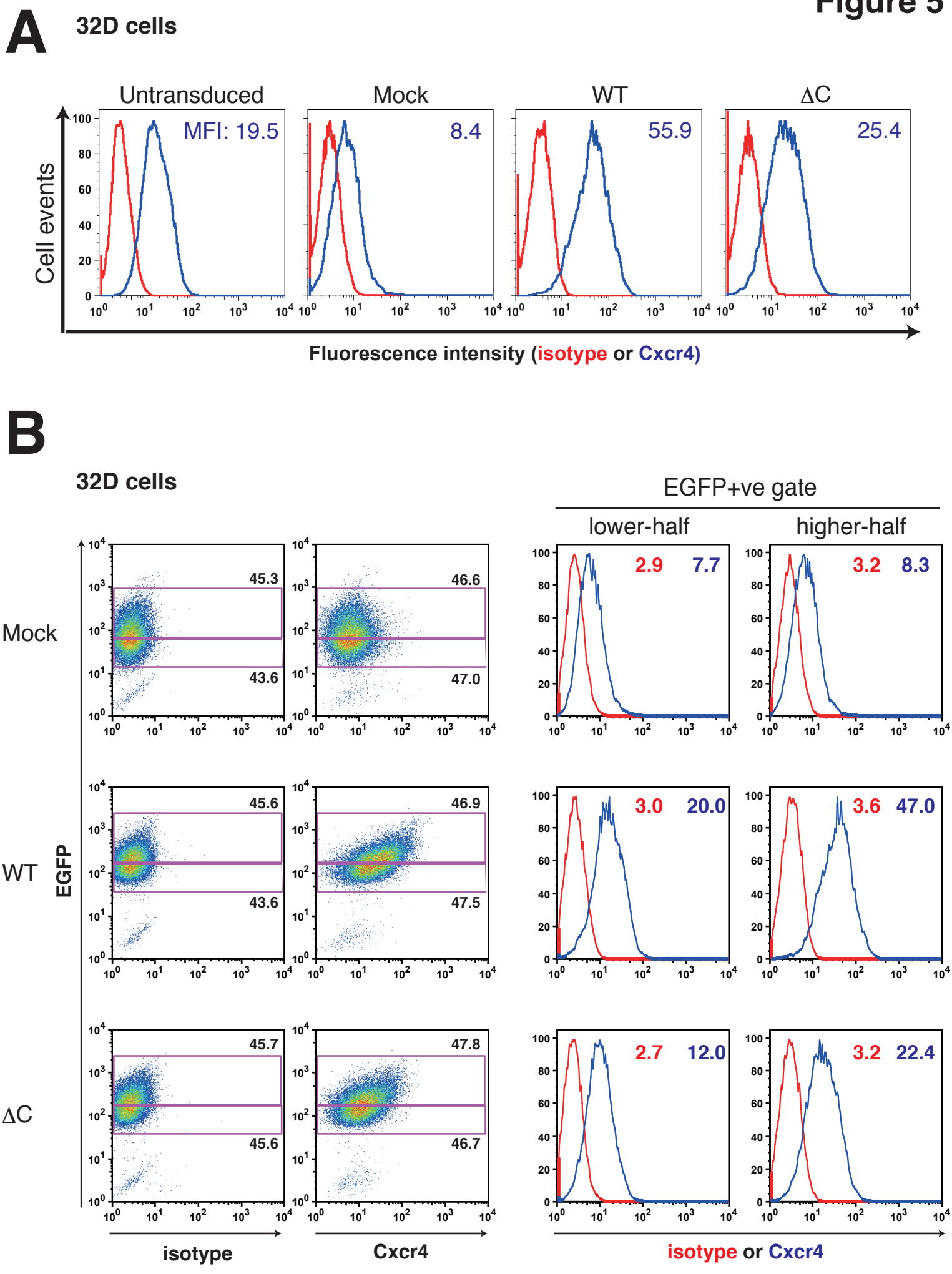
A
32D cells
Untransduced
Mock
WT
ΔC
MFI: 19.5
8.4
55.9
25.4
Cell events
Fluorescence intensity (isotype or Cxcr4)
B
32D cells
EGFP+ve gate
lower-half
higher-half
Mock
WT
ΔC
EGFP
45.3
43.6
46.6
47.0
2.9
7.7
3.2
8.3
45.6
43.6
46.9
47.5
3.0
20.0
3.6
47.0
45.7
45.6
47.8
46.7
2.7
12.0
3.2
22.4
isotype
Cxcr4
isotype or Cxcr4

Figure 6

HS(P)Cs

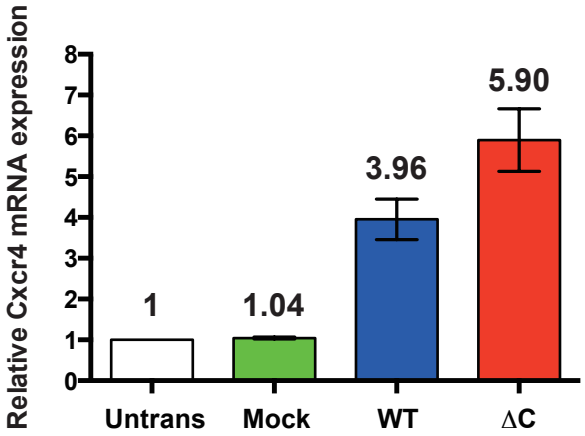

Figure 7

HSPCs

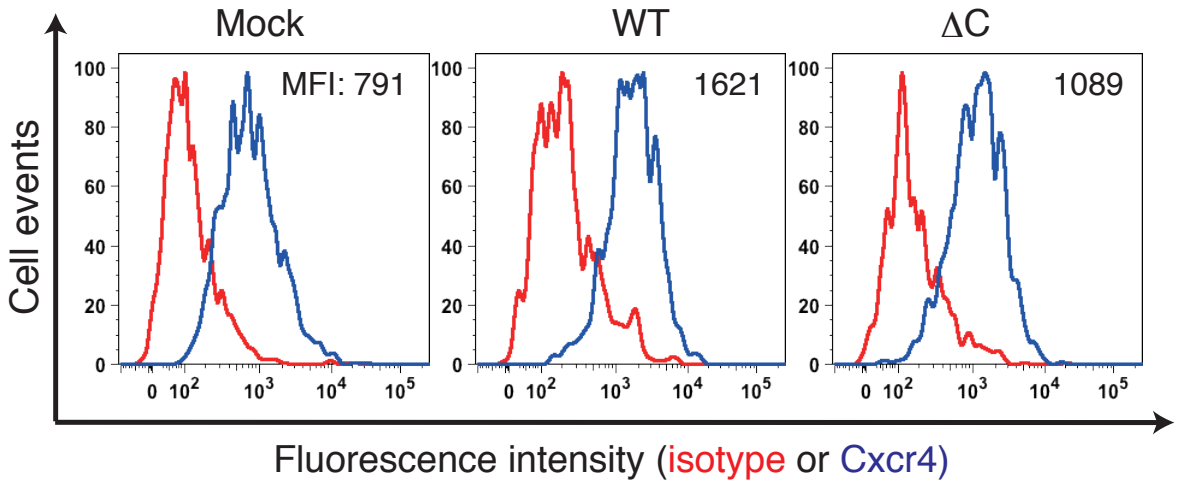

Figure 8

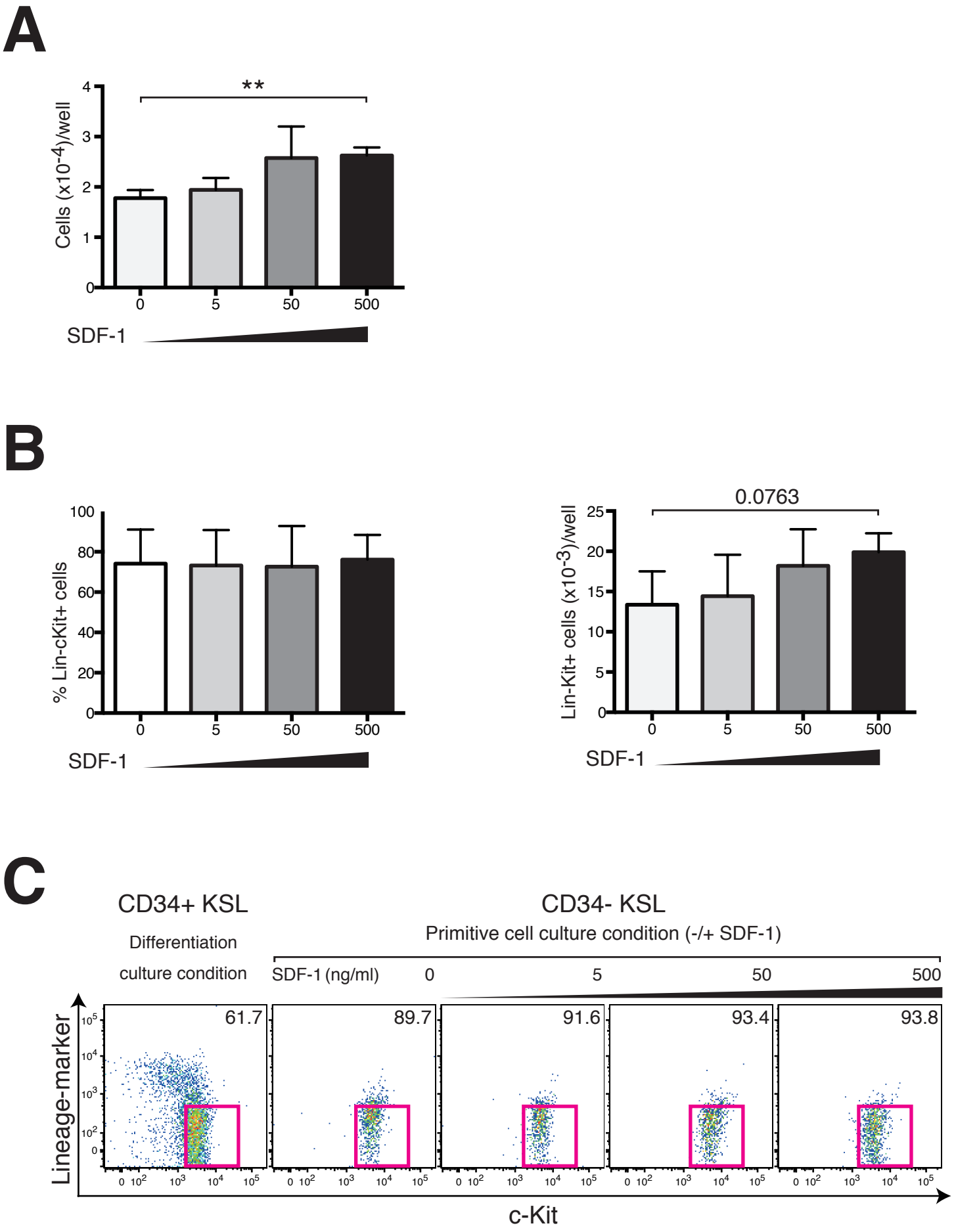
A
**
Cells (x10-4)/well
0
1
2
3
4
0
5
50
500
SDF-1
B
% Lin-cKit+ cells
0
20
40
60
80
100
0
5
50
500
SDF-1
0.0763
Lin-Kit+ cells (x10-3)/well
0
5
10
15
20
25
0
5
50
500
SDF-1
C
CD34+ KSL
CD34- KSL
Differentiation
culture condition
Primitive cell culture condition (-/+ SDF-1)
SDF-1 (ng/ml)
0
5
50
500
Lineage-marker
c-Kit
61.7
89.7
91.6
93.4
93.8

Figure 9

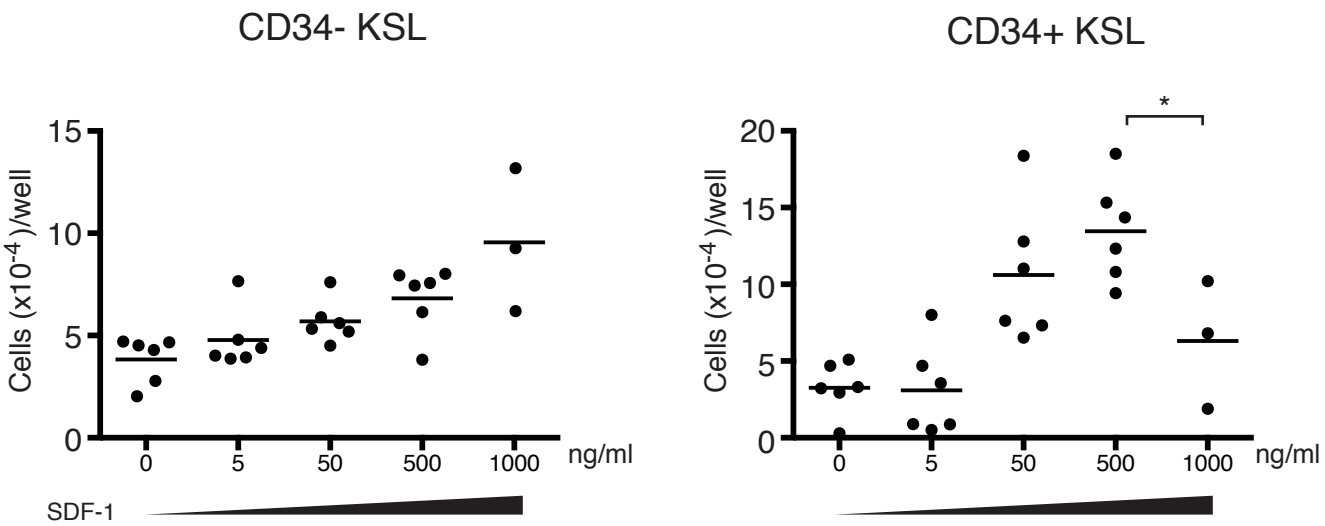
CD34- KSL
CD34+ KSL
Cells (x10-4)/well
15
10
5
0
20
0
5
50
500
1000
ng/ml
SDF-1
*

Figure 10

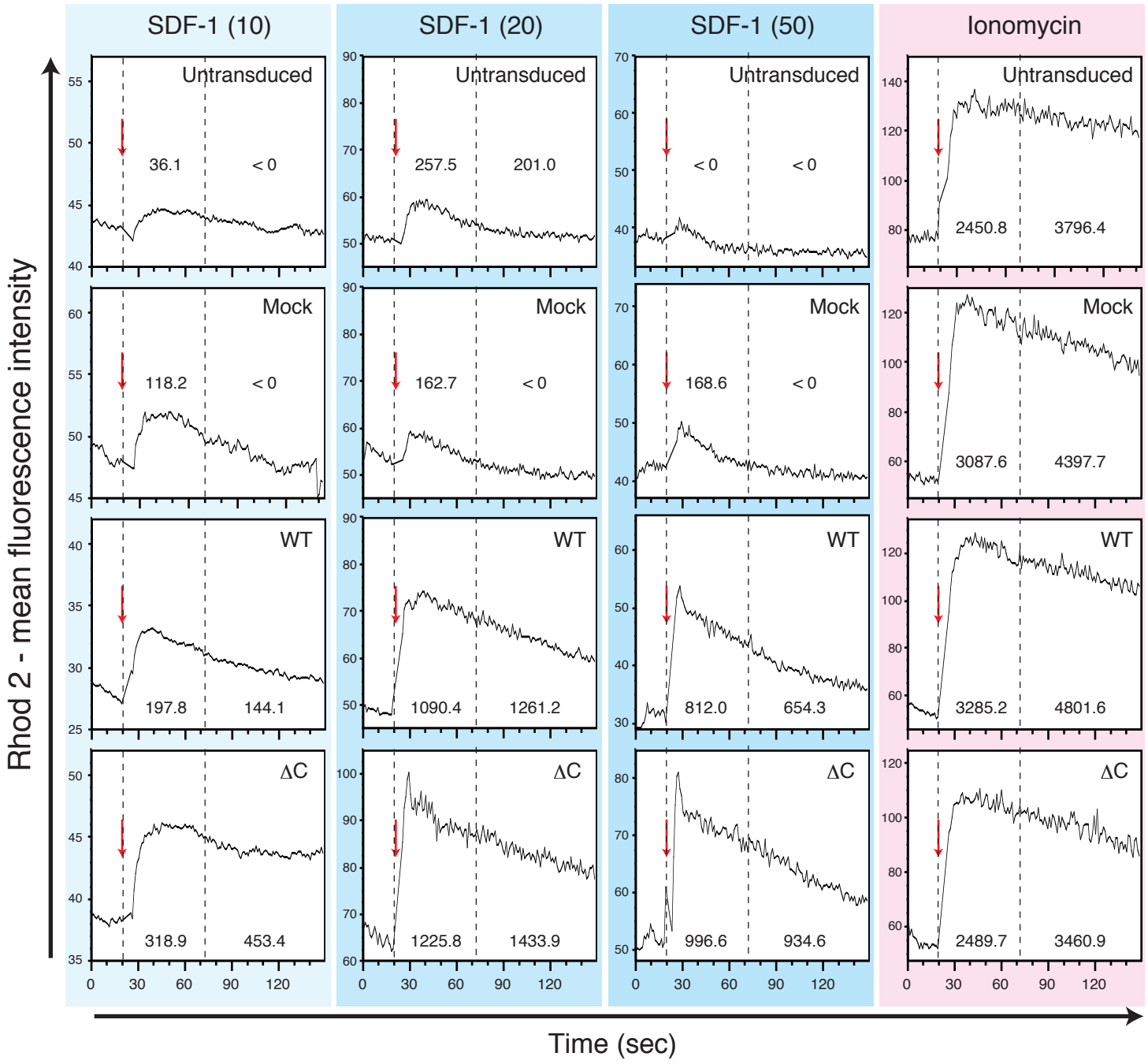
SDF-1 (10)
SDF-1 (20)
SDF-1 (50)
Ionomycin
Untransduced
Mock
WT
ΔC
36.1
< 0
257.5
201.0
< 0
< 0
2450.8
3796.4
118.2
< 0
162.7
< 0
168.6
< 0
3087.6
4397.7
197.8
144.1
1090.4
1261.2
812.0
654.3
3285.2
4801.6
318.9
453.4
1225.8
1433.9
996.6
934.6
2489.7
3460.9
Rhod 2 - mean fluorescence intensity
Time (sec)

A HS(P)Cs SDF-1 100ng/ml

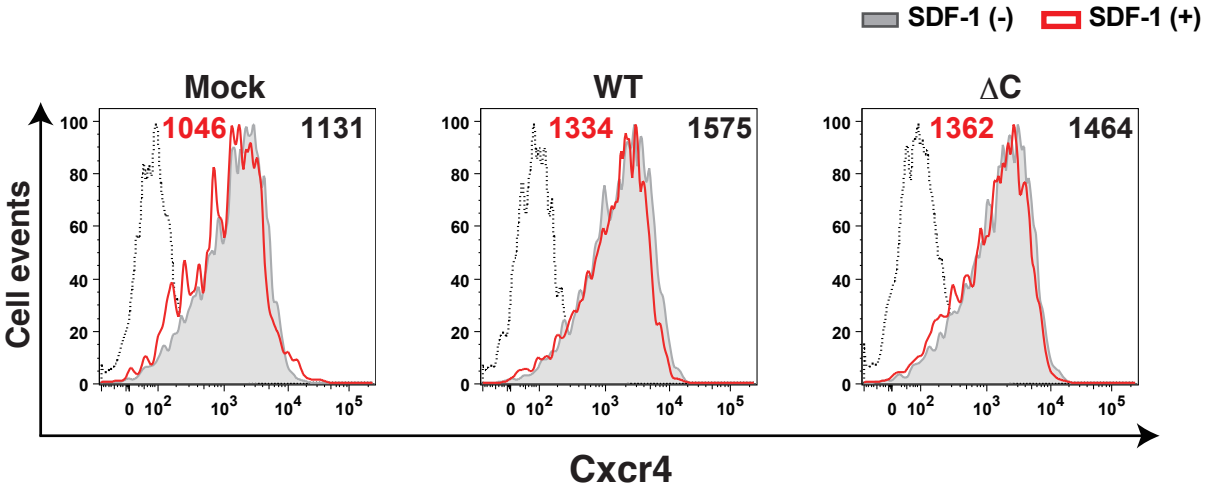

B HS(P)Cs SDF-1 500ng/ml

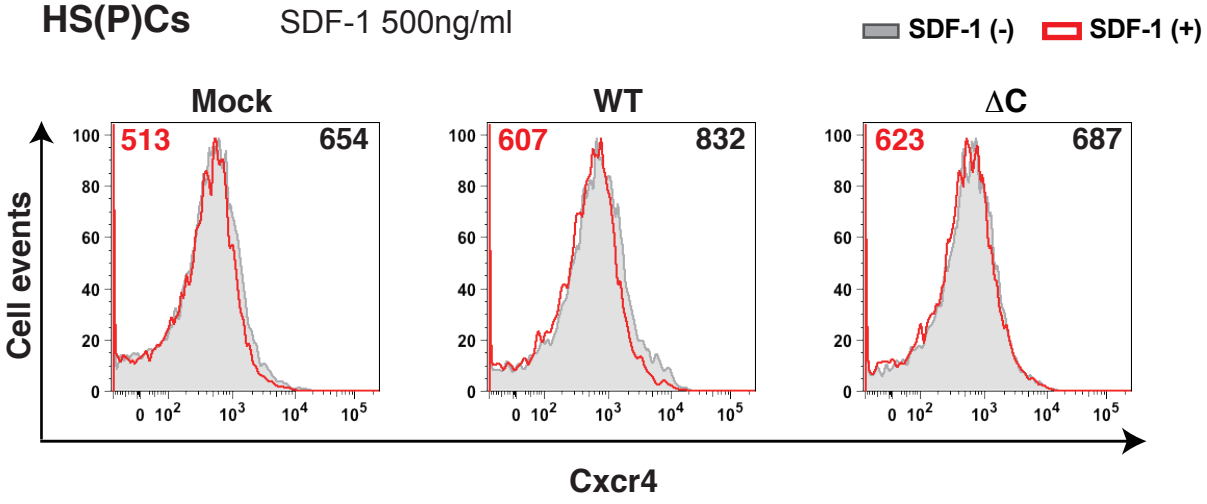

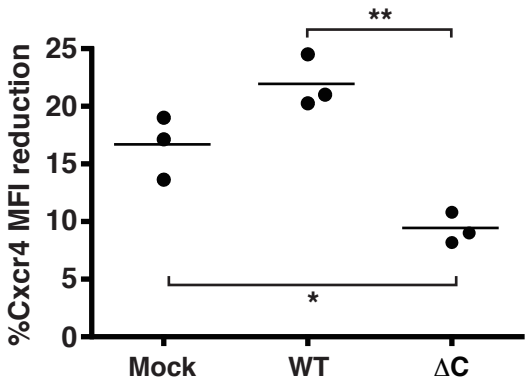

Figure 12

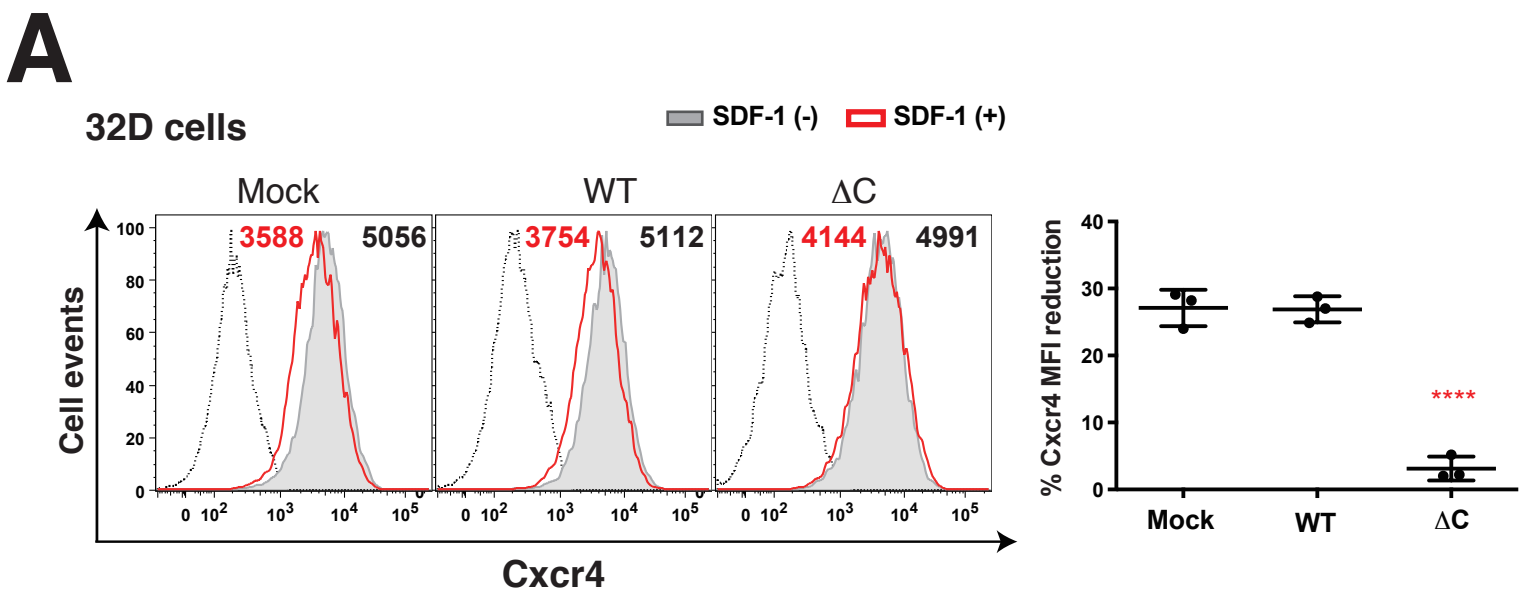
A
32D cells
SDF-1 (-)
SDF-1 (+)
Mock
WT
ΔC
3588
5056
3754
5112
4144
4991
Cell events
Cxcr4
% Cxcr4 MFI reduction
****
Mock
WT
ΔC

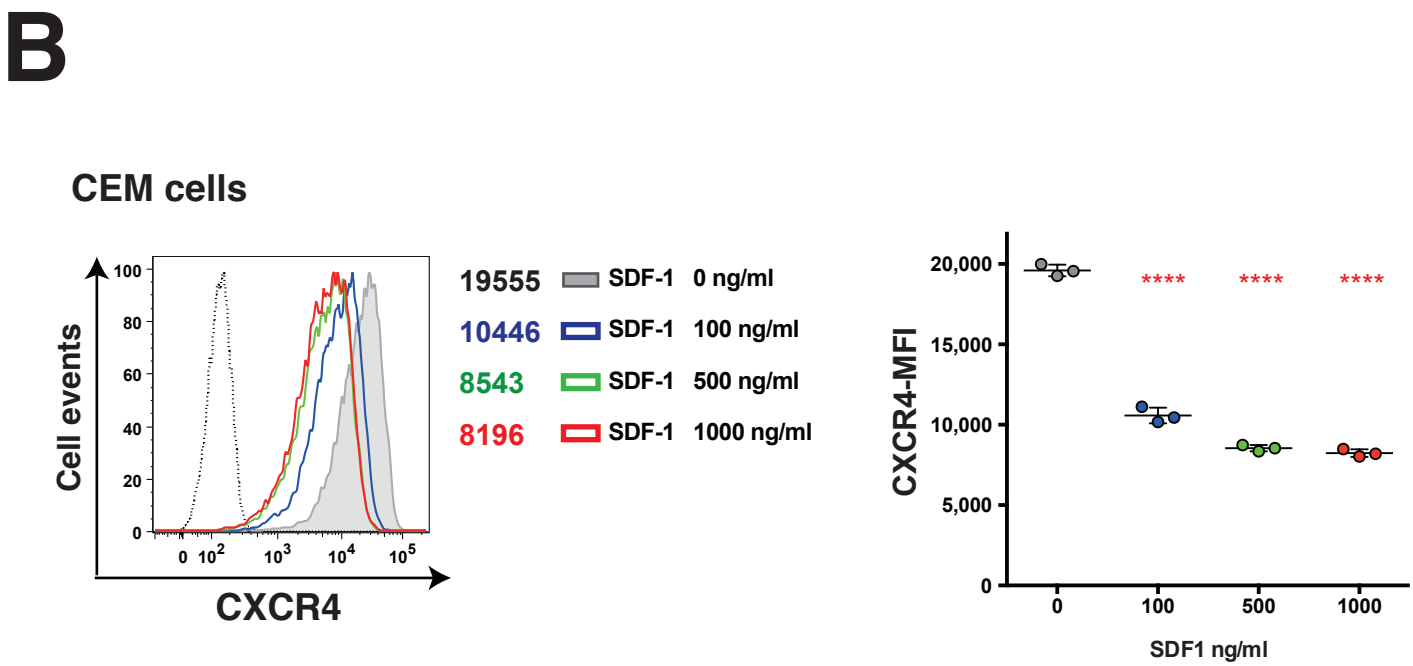
B
CEM cells
Cell events
CXCR4
19555 SDF-1 0 ng/ml
10446 SDF-1 100 ng/ml
8543 SDF-1 500 ng/ml
8196 SDF-1 1000 ng/ml
CXCR4-MFI
****
****
****
SDF1 ng/ml

Figure 13

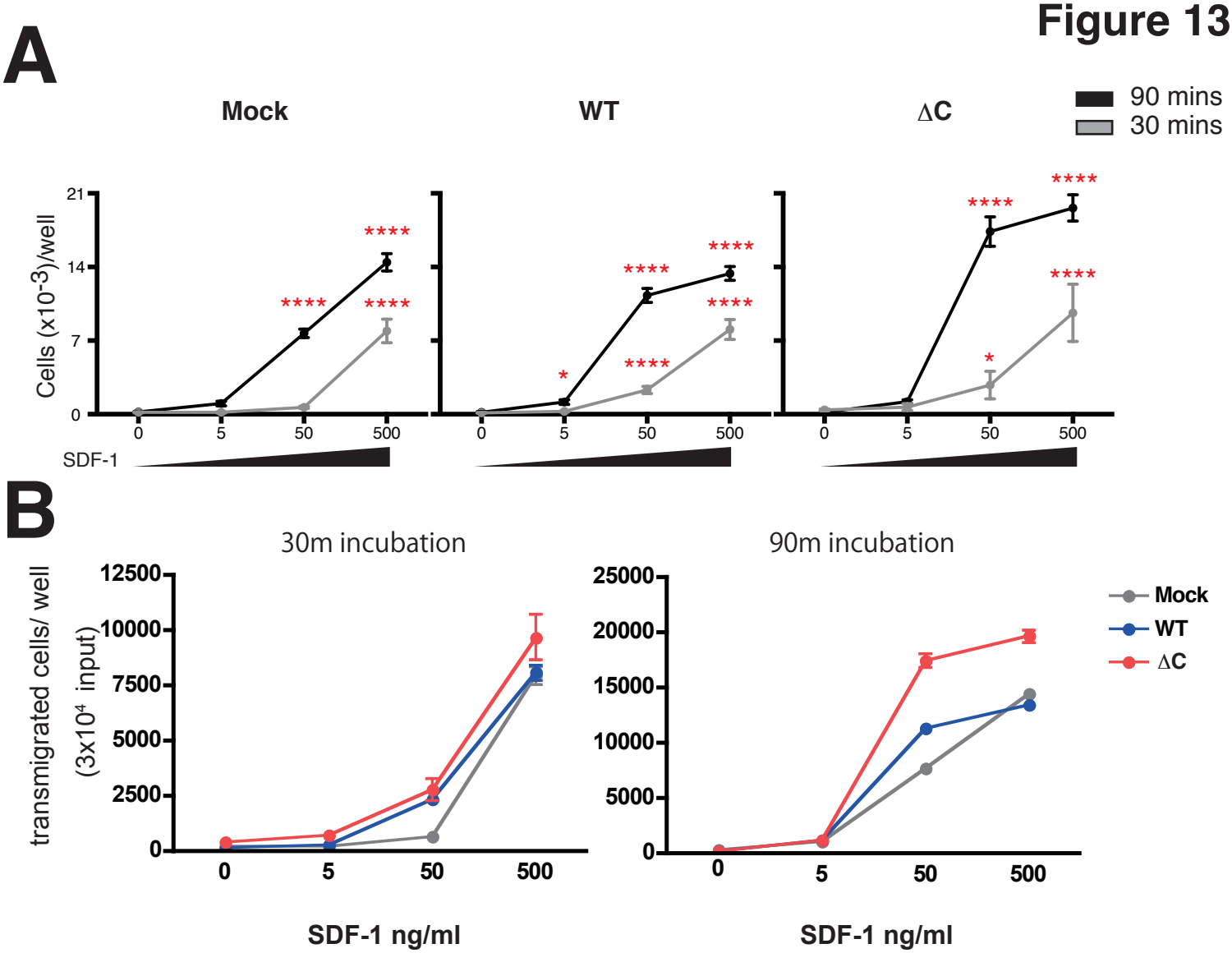
A
Mock
WT
ΔC
90 mins
30 mins
Cells (x10-3)/well
21
14
7
0
0
5
50
500
SDF-1
****
*
B
30m incubation
90m incubation
transmigrated cells/ well
(3x10⁴ input)
12500
10000
7500
5000
2500
0
25000
20000
15000
10000
5000
0
0
5
50
500
SDF-1 ng/ml
Mock
WT
ΔC
C
30m incubation
SDF 0
SDF 5
SDF 50
SDF 500
transmigrated cells/ well
1250
1000
750
500
250
0
12500
10000
7500
5000
2500
0
***
**
Mock
WT
ΔC
90m incubation
2000
1500
1000
500
0
25000
20000
15000
10000
5000
0

Figure 14

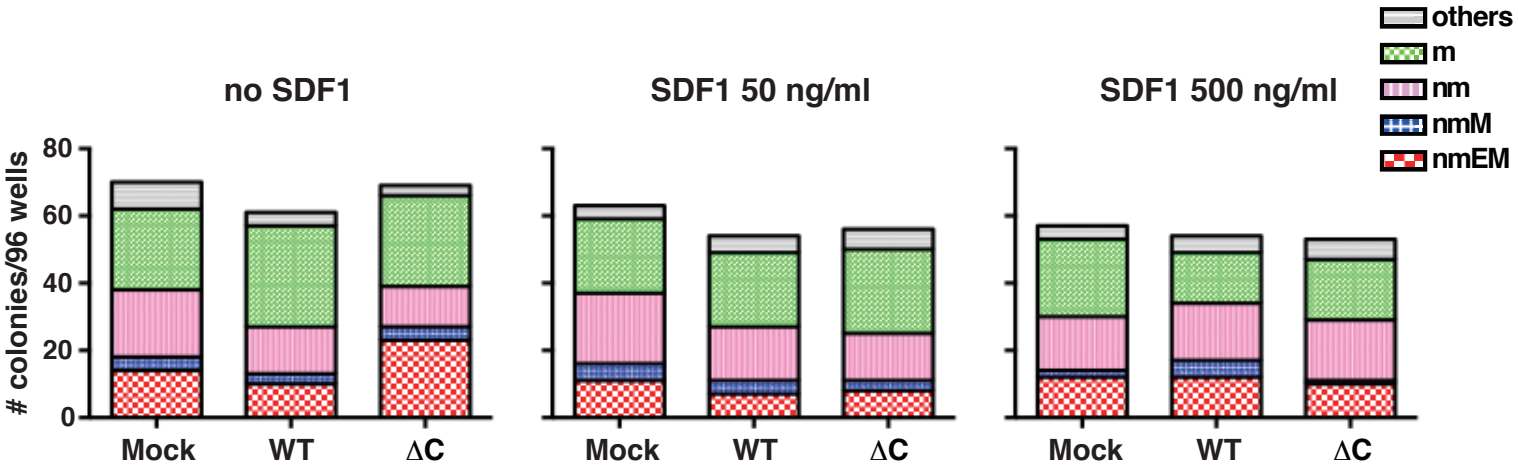
no SDF1
SDF1 50 ng/ml
SDF1 500 ng/ml
others
m
nm
nmM
nmEM
colonies/96 wells
80
60
40
20
0
Mock
WT
ΔC
Mock
WT
ΔC
Mock
WT
ΔC

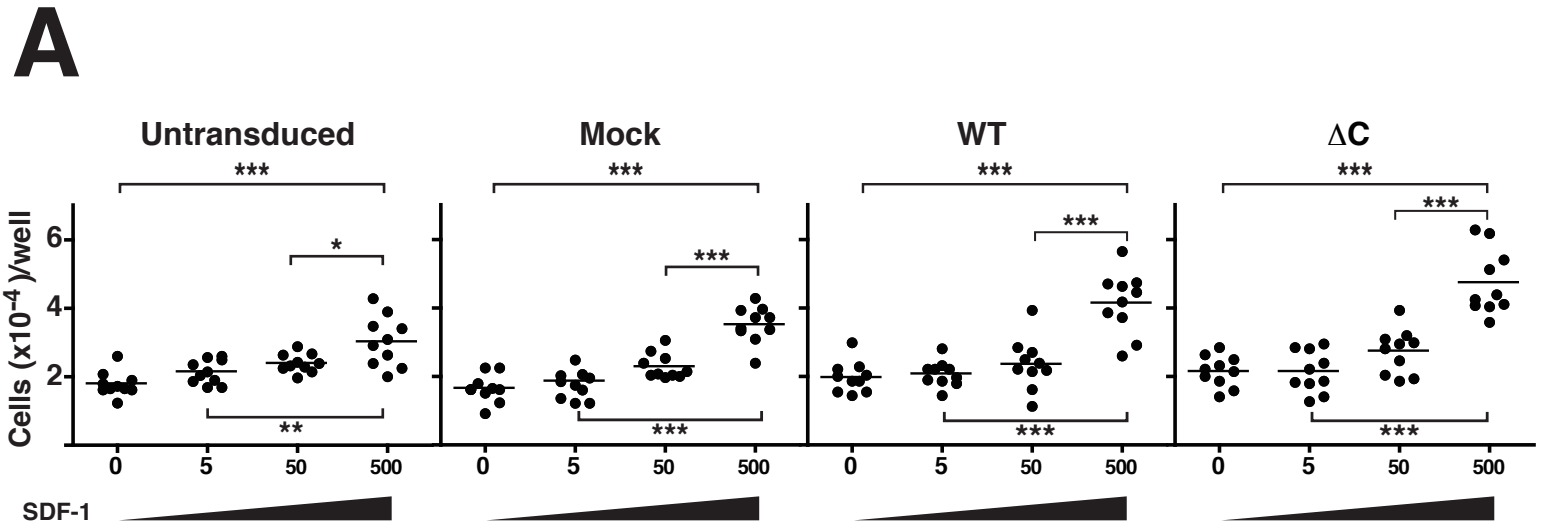
A
Untransduced
Mock
WT
ΔC
Cells (x10⁻⁴)/well
SDF-1
0
5
50
500

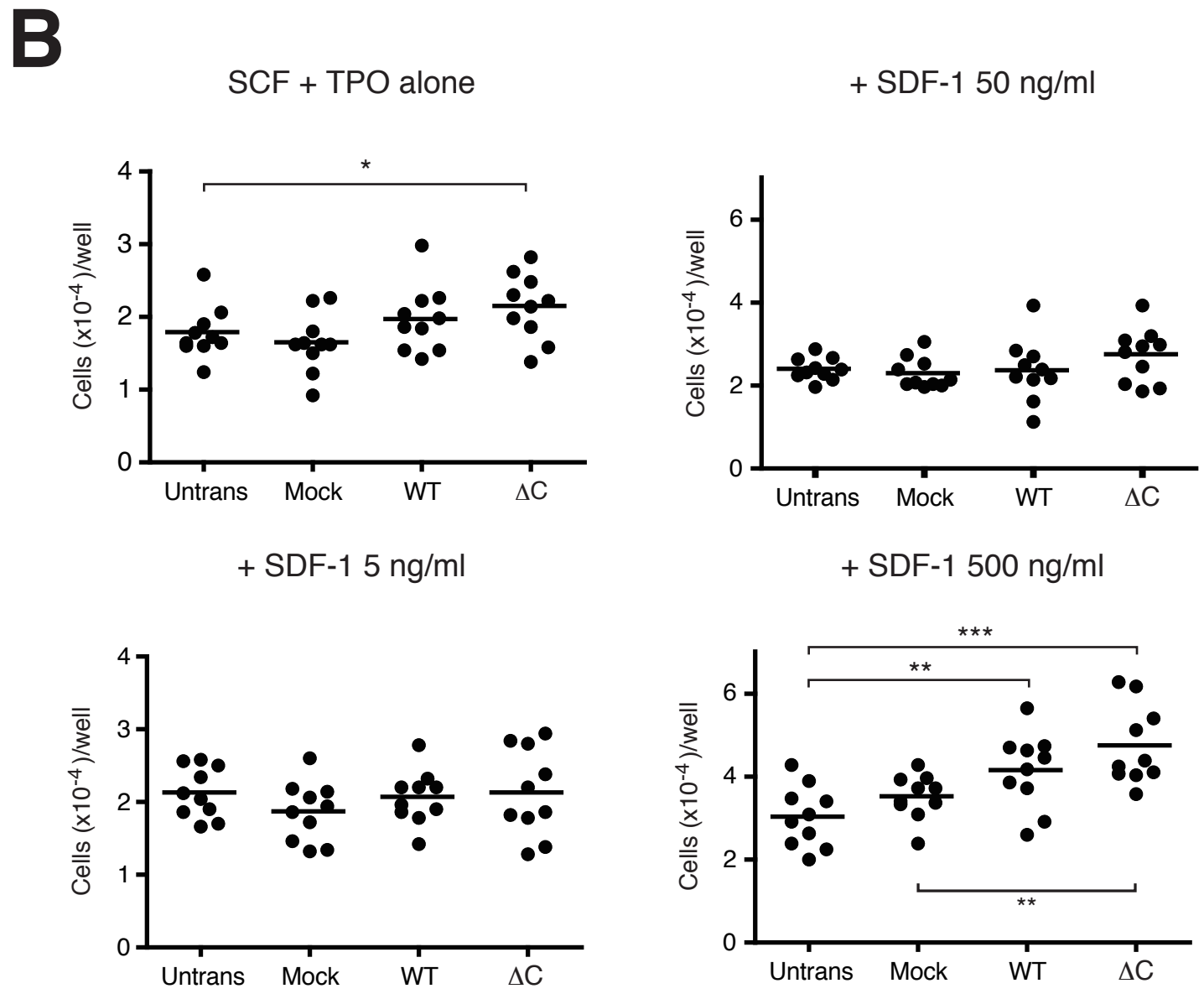
B
SCF + TPO alone
+ SDF-1 50 ng/ml
+ SDF-1 5 ng/ml
+ SDF-1 500 ng/ml
Cells (x10⁻⁴)/well
Untrans
Mock
WT
ΔC

A

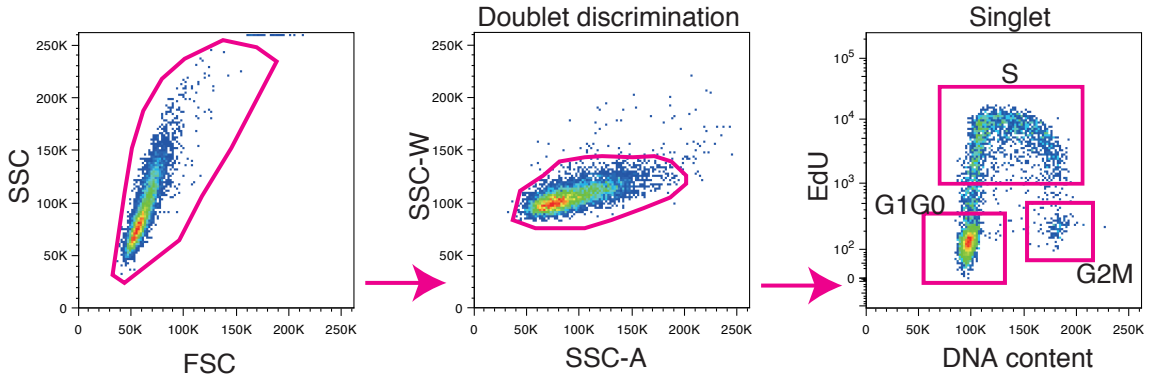
Doublet discrimination
Singlet
SSC
FSC
SSC-W
SSC-A
EdU
DNA content
S
G1G0
G2M
0
50K
100K
150K
200K
250K

B

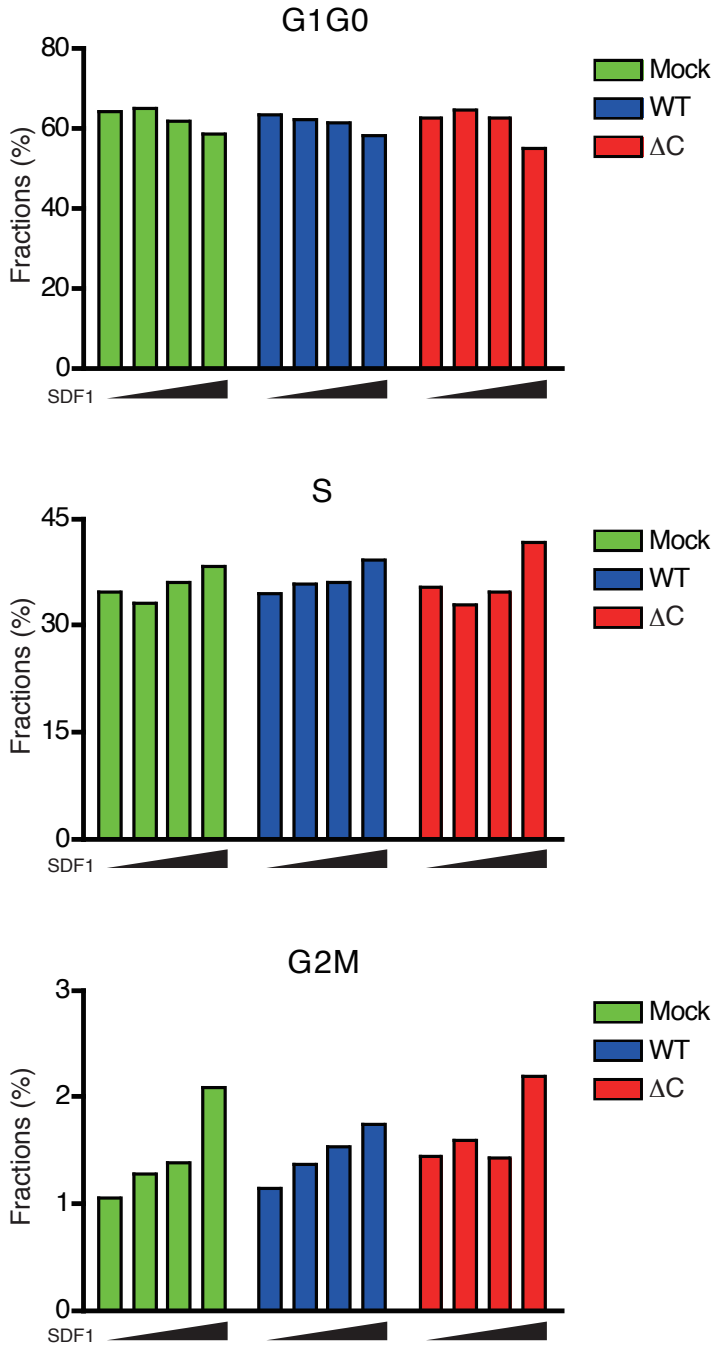
G1G0
S
G2M
Fractions (%)
SDF1
Mock
WT
ΔC

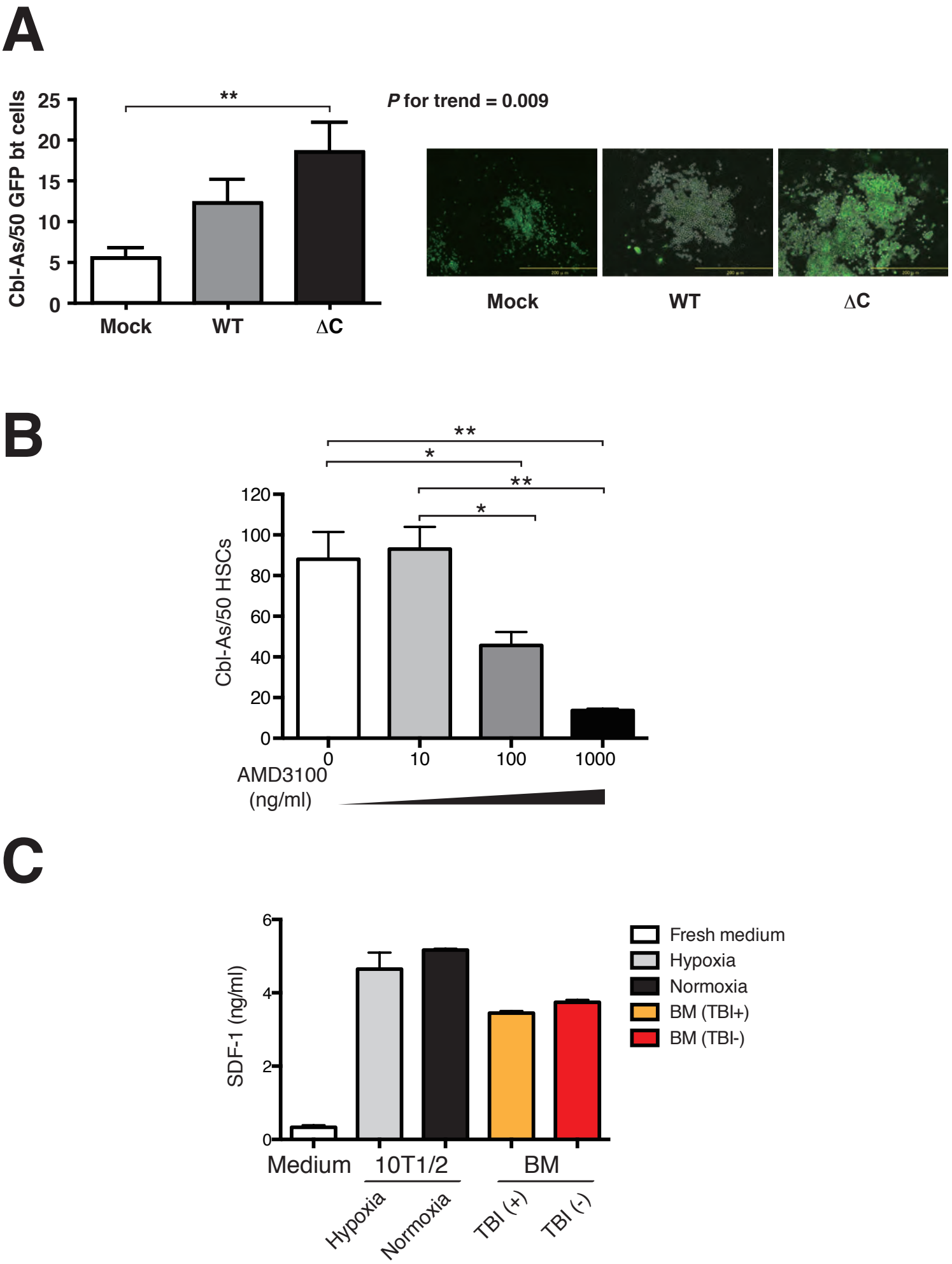
A
Cbl-As/50 GFP bt cells
25
20
15
10
5
0
**
P for trend = 0.009
Mock
WT
ΔC
Mock
WT
ΔC
B
Cbl-As/50 HSCs
120
100
80
60
40
20
0
**
*
**
*
0
10
100
1000
AMD3100
(ng/ml)
C
SDF-1 (ng/ml)
6
4
2
0
Medium
10T1/2
BM
Hypoxia
Normoxia
TBI (+)
TBI (-)
Fresh medium
Hypoxia
Normoxia
BM (TBI+)
BM (TBI-)

Figure 18

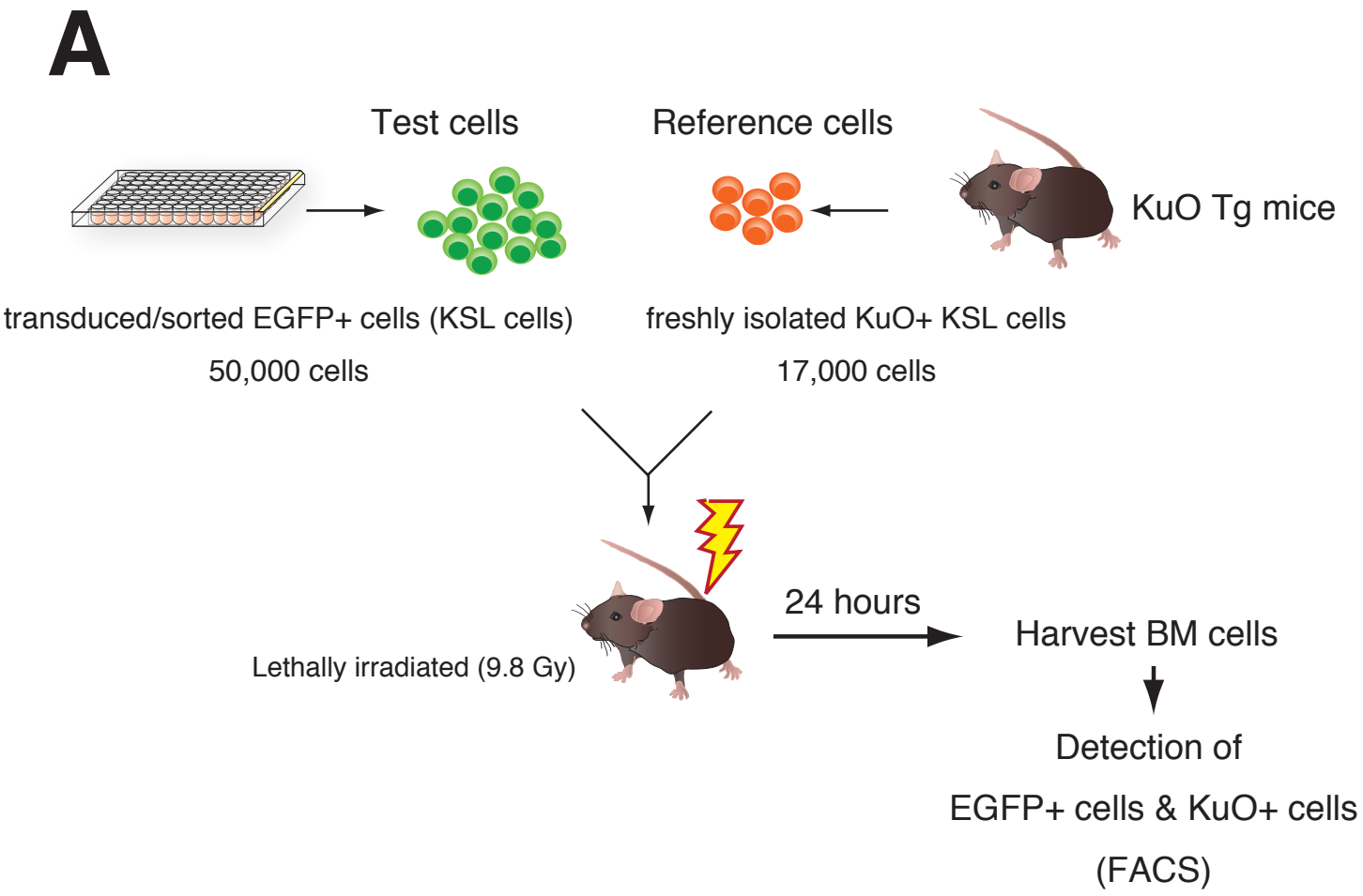
A
Test cells
Reference cells
KuO Tg mice
transduced/sorted EGFP+ cells (KSL cells)
50,000 cells
freshly isolated KuO+ KSL cells
17,000 cells
Lethally irradiated (9.8 Gy)
24 hours
Harvest BM cells
Detection of
EGFP+ cells & KuO+ cells
(FACS)

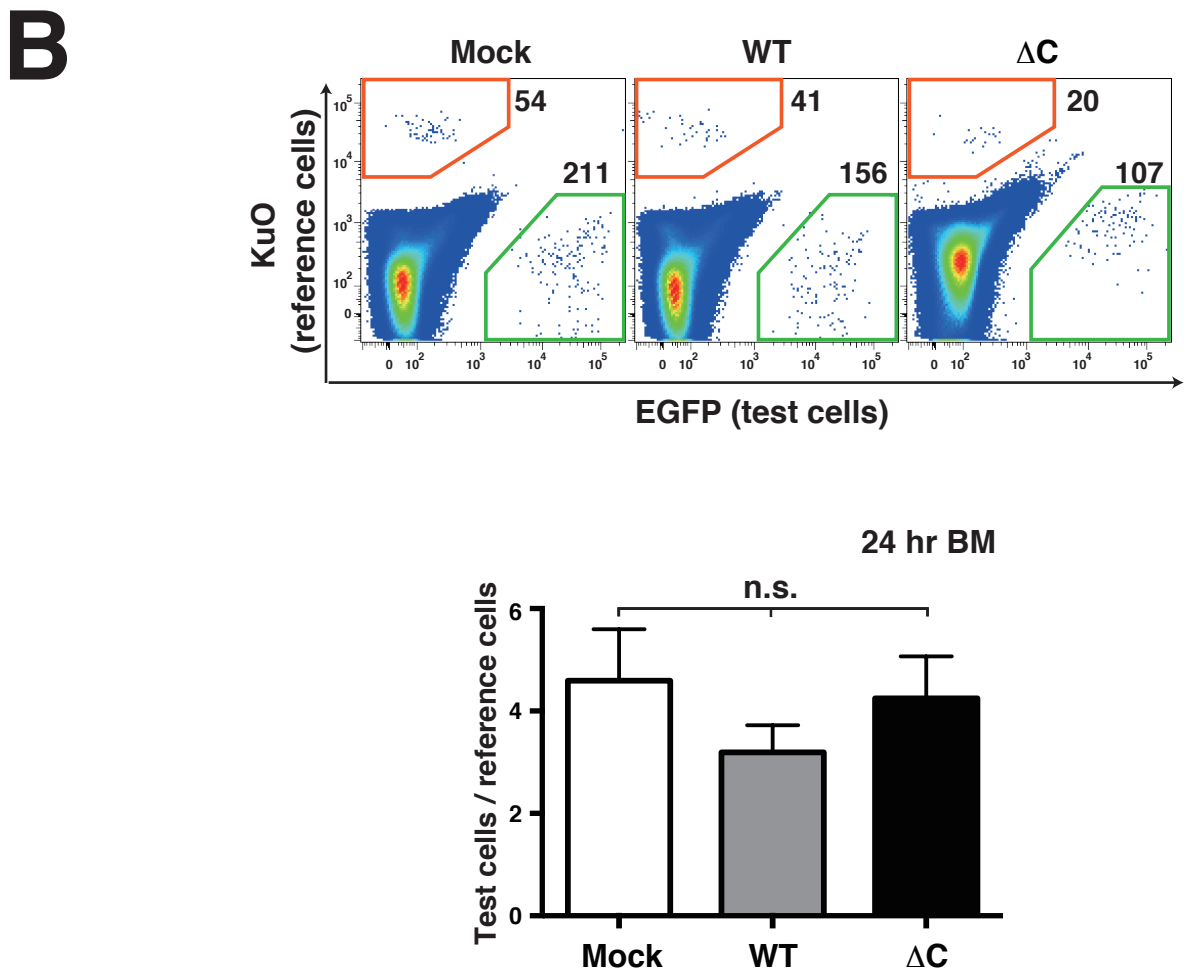
B
Mock
WT
ΔC
54
211
41
156
20
107
KuO
(reference cells)
EGFP (test cells)
24 hr BM
n.s.
Test cells / reference cells
Mock
WT
ΔC

Figure 19

A

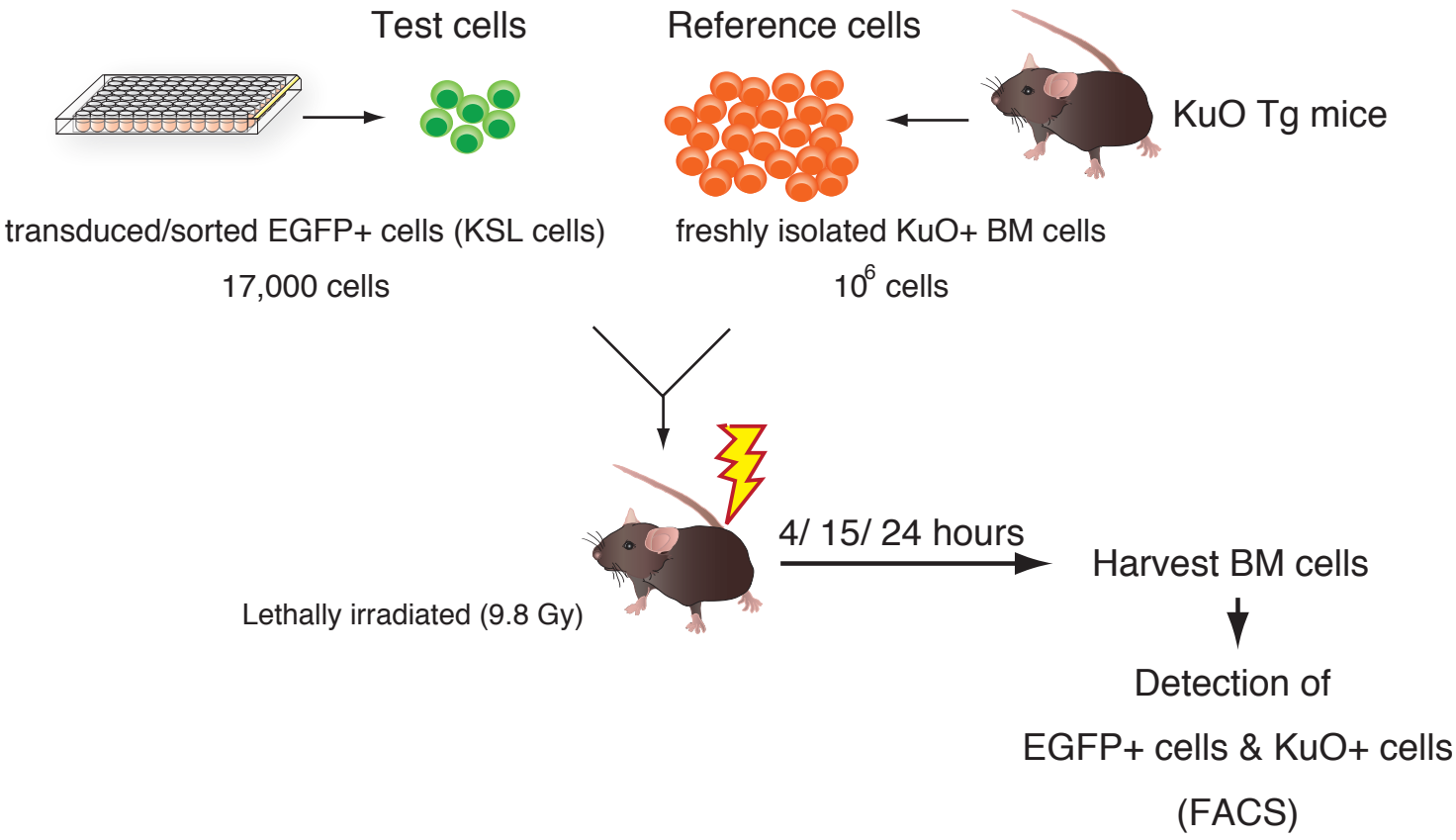
Test cells
Reference cells
KuO Tg mice
transduced/sorted EGFP+ cells (KSL cells)
17,000 cells
freshly isolated KuO+ BM cells
10^6 cells
Lethally irradiated (9.8 Gy)
4/ 15/ 24 hours
Harvest BM cells
Detection of
EGFP+ cells & KuO+ cells
(FACS)

B

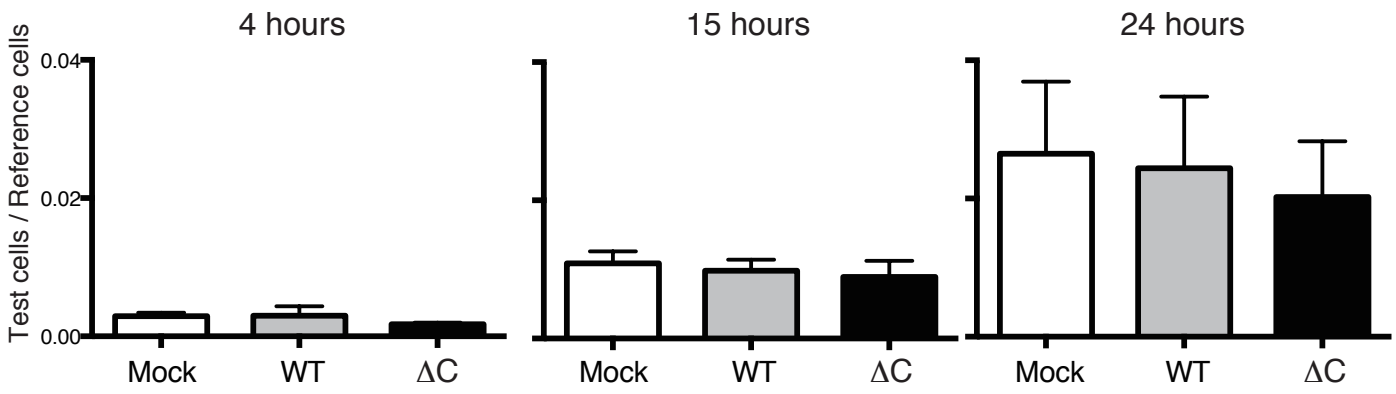
4 hours
15 hours
24 hours
Test cells / Reference cells
0.04
0.02
0.00
Mock
WT
ΔC
Mock
WT
ΔC
Mock
WT
ΔC

Figure 20

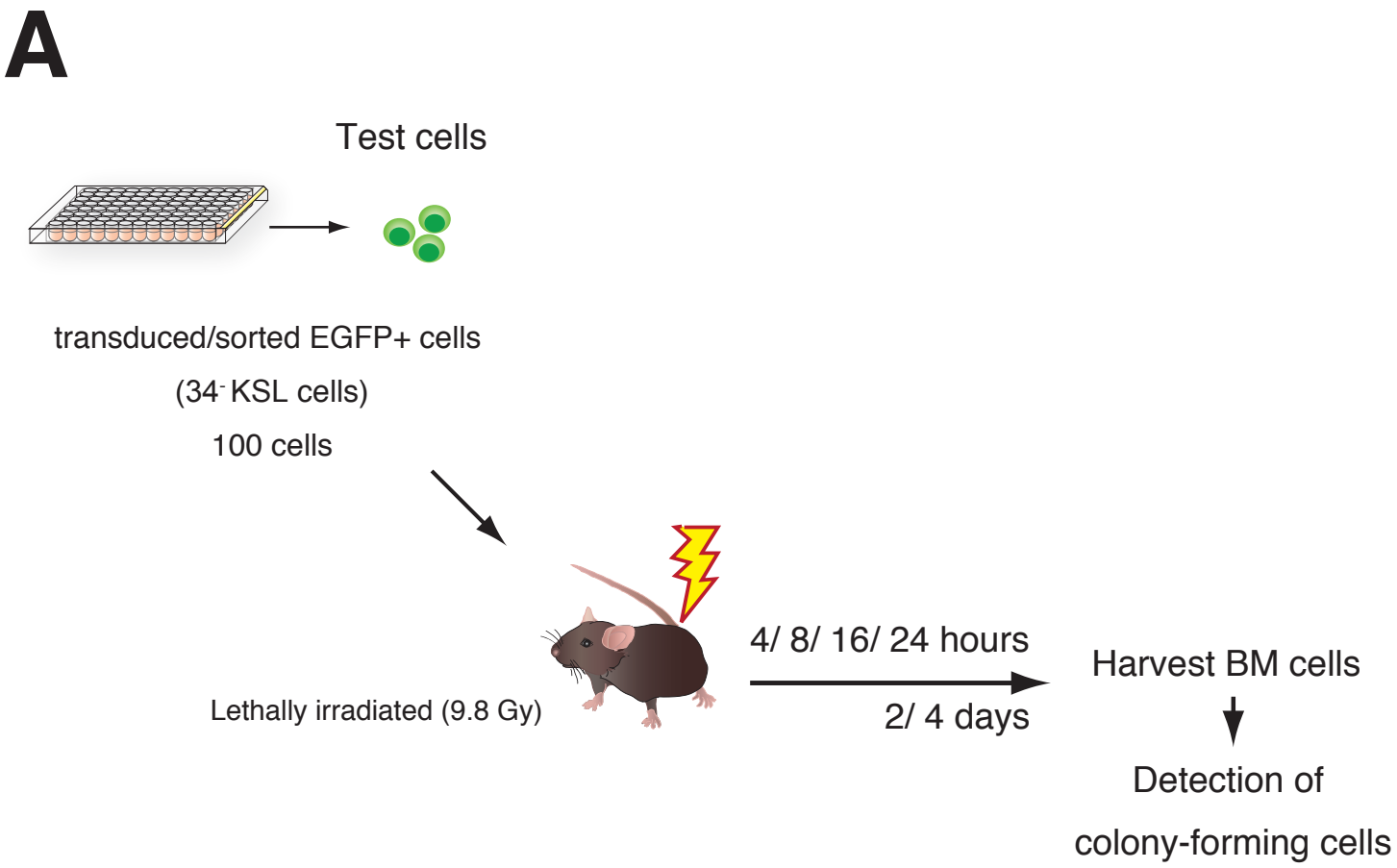
A
Test cells
transduced/sorted EGFP+ cells
(34- KSL cells)
100 cells
Lethally irradiated (9.8 Gy)
4/ 8/ 16/ 24 hours
2/ 4 days
Harvest BM cells
Detection of
colony-forming cells

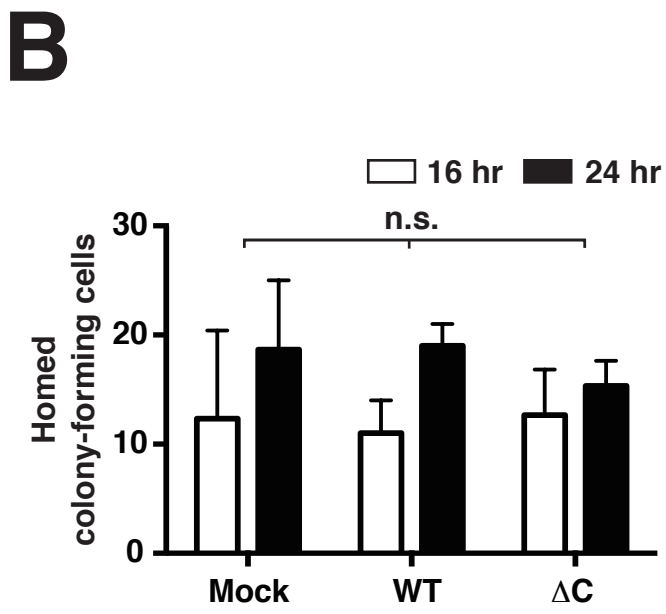
B
16 hr
24 hr
n.s.
Homed
colony-forming cells
30
20
10
0
Mock
WT
ΔC

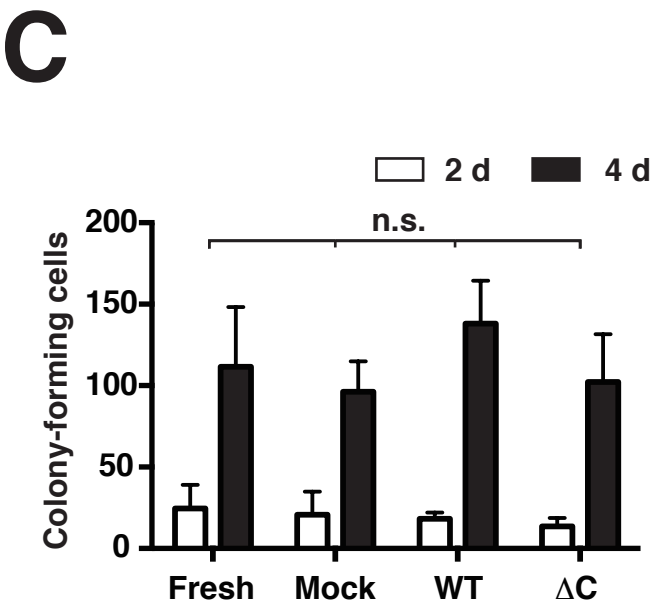
C
2 d
4 d
n.s.
Colony-forming cells
200
150
100
50
0
Fresh
Mock
WT
ΔC

A

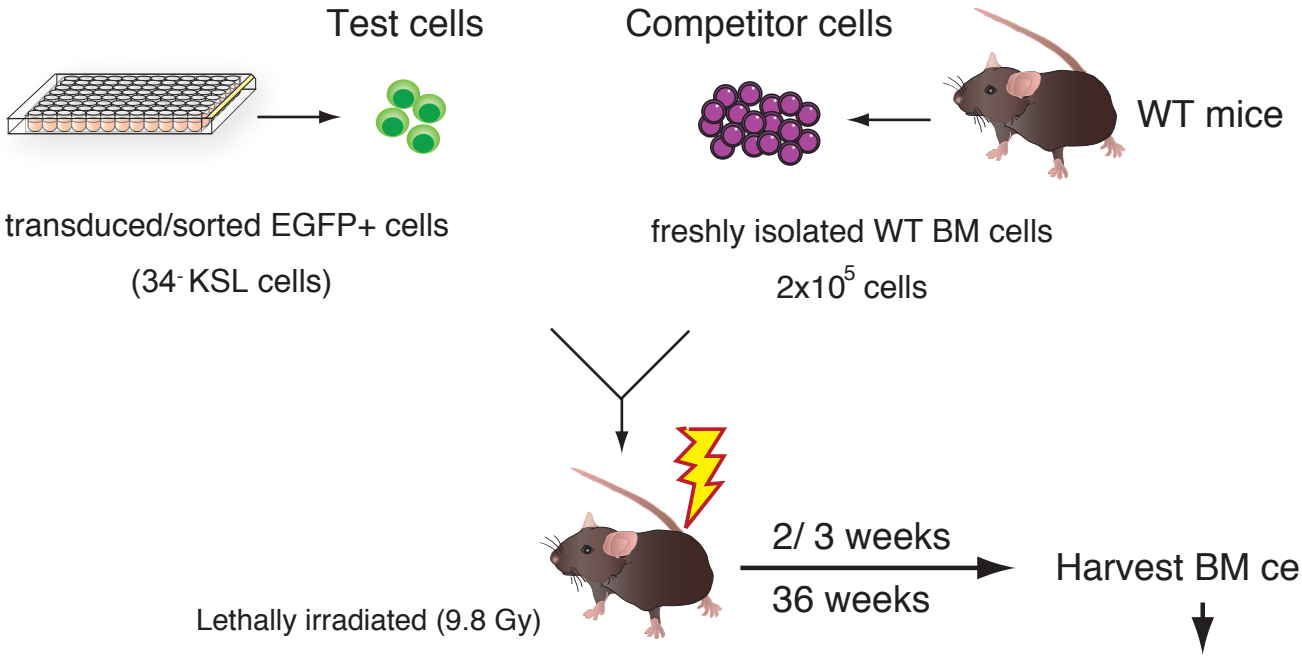
Test cells
Competitor cells
WT mice
transduced/sorted EGFP+ cells
(34- KSL cells)
freshly isolated WT BM cells
2x10^5 cells
Lethally irradiated (9.8 Gy)
2/ 3 weeks
36 weeks
Harvest BM cells
Detection of
donor cells
(FACS)

B

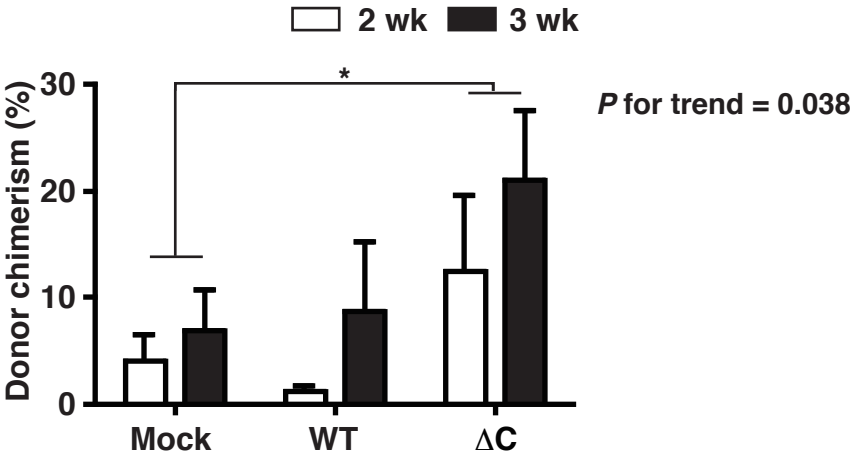
2 wk
3 wk
Donor chimerism (%)
30
20
10
0
*
P for trend = 0.038
Mock
WT
ΔC

C

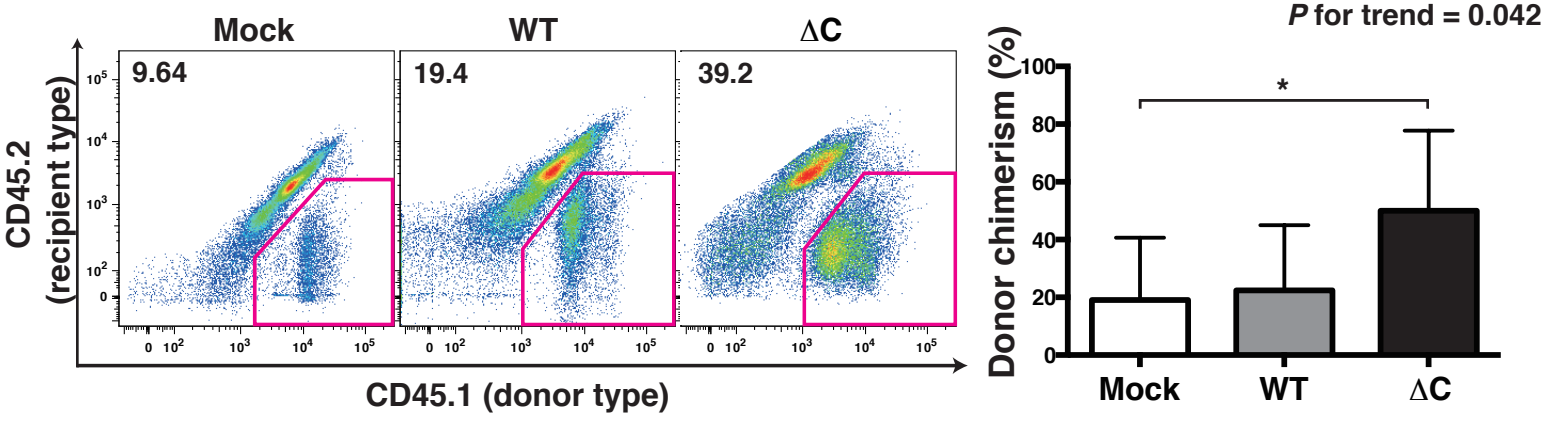
Mock
WT
ΔC
9.64
19.4
39.2
CD45.2
(recipient type)
CD45.1 (donor type)
36 wk BM
P for trend = 0.042
Donor chimerism (%)
100
80
60
40
20
0
*
Mock
WT
ΔC

Figure 22

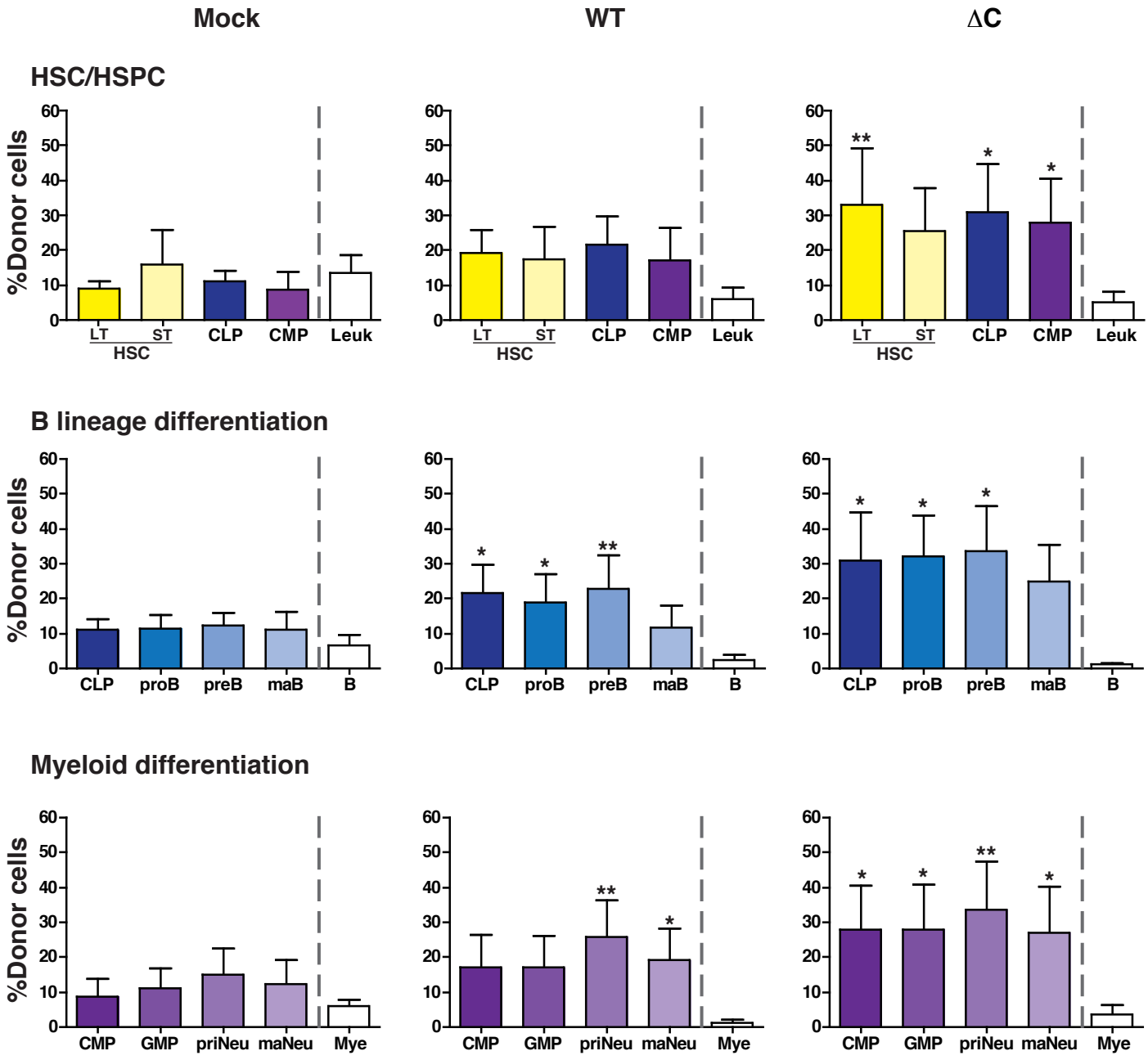
Mock
WT
ΔC
HSC/HSPC
%Donor cells
LT
ST
HSC
CLP
CMP
Leuk
B lineage differentiation
proB
preB
maB
B
Myeloid differentiation
GMP
priNeu
maNeu
Mye

Figure 23

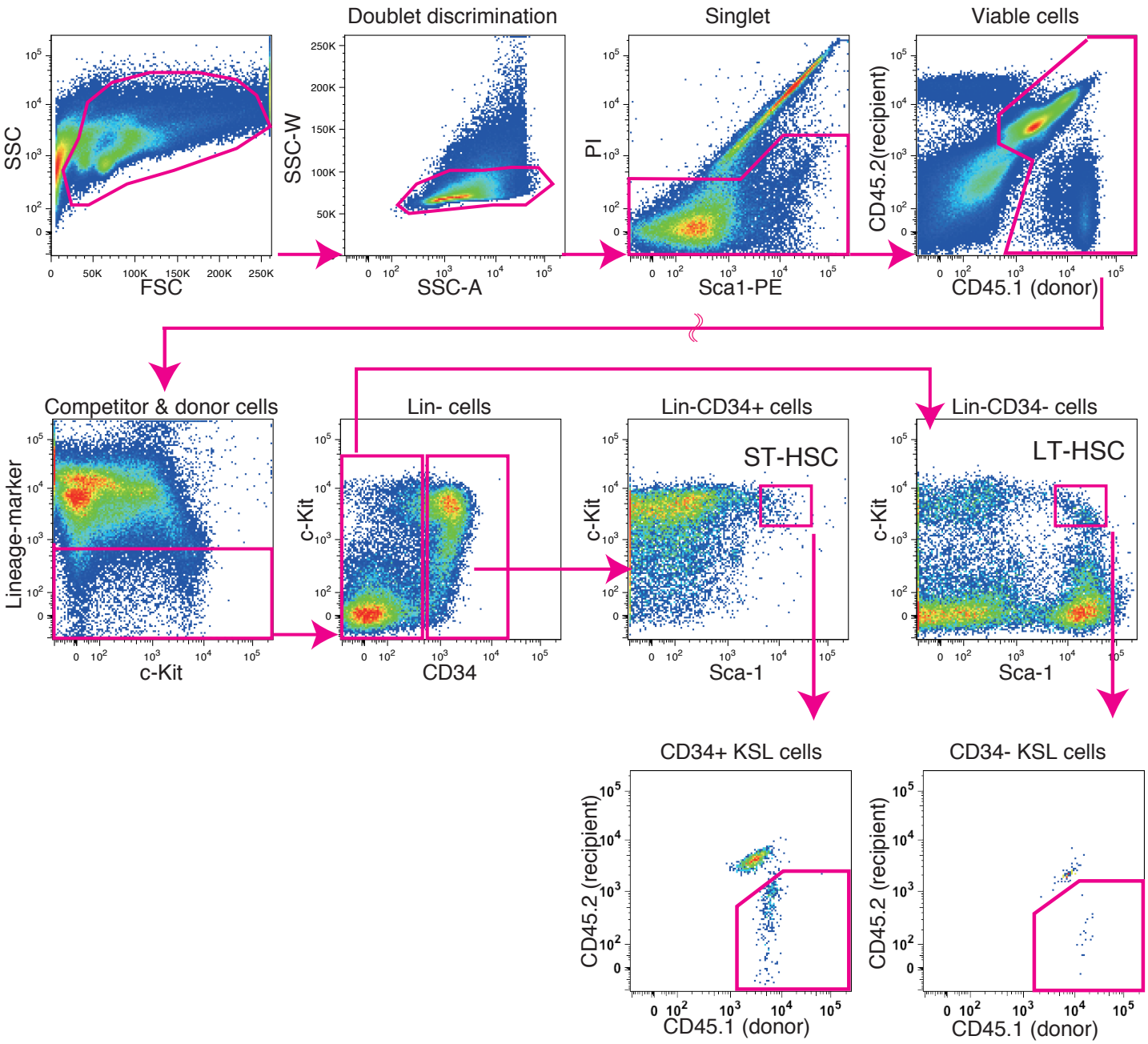
Doublet discrimination
Singlet
Viable cells
SSC
FSC
SSC-W
SSC-A
PI
Sca1-PE
CD45.2(recipient)
CD45.1 (donor)
Competitor & donor cells
Lineage-marker
c-Kit
Lin- cells
CD34
Lin-CD34+ cells
ST-HSC
Sca-1
Lin-CD34- cells
LT-HSC
CD34+ KSL cells
CD34- KSL cells

Figure 24

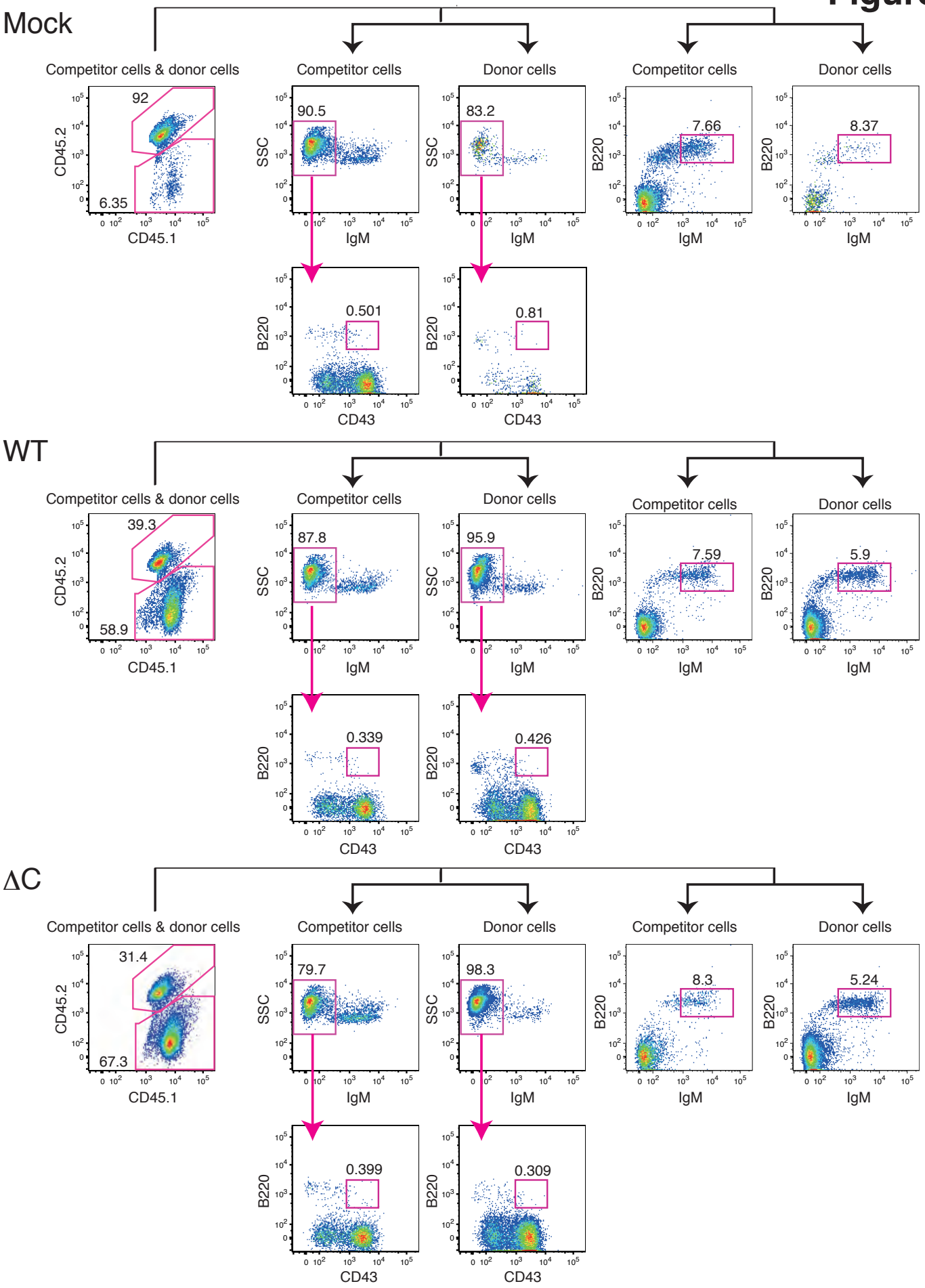
Mock
Competitor cells & donor cells
92
6.35
CD45.2
CD45.1
Competitor cells
90.5
SSC
IgM
0.501
B220
CD43
Donor cells
83.2
SSC
IgM
0.81
B220
CD43
Competitor cells
7.66
B220
IgM
Donor cells
8.37
B220
IgM
WT
Competitor cells & donor cells
39.3
58.9
CD45.2
CD45.1
Competitor cells
87.8
SSC
IgM
0.339
B220
CD43
Donor cells
95.9
SSC
IgM
0.426
B220
CD43
Competitor cells
7.59
B220
IgM
Donor cells
5.9
B220
IgM
ΔC
Competitor cells & donor cells
31.4
67.3
CD45.2
CD45.1
Competitor cells
79.7
SSC
IgM
0.399
B220
CD43
Donor cells
98.3
SSC
IgM
0.309
B220
CD43
Competitor cells
8.3
B220
IgM
Donor cells
5.24
B220
IgM

Figure 25

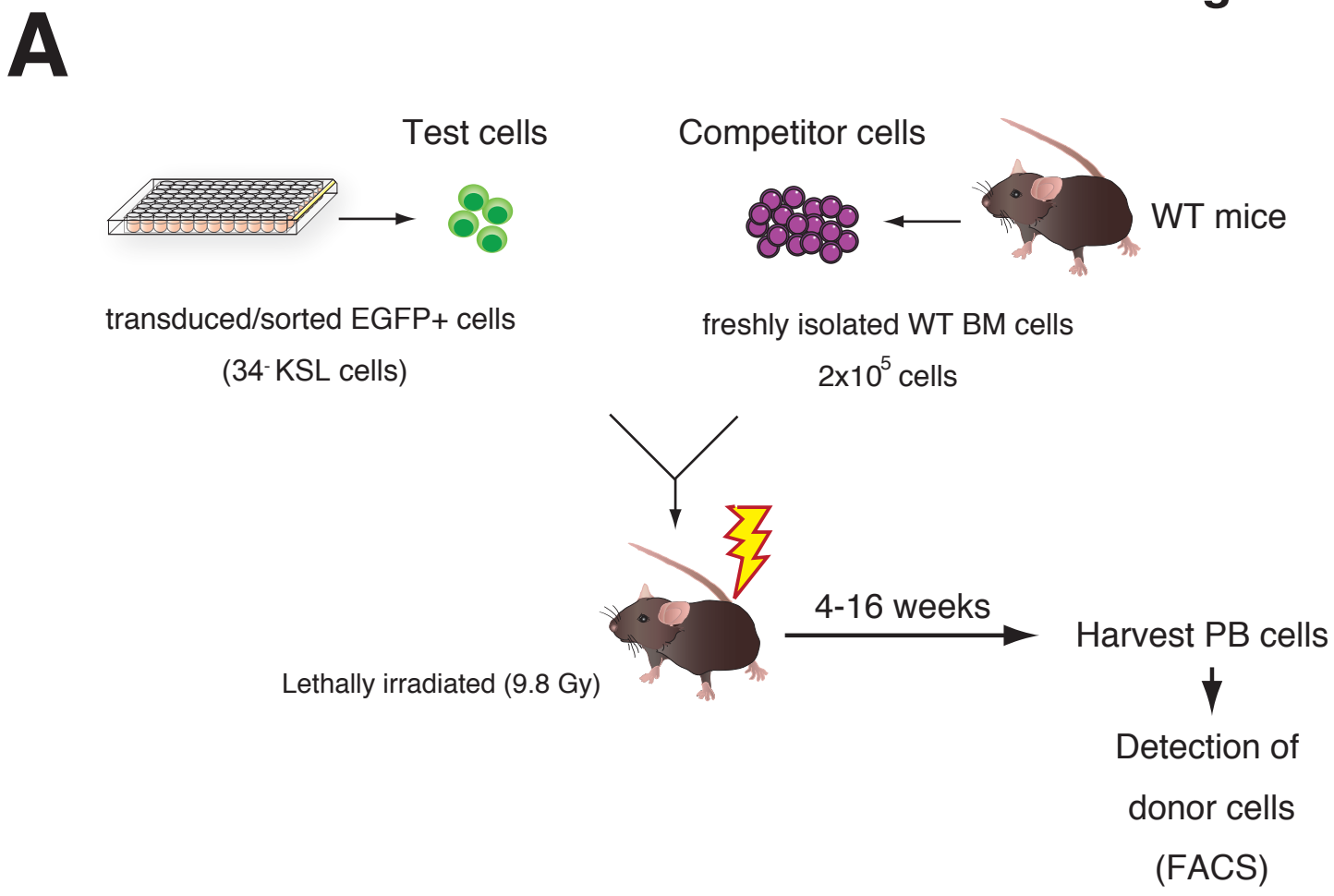
A
Test cells
Competitor cells
WT mice
transduced/sorted EGFP+ cells
(34- KSL cells)
freshly isolated WT BM cells
2x10^5 cells
Lethally irradiated (9.8 Gy)
4-16 weeks
Harvest PB cells
Detection of
donor cells
(FACS)

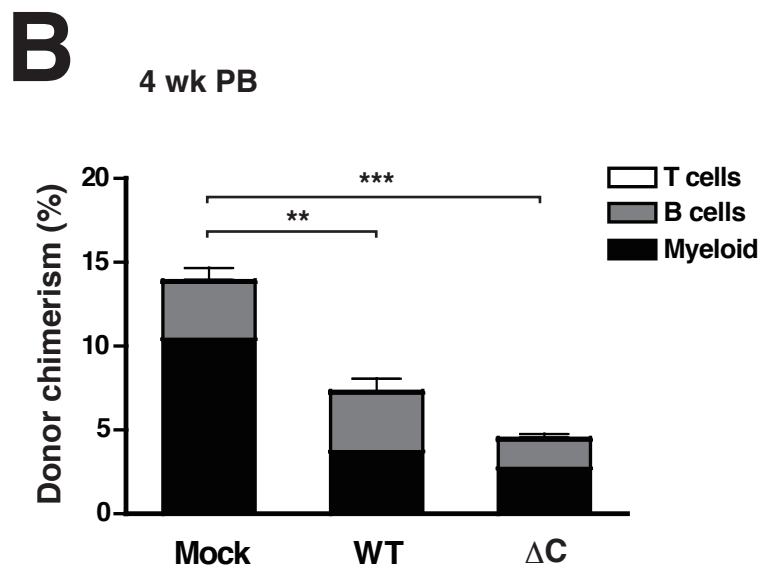
B
4 wk PB
Donor chimerism (%)
20
15
10
5
0
***
**
T cells
B cells
Myeloid
Mock
WT
ΔC

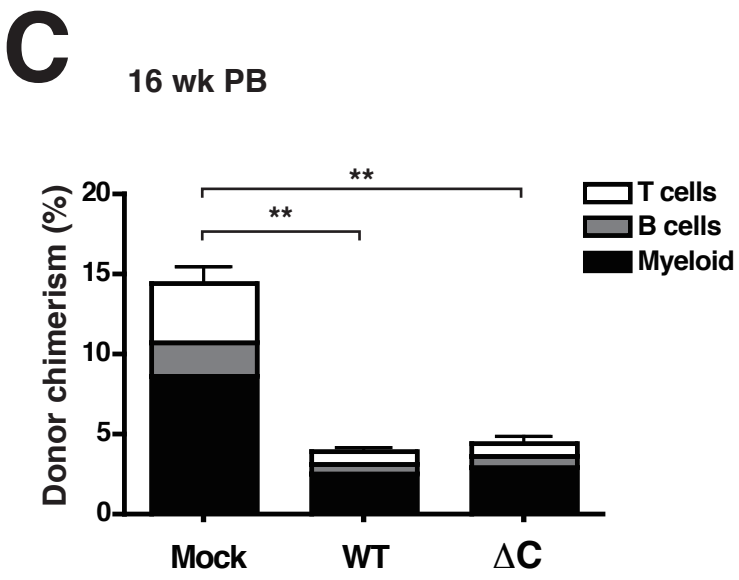
C
16 wk PB
Donor chimerism (%)
20
15
10
5
0
**
**
T cells
B cells
Myeloid
Mock
WT
ΔC

Figure 26

A

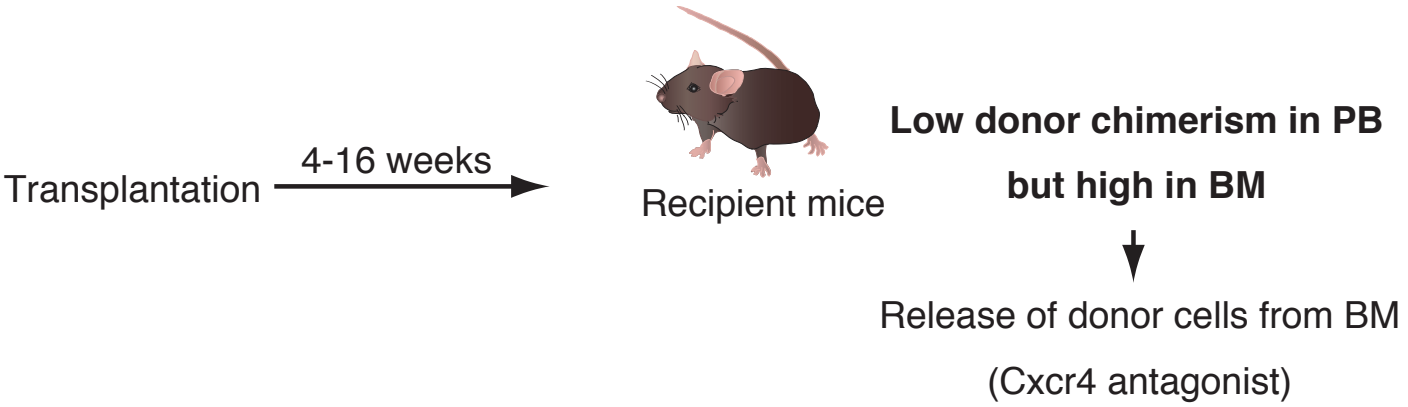

B

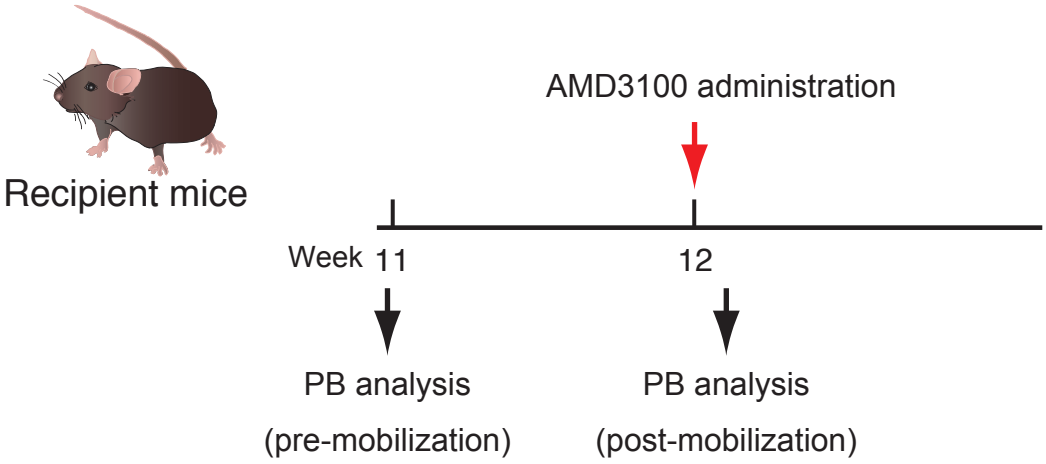

C

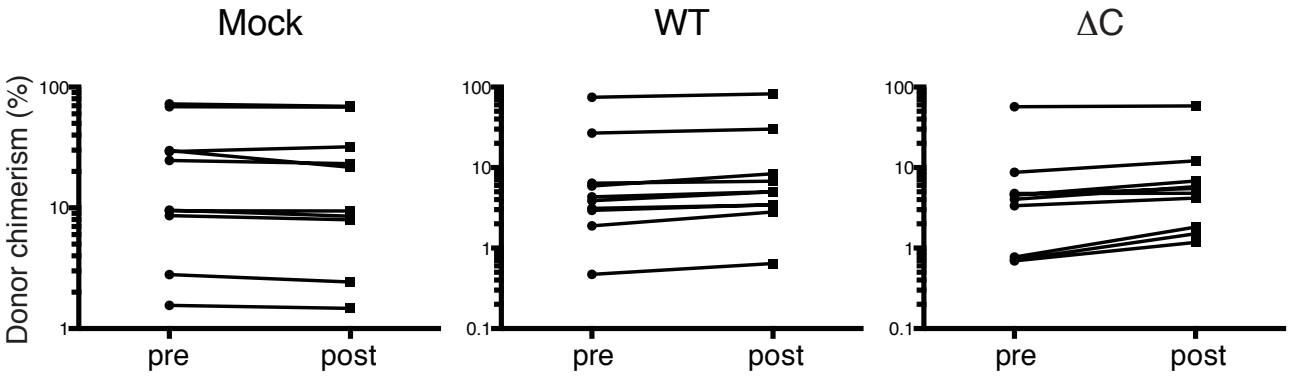

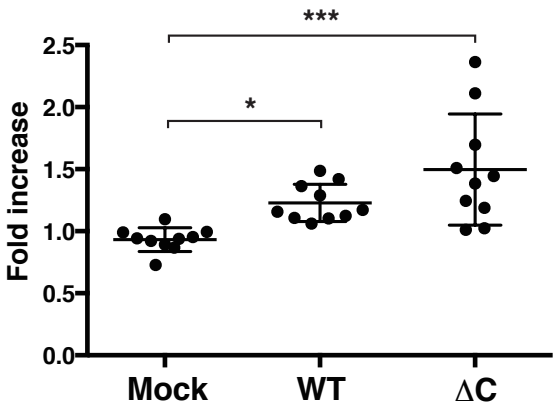

Figure 27

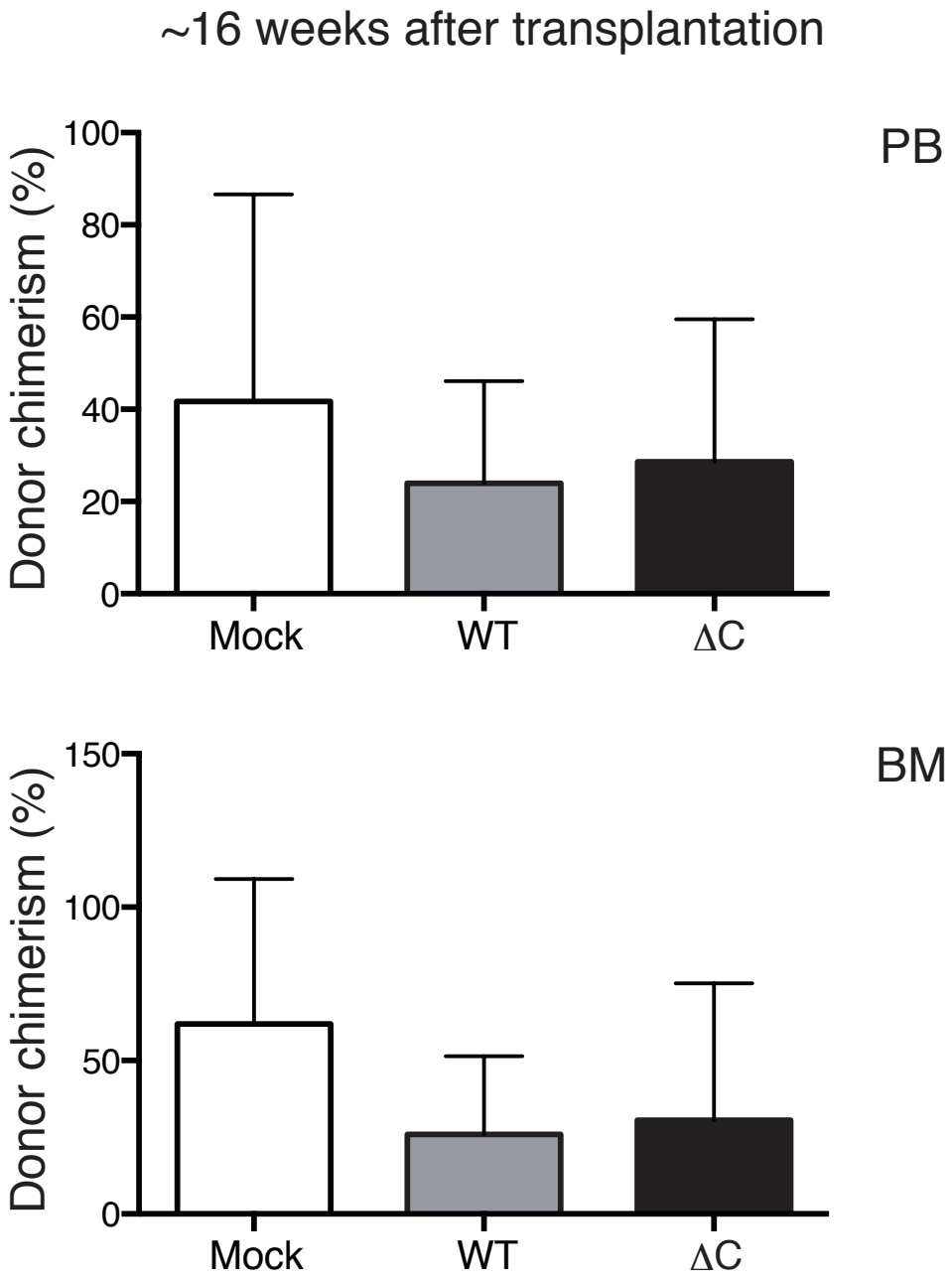
~16 weeks after transplantation
PB
Donor chimerism (%)
100
80
60
40
20
0
Mock
WT
ΔC
BM
Donor chimerism (%)
150
100
50
0
Mock
WT
ΔC

Figure 28

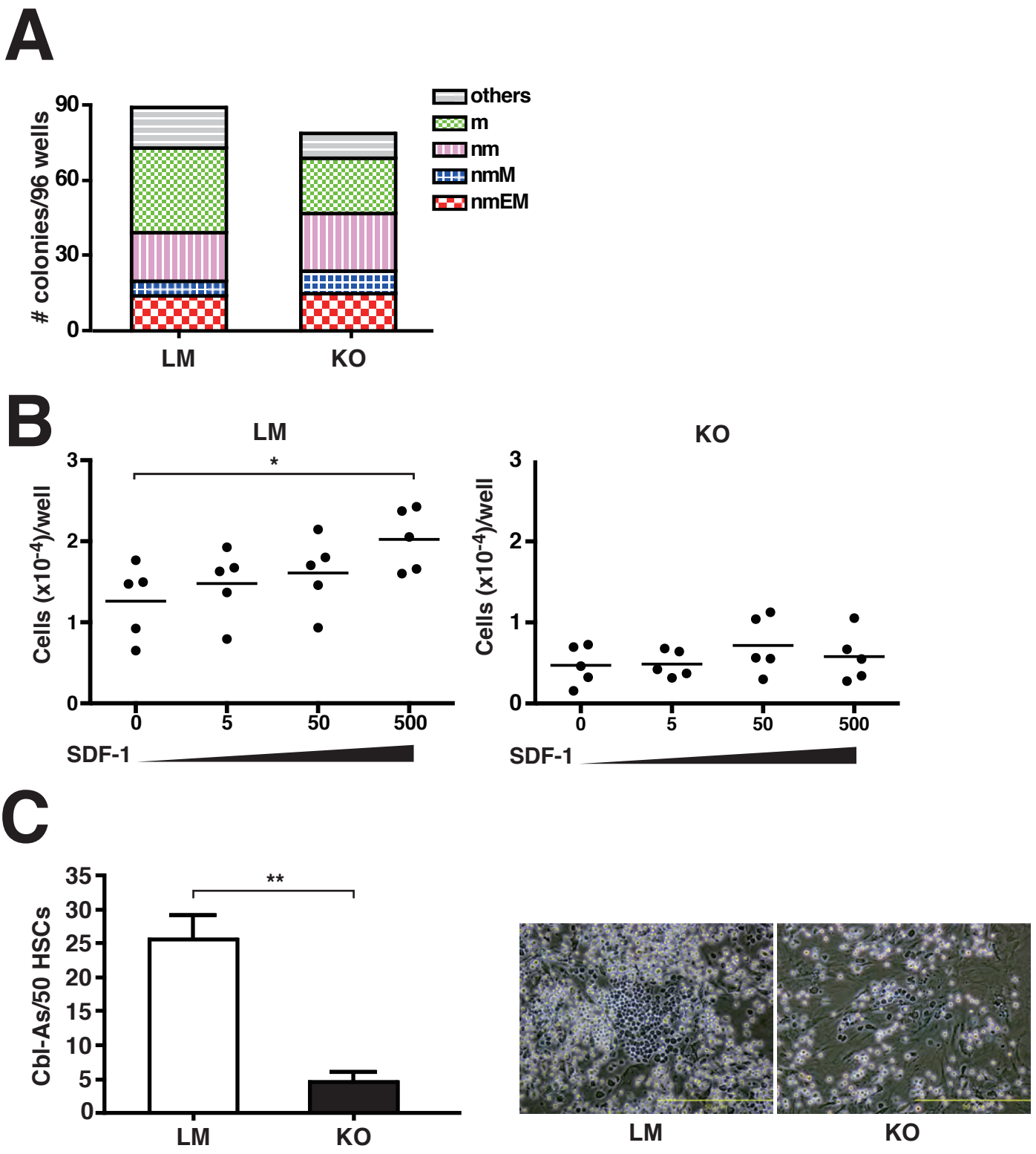
A
colonies/96 wells
90
60
30
0
LM
KO
others
m
nm
nmM
nmEM
B
LM
KO
Cells (x10-4)/well
3
2
1
0
*
0
5
50
500
SDF-1
C
Cbl-As/50 HSCs
35
30
25
20
15
10
5
0
**
LM
KO

Figure 29

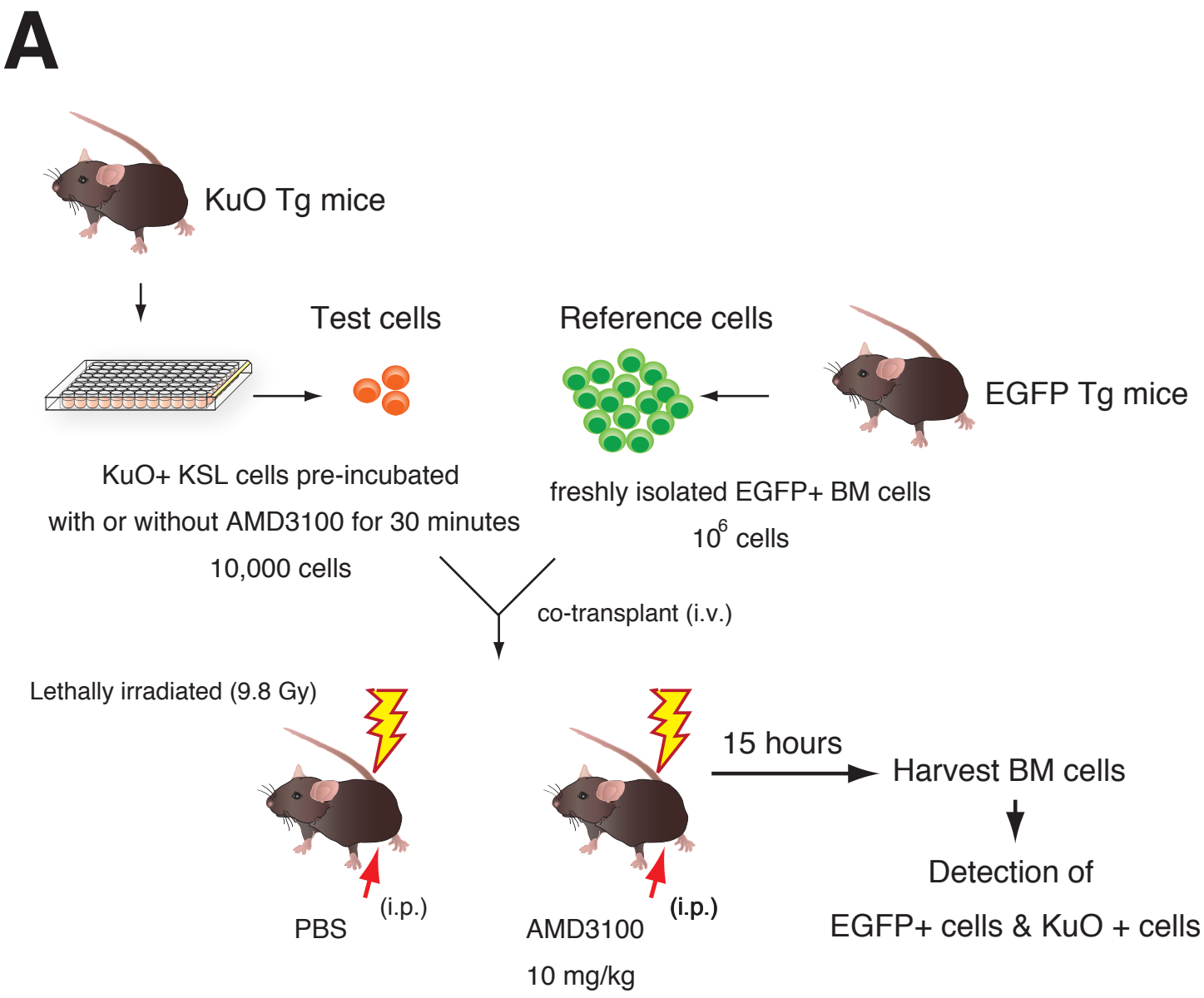
A
KuO Tg mice
Test cells
Reference cells
EGFP Tg mice
KuO+ KSL cells pre-incubated
with or without AMD3100 for 30 minutes
10,000 cells
freshly isolated EGFP+ BM cells
10^6 cells
co-transplant (i.v.)
Lethally irradiated (9.8 Gy)
15 hours
Harvest BM cells
Detection of
EGFP+ cells & KuO + cells
(i.p.)
PBS
(i.p.)
AMD3100
10 mg/kg

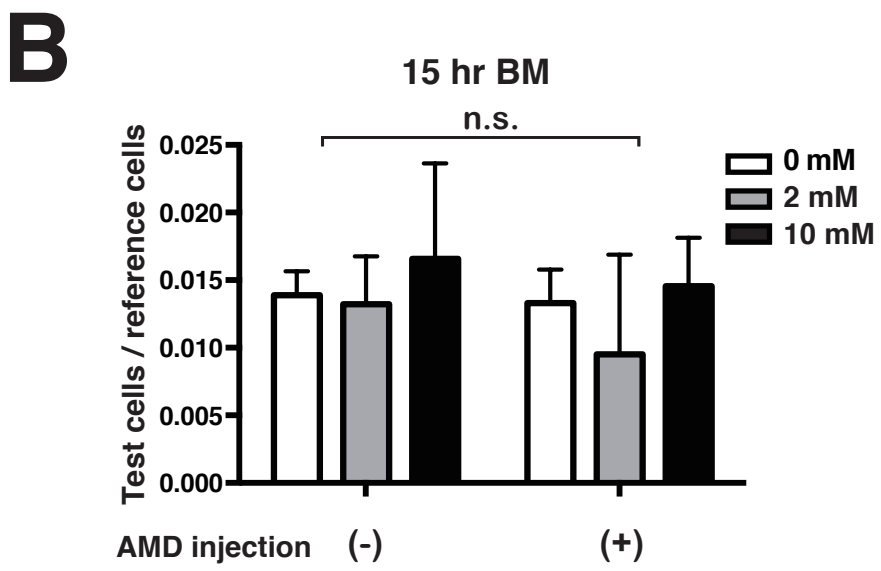
B
15 hr BM
n.s.
Test cells / reference cells
0.025
0.020
0.015
0.010
0.005
0.000
0 mM
2 mM
10 mM
AMD injection
(-)
(+)

Figure 30

A

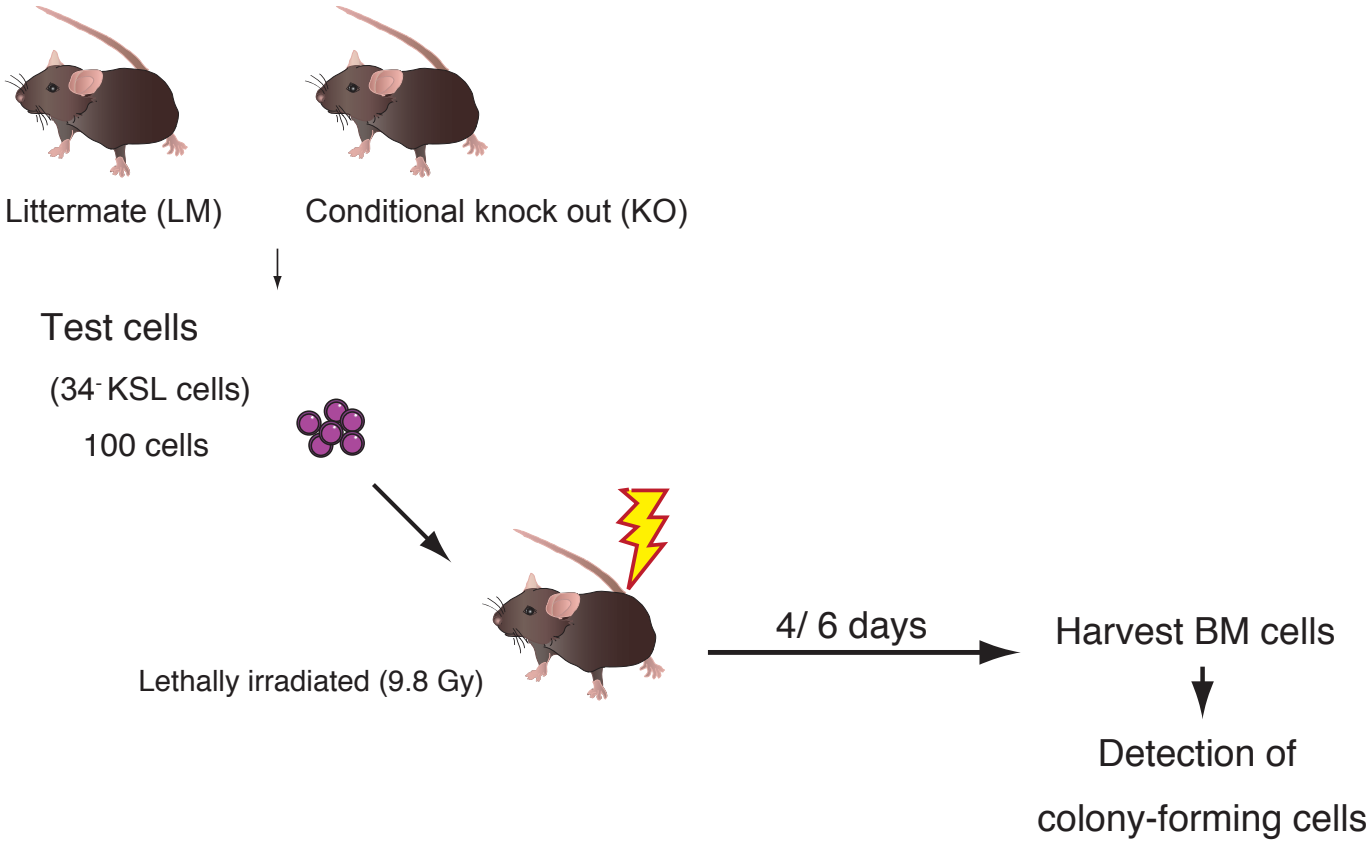
Littermate (LM)
Conditional knock out (KO)
Test cells
(34- KSL cells)
100 cells
Lethally irradiated (9.8 Gy)
4/ 6 days
Harvest BM cells
Detection of
colony-forming cells

B

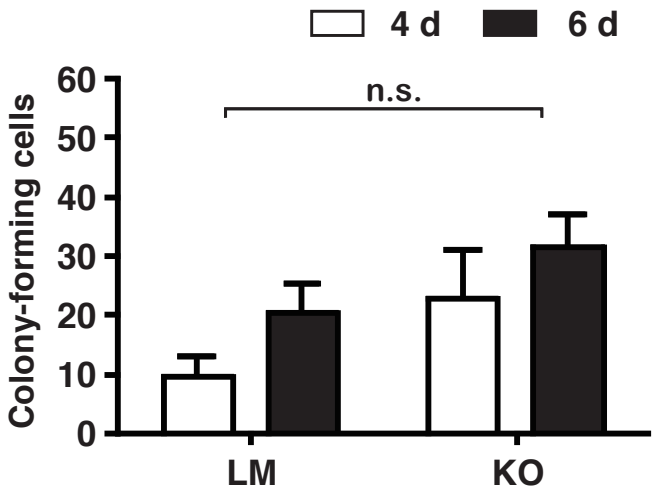
4 d
6 d
n.s.
Colony-forming cells
60
50
40
30
20
10
0
LM
KO

Figure 31

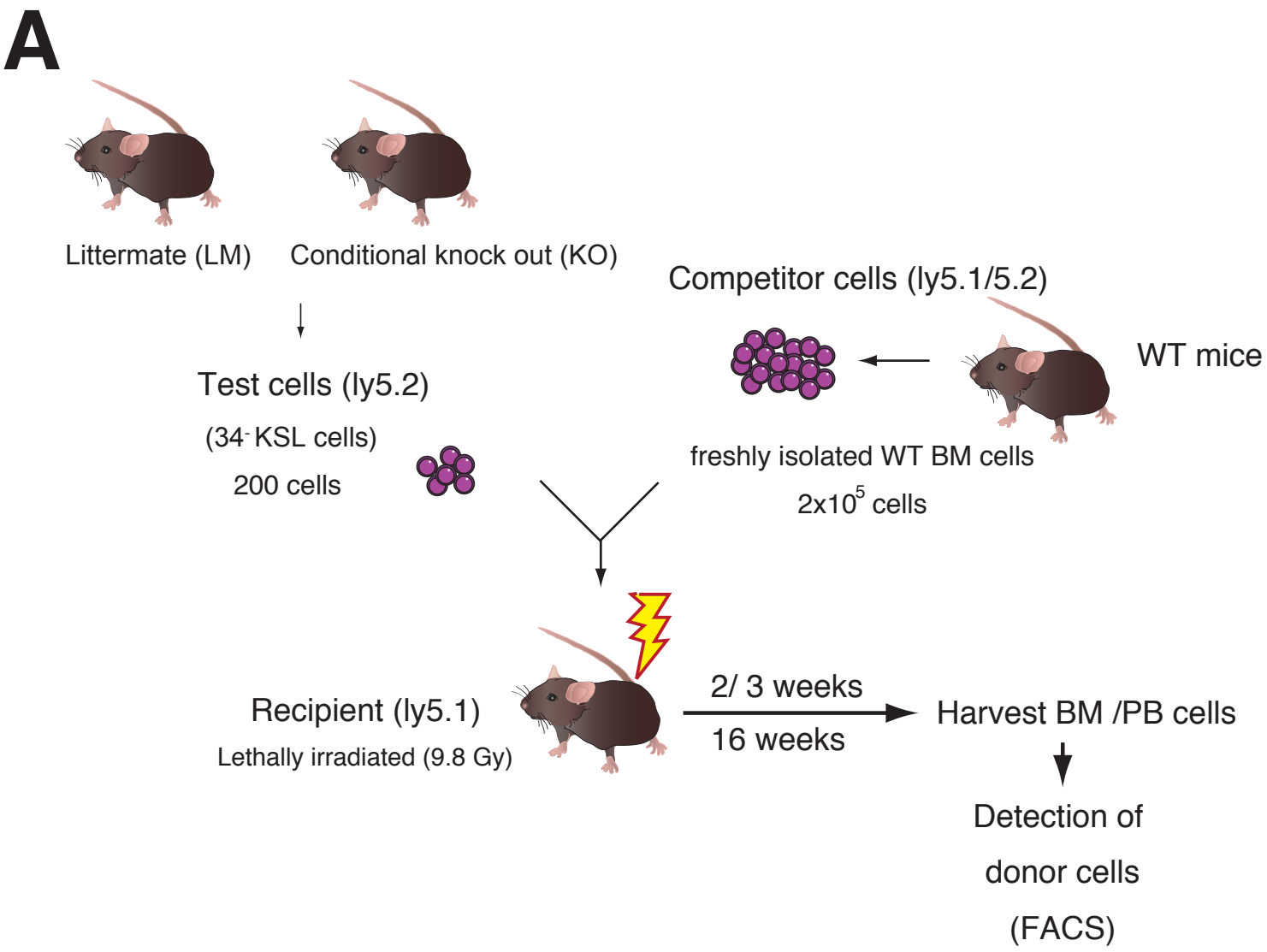
A
Littermate (LM)
Conditional knock out (KO)
Test cells (ly5.2)
(34- KSL cells)
200 cells
Competitor cells (ly5.1/5.2)
WT mice
freshly isolated WT BM cells
2x10^5 cells
Recipient (ly5.1)
Lethally irradiated (9.8 Gy)
2/ 3 weeks
16 weeks
Harvest BM /PB cells
Detection of
donor cells
(FACS)

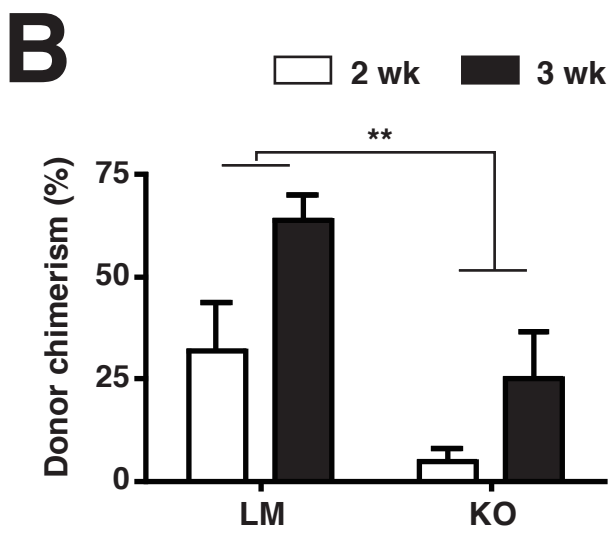
B
2 wk
3 wk
**
Donor chimerism (%)
75
50
25
0
LM
KO

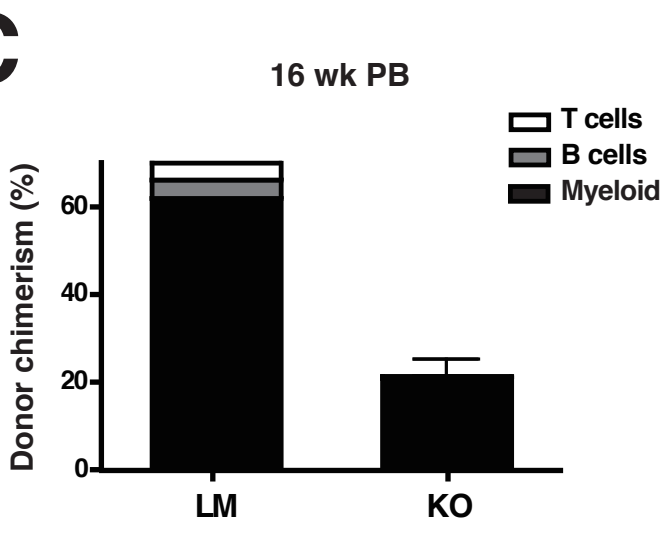
C
16 wk PB
T cells
B cells
Myeloid
Donor chimerism (%)
60
40
20
0
LM
KO

Figure 32

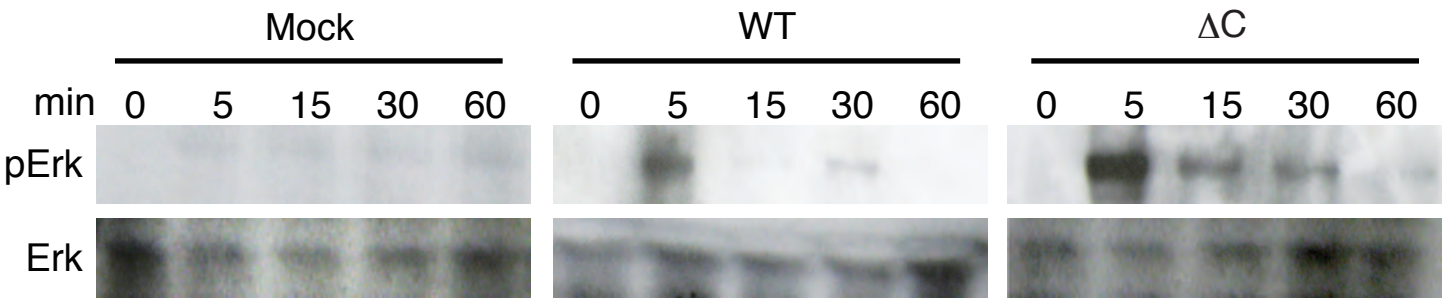

Figure 33

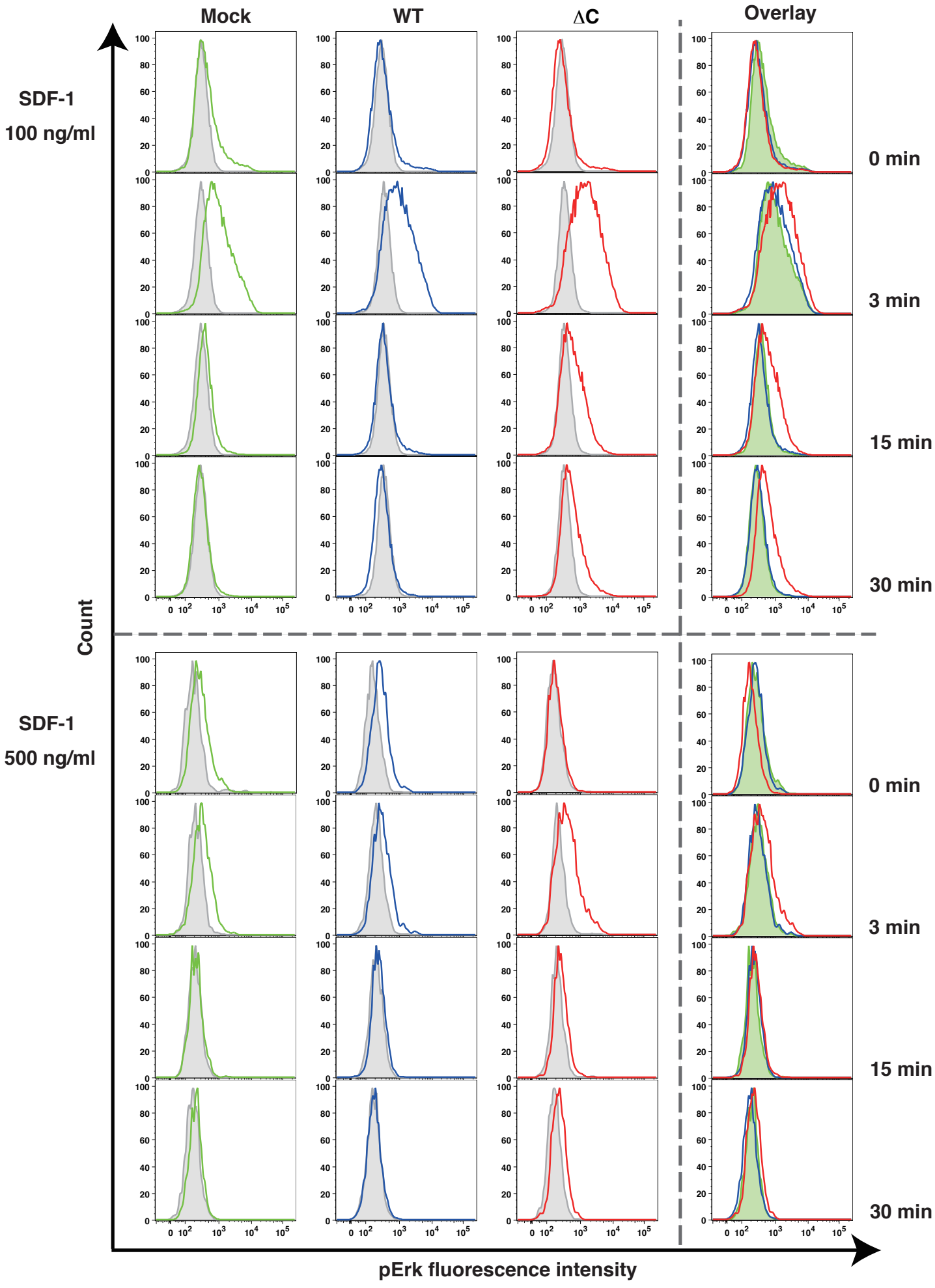
Mock
WT
ΔC
Overlay
SDF-1
100 ng/ml
SDF-1
500 ng/ml
0 min
3 min
15 min
30 min
Count
pErk fluorescence intensity

Figure 34

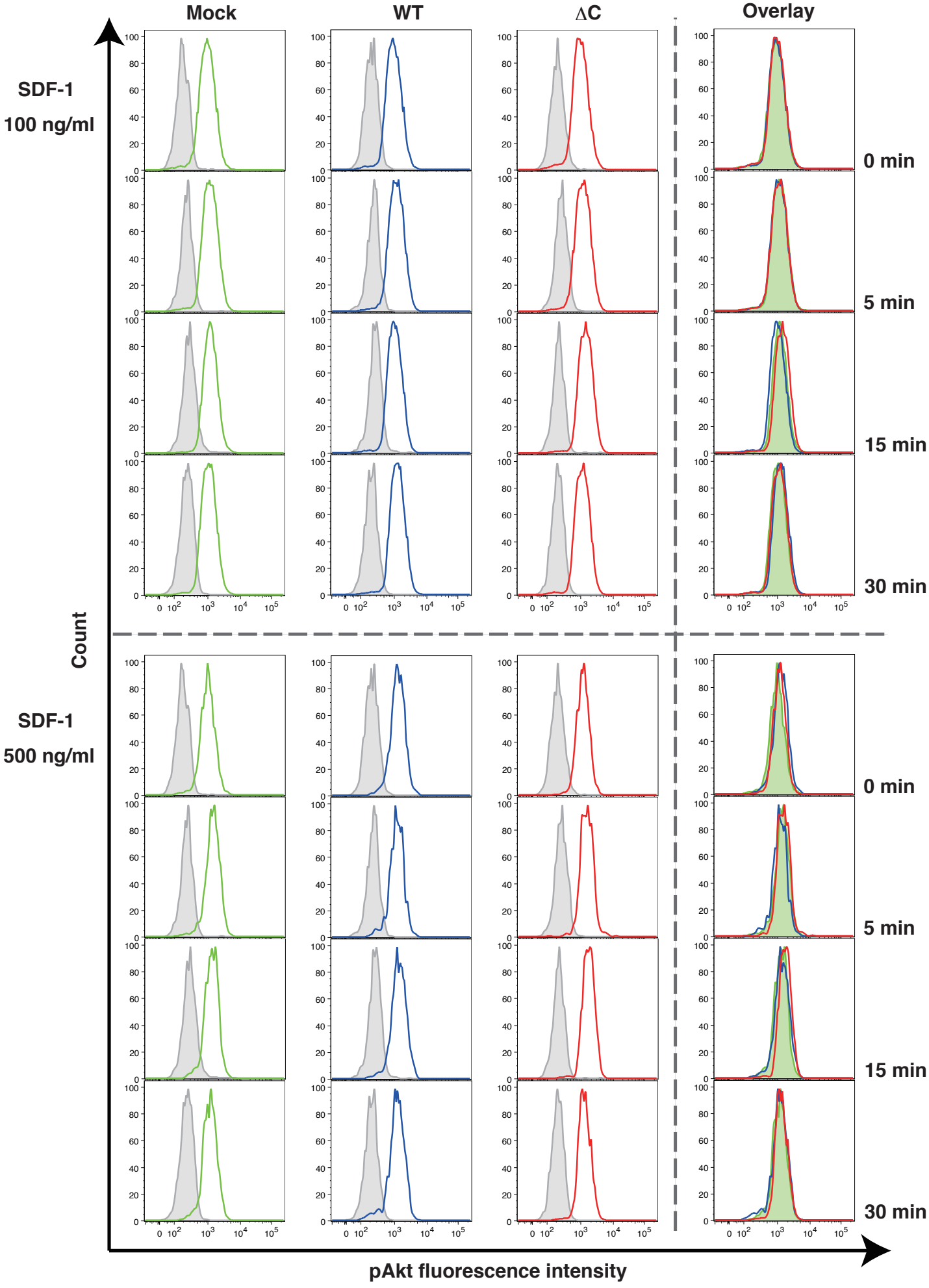
Mock
WT
ΔC
Overlay
SDF-1
100 ng/ml
SDF-1
500 ng/ml
0 min
5 min
15 min
30 min
Count
pAkt fluorescence intensity

Figure Legend

Figure 1. Schematic representation of experimental procedures and retroviral vectors. **(A)** A schema of gain-of-function and loss-of-function experiments. **(B)** Shown is a schema of the pGCDNsam-IRES-EGFP retroviral vector and its derivatives, with one harboring WT-*Cxcr4* cDNA and the other C-terminal-truncation-type (ΔC) *Cxcr4*. MoMLV: Moloney murine leukemia virus LTR; Ψ^+: packaging signal; S.D.: splice donor; S.A.: splice acceptor; IRES: internal ribosomal entry site; PCMV: PCC4 cell-passaged myeloproliferative sarcoma virus LTR.

Figure 2. Human CXCR4 and murine Cxcr4 share almost identical C-terminal tail amino-acid sequences.

Top: A schema of human CXCR4. Amino-acid residues at beginning and end of cytoplasmic tail are numbered. Amino-acid residue 334 (R334X, WHIM syndrome mutation) is also indicated.

Bottom: Comparison of amino-acid sequences in C-terminal tails of CXCR4/Cxcr4. Of 45 residues shown, only three (blue: human, green: mouse) differ between human and mouse (93.3% identity). Shared serine and threonine residues are shown in orange. The 19 amino-acid residues missing in WHIM patients and in the murine mutant used in this study are identical in sequence.

Figure 3. EGFP expression analysis.

(A) Representative flow cytometry plots obtained by analyzing EGFP expression in transduced HS(P)Cs. Cells were analyzed ~72 hours after virus exposure (corresponding to day 4 in the schematic representation in Fig. 1). **(B)** Retention of EGFP reporter expression in donor cells after transplantation. Typical examples of assessment show EGFP positivity in PB leukocytes gated on donor-type marker $CD45.1^+$ cells. The data from representative mice that received transduced and $EGFP^+$-sorted HS(P)Cs in a series of competitive repopulation assays are shown (transplantation #3, see Table 2B).

Figure 4. Characterization of HS(P)Cs engineered to overexpress exogenous Cxcr4 receptors.

(A) Assessment of cell surface Cxcr4 expression in HS(P)Cs after one week of cultivation following transduction and $EGFP^+$ cell-sorting. Cxcr4 intensity (blue histograms) represents endogenous Cxcr4 expression by untransduced cells (Untransduced) and Mock-transduced cells (Mock), or the sum of both endogenous and exogenous Cxcr4 expression by transduced cells (WT, ΔC). Mean fluorescence intensity (MFI) values are shown. Red histogram: isotype control. **(B)** Cxcr4 surface expression levels are shown in conjunction with EGFP marker intensity in two-color plots. For these particular experiments, cells were used unsorted after transduction. To better demonstrate several features of Cxcr4 overexpression, overlay histograms are depicted separately by gating EGFP-dull populations and -bright populations (percentages are shown). Cxcr4 intensity (blue histograms) represents endogenous Cxcr4 expression by Mock-transduced cells (Mock), or the sum of both endogenous and exogenous Cxcr4 expression by transduced cells (WT and ΔC). MFI values are shown. Red histograms: isotype control. Note that the brighter EGFP intensity becomes, the higher Cxcr4 expression goes in cells transduced with WT- and ΔC-Cxcr4-vectors.

Figure 5. Characterization of 32D cell lines engineered to overexpress exogenous Cxcr4 receptors.

(A) Assessment of cell surface Cxcr4 expression in 32D cell lines following transduction and $EGFP^+$ cell-sorting. Cxcr4 intensity (blue histograms) represents endogenous Cxcr4 expression by untransduced cells (Untransduced) and Mock-transduced cells (Mock), or the sum of both endogenous and exogenous Cxcr4 expression by transduced cells (WT, ΔC). Mean fluorescence intensity (MFI) values are shown. Red histogram: isotype control. **(B)** Assessment of cell surface Cxcr4 expression in 32D cells following transduction and $EGFP^+$ cell-sorting. Data are shown as described in Fig. 4B.

Fig 6. Confirmation of Cxcr4 overexpression in transduced HS(P)Cs at an mRNA level.

$EGFP^+$ cells obtained by flow-cytometry sorting were subjected to quantitative RT-PCR analysis after cultivation for 7 days. For reference, one group of cells was kept in expansion medium without gene transduction (Untransduced). Copy numbers of Cxcr4 transcripts in each sample were normalized to those of GAPDH. Relative abundance (mean values ± SD, n = 3) of *Cxcr4* (assessed as sum of endogenous and exogenous transcripts where they exist) is shown by setting Untransduced values as 1.

Figure 7. Confirmation of Cxcr4 overexpression in transduced HSPCs.

Assessment of cell surface Cxcr4 expression in HSPCs after cultivation following transduction. Cxcr4 intensity (blue histograms) represents endogenous Cxcr4 expression by Mock-transduced cells (Mock), or the sum of both endogenous and exogenous Cxcr4 expression by transduced cells (WT, ΔC). Mean fluorescence intensity (MFI) values are shown. Red histogram: isotype control.

Figure 8. Baseline characteristics of proliferative response and immunophenotype alteration in *ex vivo* cultured HSCs in the context of SDF-1 stimulation.

Compare with results in main text using mostly cultured cell populations derived from purified $CD34^-$KSL cells (HSCs). Baseline response of fresh HSCs to SDF-1 and retention of primitive cell immunophenotypes were assessed using our defined serum-free culture system containing SCF and TPO. **(A)** Fresh $CD34^-$KSL cells were sorted into 96-well U-bottom plates at 50 cells/well and were counted 7 days after cultivation with the indicated concentrations (ng/ml) of SDF-1. Shown are representative data from 6 independent experiments. Mean values ± SD are shown (n = 6). $^{**}P < .01$. (B-C) Similarly treated cells were collected, stained with antibodies to c-Kit and lineage markers, and analyzed for immunophenotypes by flow cytometry. **(B)** Left: Shown is the frequency (%) in each well of cells that retained a lineage-marker negative (Lin^-), c-Kit-positive (Kit^+) phenotype (KL cells). Dead cells were excluded from analysis using propidium iodide. Right: Estimated absolute counts of KL cells in each well. **(C)** Representative immunophenotypes of cultured HSCs in each condition. Results for a control culture of $CD34^+$ KSL cells (multipotent

progenitors) in medium containing SCF, TPO, EPO, and IL-3 are also shown for comparison. Percentage of cells residing within the given gates is shown. Note that ~90% of cells still retain a "KL cell" phenotype despite substantial expansion in cell numbers over 7 days.

Figure 9. Resistance to SDF-1-induced receptor desensitization in murine HSCs observed via proliferative response in a defined culture system.

Proliferation ability of HSCs and multipotent progenitors (MPPs: $CD34^+$ KSL) in response to varying concentrations of SDF-1. Test HSCs or MPPs were sorted at 50 cells/well into 96-well plates and were counted 7 days after cultivation in serum-free basal medium (containing SCF and TPO) without or with different concentrations of SDF-1. Flt-3 ligand (50 ng/ml) and IL-6 (10 ng/ml) were added to support the proliferation of MPPs. Addition of SDF-1 at an extremely high concentration (1,000 ng/ml) evoked signs of Cxcr4 desensitization in MPPs, while it further enhanced HSCs proliferation. Data shown represent 2 independent experiments (n = 6). Mean values are indicated as bars. $*P < .05$.

Figure 10. Stepwise enhancement in SDF-1-mediated Ca^{2+} influx response in 32D cells by gain-of-function *Cxcr4* modification.

Shown is Ca^{2+} influx response assessed in a series of 32D cell lines. Viable cells loaded with the fluorescent calcium indicator Rhod-2 were subjected to flow cytometry analysis. After initiation of data acquisition for Rhod-2 fluorescence, the assay tube was removed from a FACSCalibur at 20 seconds, the stimulant was added (red arrows), and the tube was immediately restored for analysis followed by continuous data acquisition for up to 150 seconds overall. Rhod-2 fluorescence was analyzed by gating on $EGFP^+$ cells to ensure accuracy. The Ca^{2+} influx kinetics in response to the given stimulants was represented as the values of Rhod-2 MFI, using FlowJo software. For comparison, the raw values of "area under the curve" (AUC) were estimated in each time frame (0-20 sec, baseline; 20-70 sec, early phase; 70-150 sec, late phase). Shown are corrected AUC values for early and late phases. These were calculated as corrected AUC value for, *e.g.*, an early phase sample = raw AUC (early phase) – [raw AUC (baseline) x 50 (acquisition time length for early phase)/20 (acquisition time length for baseline phase)]. Where values fall below zero, "< 0" is indicated. Of note is that AUC assessment revealed that the ΔC-Cxcr4-expressing cells

showed enhanced Ca^{2+} influx response compared with those overexpressing WT-Cxcr4. All data were analyzed in duplicate. Representative data are shown.

Figure 11. Receptor internalization analysis in HS(P)Cs.

(A) Receptor internalization. Cultured and sorted HS(P)Cs were left unstimulated or were stimulated with SDF-1 (100 ng/ml) for 30 minutes, after which surface expression of Cxcr4 was compared by flow cytometry. **(B)** Cxcr4 receptor internalization was tested by using 100 ng/ml SDF-1. Gray/Black: unstimulated; Red: stimulated with SDF-1. As a negative control, data for unstained cells (stimulated) are included as dotted histograms. Estimated MFI values are shown in the corresponding colors. Percent reduction of Cxcr4 expression was calculated as described (Materials and Methods). Shown are representative data from 3 independent experiments.

Figure 12. Receptor internalization analysis in 32D cells.

(A) Receptor internalization analysis of a series of 32D cells. Transduced and sorted 32D cells were left unstimulated or were stimulated with SDF-1 (100 ng/ml) for 30 minutes, after which surface expression of Cxcr4 was compared by flow cytometry. Gray/Black: unstimulated; Red: stimulated with SDF-1. As a negative control, data for unstained cells (stimulated) are included as dotted histograms. Estimated MFI values are shown in the corresponding colors. Percent reduction of Cxcr4 expression was calculated as described (Materials and Methods). Mean values are indicated as bars (n = 3, ****$P < .0001$). **(B)** CXCR4 receptor internalization assessment in a human T cell line, CEM. CEM cells were left unstimulated or were stimulated with varying concentrations of SDF-1 for 30 minutes, after which surface expression of CXCR4 was compared by flow cytometry. Gray/Black: unstimulated; colored: stimulated with SDF-1 at the indicated concentration. As a negative control, data of unstained cells (unstimulated) are included as a dotted histogram. Estimated MFI values are shown in the corresponding colors. Cells were tested in triplicate; the MFI values are shown as plots. Mean values ± SD are indicated (n = 3, ****$P < .0001$).

Figure 13. Step-wise enhancement of chemotactic responses to SDF-1 in murine HS(P)Cs.

Shown are the results obtained by a comprehensive transwell migration assay testing varying SDF-1 concentrations at two time points. Numbers of cells that transmigrated to lower chambers in response to varying concentrations of SDF-1, estimated at the indicated time points, are shown as representative data from 2 independent experiments with 5 replicates per group. $*P < .05$, $**P < .01$, $***P < .001$, $****P < .0001$. Same data are shown with different way of expression. **(A)** Data are shown by groups. **(B)** Data are shown by incubation times. **(C)** Data are shown by concentrations.

Figure 14. Colony forming assay of Cxcr4-modified HS(P)Cs in single-cell cultures.

Single-cell cultures in the presence of SCF, TPO, IL-3, and EPO as baseline cocktail. Cultures were maintained either with no other additives (no SDF-1) or added exogenous SDF-1 at the indicated concentrations (SDF-1 50 or 500 ng/ml). Shown are colony numbers (numbers of positive wells in a 96-well plate) and the colony types assessed on day 11. Cell composition morphologically determined in each colony was represented by a single or combination of the following letters; m: macrophage, n: neutrophil, E: Erythroblast, M: Megakaryocyte. For example, "m" means a colony containing only macrophages, whereas "nm" and "nmM" represent colonies composed of a mixture of corresponding cell lineages. "nmEM" represents colonies derived from "uncommitted "single cells with high potential for multilineage differentiation within a myeloid compartment.

Figure 15. Augmentation of Cxcr4 signaling in HS(P)Cs correlates with enhanced proliferative responses in the presence of SDF-1 in high concentrations.

(A) Proliferation ability of *Cxcr4*-modified cells in response to SDF-1. Test HS(P)Cs were sorted at 50 cells/well into 96-well plates and were counted 7 days after cultivation in serum-free basal medium (containing SCF and TPO) alone or in the presence of SDF-1. Data shown represent 3 independent experiments (n = 10). **(B)** Same data are shown and expressed according to different concentrations of SDF-1 in the culture medium. Mean values are indicated as bars. $*P < .05$, $**P < .01$, $***P < .001$. Untransduced: untransduced control.

Figure 16. Cell cycle status of transduced HS(P)Cs growing in liquid culture.

Representative profiles of EdU labeling and cell cycle dye staining in retrovirus-transduced HS(P)Cs. $EGFP^+$ cells were sorted and cultured for 7 days in serum-free basal medium containing SCF and TPO with or without SDF-1. EdU (2.5 mM) was added 3 hours before the end of incubation to label cells progressing through the cell cycle. **(A)** Dual-parameter dot plot diagram to determine cell cycle status. Top panel, right: APC fluorescence (EdU-positive cells) plotted against DNA content (cell cycle dye 405 staining) to identify cells in G1G0, S, and G2M phases after doublet discrimination. **(B)** Percentages of cells in different phases of cell cycle. Black triangles shown below each set of four histograms represent varying concentrations of SDF-1. From left to right, each histogram corresponds to 0, 5, 50, and 500 ng/ml. Green: Mock, blue: WT, red: ΔC. Differences among samples were subtle but significant: More ΔC-Cxcr4-treated cells were in S-phase and fewer were in G0/G1 phase than was the case for other cells (Mock and WT) in the presence of 500 ng/ml SDF-1, consistent with their proliferation properties (Figure 15).

Figure 17. Augmentation of Cxcr4 signaling in HS(P)Cs correlates with enhanced proliferative responses in the presence of feeder cell layers.

(A) Ability of *Cxcr4*-modified HS(P)Cs to form cobblestone-like areas (Cbl-As) in the presence of feeder cells. Test cells were directly sorted onto a feeder layer of C3HT101/2 cells at 50 cells/well. Numbers of areas per well evaluated on day 10 are shown as mean values ± SD (n = 4, representative of 3 independent experiments). $^{**}P < .01$. Right: Photo images of representative view fields are shown. Scale bars represent 200 μm. **(B)** Dose-related inhibition of HSC cobblestone-like area formation by blocking the Sdf-1/Cxcr4 axis in the C3H 10T1/2 cell layer culture. $CD34^-$KSL cells were directly sorted onto a feeder layer of C3H 10T1/2 cells and cultivated in defined medium with or without the CXCR4 receptor antagonist AMD3100 at 10, 100, and 1000 ng/ml. AMD3100 exposure was maintained steadily throughout culture by fresh medium replacement every 2-3 days. Numbers of areas per well evaluated on day 14 are shown as mean values ± SD (n = 4 per condition, representative of 2 independent experiments). $^{*}P < .05$, $^{**}P < .01$. **(C)** Presence of measurable Sdf-1 in conditioned medium of C3H 10T1/2 feeder cells and in bone marrow (BM) cavities. Fresh medium was included as control (Medium). After

establishing an irradiated C3H 10T1/2 (10T1/2) feeder cell layer in 6-well plates, medium samples were obtained 3 days after re-feeding and culturing cells in either normoxic or hypoxic conditions (~20% O_2, Normoxia; ~5% O_2, Hypoxia). BM fluid samples were obtained as supernatants by flushing out the BM cavity in 500 ml PBS using sets of femurs, tibias, pelvic bones, and upper forelimb bones from individual mice, followed by centrifugation to exclude cells. Mice were used either unirradiated [TBI (-)] or 24 hours after irradiation [TBI (+)] at 9.7 Gy. Sdf-1 concentrations were quantified by ELISA. Samples were assessed in triplicate. Data are shown as mean values ± SD.

Figure 18 Cxcr4 signal-augmentation in HSPCs does not enhance the homing process.
(A) A schema of a homing assay using HSPCs as test cells. $EGFP^+$ cultured KSL cells were transplanted into lethally-irradiated recipients at 50,000 cells per mouse (Test cells). Each recipient mouse simultaneously received 17,000 fresh KSL cells expressing the fluorescent marker KuO (KuO^+ cells) as reference control (Reference cells). Approximately 24 hours later, as many bone marrow cells as possible were obtained from 6 long bones (pelvic bones, femurs, and tibias) of each mouse to estimate the numbers of $EGFP^+$ and KuO^+ cells contained, with these regarded as "BM-homed" cells. **(B) A** homing assay using cultured HSPCs, either Mock-virus-treated (Mock) or expressing either wild-type (WT) or C-terminal truncated-type (ΔC) exogenous Cxcr4 receptors. Twenty-four hours later, homing events were quantified in recipient BM as KuO^+ and $EGFP^+$ cells (red and green gates respectively). Representative flow cytometry analysis is shown at upper panel. Shown are the event ratios of $EGFP^+$ (test cells) to KuO^+ (reference cells) expressed as means ± SD (n = 5 for each group).

Figure 19. Tracking *in vivo* fates of Cxcr4-modified HSPCs in homing processes.
Tracking *in vivo* fates within recipient BM of reconstituting HSPCs with or without overexpression of exogenous Cxcr4 receptors. **(A)** A schema of a homing assay using HSPCs as test cells. $EGFP^+$ cultured HSPCs were transplanted into lethally-irradiated recipients at 17,000 cells per mouse (Test cells). Each recipient mouse simultaneously received 10^6 fresh BM cells expressing fluorescent marker KuO (KuO^+ cells) as reference control (Reference cells). BM cells subsequently were obtained from recipient left femur

and tibia. Approximately $2x10^6$ viable cells per sample were analyzed for numbers of $EGFP^+$ and KuO^+ cells contained, with these regarded as "BM-homed" cells. **(B)** Homing assay using cultured HSPCs, either Mock-virus-treated (Mock) or expressing either wild-type (WT) or C-terminal truncated (ΔC) exogenous Cxcr4 receptors. Test and reference cells were transplanted as described above. Four, 15, and 24 hours later, homing events were quantified in recipient BM. Shown are the event ratios of $EGFP^+$ cells (Test cells) to KuO^+ cells (Reference cells) expressed as means ± SD (n = 5 for each group) from 2 independent experiments.

Figure 20. Tracking *in vivo* fates of Cxcr4-modified HS(P)Cs in homing processes.

Tracking *in vivo* fates within recipient BM of reconstituting HS(P)Cs with or without overexpression of gain-of-function Cxcr4 receptors. **(A)** A schema of a homing assay using HS(P)Cs as the sole test cells. $EGFP^+$ cultured HS(P)Cs were transplanted into lethally-irradiated recipients at 100 cells per mouse. **(B, C)** Assessment of BM homing/early repopulation processes. Shown are numbers of CFCs detected in BM of each mouse that received either fresh unmodified HSCs or HS(P)Cs (100 cells per mouse) alone after lethal-dose irradiation. Shown are the results obtained at 16 hours (open histograms) and 24 hours (closed histograms) after transplantation (B), or at 2 days (open histograms) and 4 days (closed histograms) after transplantation (C). Data are expressed as means ± SD (n = 4, representative of 3 independent experiments).

Figure 21. Tracking *in vivo* fates of Cxcr4-modified HS(P)Cs in BM repopulation.

(A) A schema of a competitive repopulation assay using HS(P)Cs as test cells. $EGFP^+$ cultured HS(P)Cs were transplanted into lethally-irradiated recipients. Each recipient mouse simultaneously received $2x10^5$ fresh BM cells competitor cells. Recipient BM was analyzed at specific time points as indicated. **(B)** Donor cell chimerism assessment in competitive repopulation assays. Shown are donor cell chimerism values in recipient BM at week 2 (open histograms) and week 3 (closed histograms). Mean values ± SD are shown (n = 4, representative of 4 independent experiments). $*P < .05$ (ΔC vs. Mock). Values of *P* for trend are shown. **(C)** Donor cell chimerism in long-term recipient BM at week 36. Shown is representative flow cytometry analysis of donor cell chimerism in mice transplanted with

treated HS(P)Cs in a competitive repopulation assay. Graphic representation of chimerism analysis is also shown as mean values ± SD (n = 5, representative of 3 independent experiments). *$P < .05$ (ΔC vs. Mock). Values of P for trend are shown.

Figure 22. Continuous expression of gain-of-function receptors in HS(P)Cs enhanced BM repopulation, by donor cells throughout developmental stages.

Donor cell chimerism assessed 36 weeks after transplantation in long-term recipient BM (colored histograms) and PB (white histograms) for multiple hematopoietic subfractions. Top: Stem cells, progenitor cells, and PB leucocytes (HSC/HSPC). Middle: Differentiation path along B cell development (B lineage differentiation). Bottom: Differentiation path along myeloid development (Myeloid differentiation). Detailed marker combinations used to define each population are listed (see Materials and Methods). Data analyzed by Dunnett's multiple comparison test with peripheral chimerism as control. *$P < .05$, **$P < .01$. LT-HSC: long-term hematopoietic stem cells, ST-HSC: short-term hematopoietic stem cells, CLP: common lymphoid progenitors, CMP: common myeloid progenitors, all in BM. Leuk: leukocytes in PB. proB: pro-B cells, preB: pre-B cells, maB: mature B cells, all in BM. B: B cells in PB. GMP: granulocyte/macrophage progenitors, priNeu: primitive neutrophils, maNeu: mature neutrophils, all in BM. Mye: myeloid cells in PB.

Figure 23. Detailed analysis of donor cell chimerism in multiple cell fractions in recipient BM.

Shown is the representative step-by-step gating strategy used for the analysis shown in Figure 22 (example: analysis of LT-HSC and ST-HSC populations for a recipient mouse in the WT-Cxcr4 treatment group).

Figure 24. Comparative analysis of B cell lineage development in long-term recipient BM.

Shown are the representative step-by-step gating strategy and FACS plots used to analyze development characteristics of B cell lineages in recipient BM. The competitor and donor cells co-existing in the same recipient BM were separately gated and analyzed for pro-B

($IgM^-B220^+CD43^+$) and mature B (IgM^+ $B220^+$) cell populations. Similar percentages of not only pro-B cells but also IgM^+ B cells are shown in both competitor and donor cell populations within the same recipient BM, revealing no gross abnormality in B cell-lineage differentiation in Cxcr4-modified cells.

Figure 25. Continuous expression of gain-of-function receptors in HS(P)Cs leads to impaired peripheral reconstitution.

(A) A schema of a competitive repopulation assay using HS(P)Cs as test cells. $EGFP^+$ cultured HS(P)Cs were transplanted into lethally-irradiated recipients. Each recipient mouse simultaneously received $2x10^5$ fresh BM cells competitor cells. Recipient PB was analyzed at specific time points as indicated. **(B-C)** Percent PB chimerism of donor cells on competitive repopulation assay 4 weeks for (B) and 16 weeks for (C) after transplantation. Donor cell chimerism was separately determined for each lineage (T cells, B cells, and myeloid cells). Shown are data represented as mean values ± SD obtained from mice each of which received 700 $EGFP^+$ cells along with 2 x 10^5 competitor cells (n = 5, representative of 3 independent experiments). $^{**}P < .01.$, $^{***}P < .001$.

Figure 26. Blunted peripheral mobilization of donor cells plays a causal role in poor PB reconstitution for Cxcr4-overexpressing cells.

(A) A schema of the rational of AMD3100 mobilization experiments. Note that donor cell chimerism is high in BM, but low in PB in the recipients of HS(P)Cs expressing exogenous Cxcr4 receptors. **(B)** A schema representative of AMD3100 mobilization. One week after the analysis of baseline donor cell chimerism, each mouse received intraperitoneal systemic injection of AMD3100 (10 mg/kg). One hour after AMD3100 injection, PB chimerism was analyzed and the fold increase of donor chimerism was calculated for each donor. **(C)** Assessment of AMD3100-induced mobilization effect on donor chimerism in long-term recipients. Top: Donor cell chimerism of individual recipients before and after mobilization. Bottom: Shown are data represented as mean values ± SD obtained from groups of recipient mice (n = 10, representative of 2 independent experiments). $^{*}P < .05$, $^{***}P < .001$.

Figure 27. Long-term hematopoietic reconstitution in secondary recipients of *Cxcr4*-modified HS(P)Cs.

Reconstitution capability of *Cxcr4*-modified HS(P)Cs was assessed by serially transplanting BM cells obtained from primary recipients (4 x 10^5 cells per mouse) into secondary recipients. Shown are mean values ± SD for donor cell chimerism in PB (top) or in BM (bottom) determined 16 weeks after transplantation.

Figure 28. The importance of the Sdf-1/Cxcr4 axis in HSC/HSPCs proliferation and colonization in the presence of stromal cells.

All loss-of-function studies used as starting materials purified HSCs harvested from either *Cxcr4* conditional KO mice or their littermate control (LM) mice similarly treated with pIpC. **(A)** Single-cell cultures in the presence of SCF, TPO, IL-3, and EPO. Shown are colony numbers and the colony types assessed on day 14. m: macrophage, n: neutrophil, E: Erythroblast, M: Megakaryocyte (classifications, see legend, Fig. 14. **(B)** Proliferation ability of either LM HSCs or *Cxcr4*-KO HSCs in response to SDF-1 (starting from 50 cells/well). Data shown represent 3 independent experiments (n = 5). Mean values are indicated as bars. $*P < .05$. **(C)** Ability of either LM HSCs or *Cxcr4*-KO HSCs to form cobblestone-like areas (Cbl-As) in a feeder layer of C3H10T1/2 cells (50 input cells/well). Left: Shown are numbers of areas per well evaluated on day 10 as mean values ± SD (n = 4, representative of 3 independent experiments). $**P < .01$. Right: Photo images of representative view fields are shown. Scale bars represent 50 μm.

Figure 29. Deletion of Cxcr4 signaling in HSPCs does not compromise the BM homing ability of the cells.

All loss-of-function studies used as starting materials purified HSCs harvested from either *Cxcr4* conditional KO mice or their littermate control (LM) mice similarly treated with pIpC. **(A)** Schematic representation of HSPC homing assay with AMD3100 blockage. A schema of homing assay using HSPCs as test cells. KuO-expressing (KuO^+), freshly isolated KSL cells were left untouched or were incubated with AMD3100 at varying concentrations for 30 minutes at 37ºC, washed, and infused into lethally-irradiated recipients at 10,000 cells (Test cells). BM cells obtained from EGFP-Tg mice ($EGFP^+$ cells; Reference cells) were

co-transplanted intravenously at 10^6 cells per recipient. In addition, one cohort of mice received PBS intraperitoneally, whereas another one received AMD3100. Fifteen hours later, BM cells were harvested, with ~2 x 10^6 viable cells per recipient analyzed for numbers of KuO^+ and $EGFP^+$ cells, with these regarded as "BM-homed" cells. **(B)** Assessment of BM homing ability using fresh HSPCs as test cells. Test cells and reference cells were obtained and treated as mentioned above. Lethally irradiated recipients received a mixture of test and reference cells. Fifteen hours later, homing events were quantified in recipient BM as KuO^+ and $EGFP^+$ cells. One group of mice received PBS intraperitoneally [AMD injection (-)], whereas another received AMD3100 [AMD injection (+)]. Shown are the event ratios of test cells (KuO^+) to reference cells ($EGFP^+$) as means ± SD (n = 4 for each group).

Figure 30. Loss-of-function studies support the idea that Sdf-1/Cxcr4 axis in highly purified HSCs is dispensable for the BM homing process.

Tracking *in vivo* fates within recipient BM of reconstituting HSCs with or without Cxcr4 receptors. **(A)** A schema of a homing assay using HSCs as the sole test cells. Purified HSCs from LM and KO mice were transplanted into lethally-irradiated recipients at 100 cells per mouse. **(B)** The similar protocol was used as described in Fig. 20. Shown are numbers of CFCs detected in BM of each mouse that received either LM HSCs or KO HSCs (100 cells per mouse) at day 4 (open histograms) and day 6 (closed histograms). Data are expressed as means ± SD (n = 5, representative of 2 independent experiments).

Figure 31. Loss-of-function studies support the idea that Sdf-1/Cxcr4 axis in HSCs is important for BM repopulation.

(A) A schema of a competitive repopulation assay using HSCs as test cells. Purified HSCs were transplanted into lethally-irradiated recipients. Each recipient mouse simultaneously received $2x10^5$ fresh BM cells as competitor cells. Recipient BM and PB cells were analyzed at specific time points as indicated. **(B)** Donor cell chimerism in recipient BM at week 2 (open histograms) and week 3 (closed histograms) is shown as mean values ± SD (n = 5, representative of 3 independent experiments). $^{**}P < .01$. **(C)** Percent PB chimerism of donor cells in a competitive repopulation assay 16 weeks after transplantation. Donor cell

chimerism was separately determined for each lineage (T cells, B cells, and myeloid cells). Shown are data represented as mean values ± SD.

Figure 32. Erk activation kinetics in 32D cells upon stimulation.

Immunoblot analysis of SDF-1-mediated Erk activation kinetics in whole cell lysates obtained from 32D cells (1 x 10^5 cells per lane) before and after stimulation with SDF-1 (100 ng/ml) for indicated times. pErk: blots specifically detected by anti-phospho-Erk1/2 antibody; Erk: blots reflecting endogenous levels of total Erk1/2 protein. Note the enhanced response in WT samples in comparison with Mock cells (5 min), and the far more enhanced one in ΔC-Cxcr4-expressing cells, showing signal more intense than that in WT cells (5 min) and later sustained Erk activation evident (15 and 30 min).

Figure 33. Augmentation of Cxcr4 signaling leads to enhanced and prolonged phosphorylation of Erk in HS(P)Cs upon SDF-1 stimulation.

Altered Erk activation kinetics. Test cells were cytokine-starved and stimulated with 100 or 500 ng/ml SDF-1 for the indicated times. The amount of phosphorylated Erk was determined by flow cytometry analysis. Top, each colored histogram represents pErk intensity at different time points upon stimulation with 100 ng/ml SDF-1. Bottom, same as top panel except for SDF-1 concentration (500 ng/ml). Gray histogram in each represents isotype-control. Overlay histogram figures are shown on the right for comparison between groups.

Figure 34. Augmentation of Cxcr4 signaling has little effect on Akt activation in cultured HS(P)Cs.

Cells transduced with Mock-virus (Mock) or with virus harboring either WT- (WT) or ΔC-type (ΔC) Cxcr4 were cytokine-starved for 6 hours and then were stimulated with SDF-1 (100 ng/ml, top panel; 500 ng/ml, bottom panel) for the indicated times. Phosphorylated Akt was quantitated by flow cytometry analysis using anti-phospho-Akt (Thr308) mAb. Histograms in color (green: Mock, blue: WT, red: ΔC) represent pAkt intensity, whereas shaded gray histograms show background intensity with isotype control mAb. Right-most panel shows the overlay between groups at indicated time points. Of note is that treatment

of cells with LY294002, a PI3 kinase inhibitor, reduced pAkt intensity to background levels (data not shown).

Tables

Table 1

(A) Antibodies and other markers used to sort donor HSCs/HSPCs and to detect donor-derived cells in multilineage hematopoietic analysis (biotinylated antibodies)

Antigen	Alternate name	Clone	Conjugation	Catalog #	Vendor
Gr-1	Ly-6G	RB6-865	Biotin	13-5931-85	eBioscience
Mac-1	CD11b	M1/70	Biotin	13-0112-85	eBioscience
Ter119	Ly-76	TER-119	Biotin	13-5921-85	eBioscience
CD4	Ly-4	RM4-5	Biotin	13-0042-85	eBioscience
CD8	Ly-2	53-6.7	Biotin	100704	BioLegend
CD45R (B220)	Ly-5	RA3-7B2	Biotin	13-0452-85	eBioscience
IL-7R	CD127	A7R34	Biotin	13-1271-85	eBioscience
IgM	-	II/41	Biotin	13-5790-85	eBioscience
CD3e	-	145-2C11	Biotin	13-0031-85	eBioscience
CD19	B4	EB19-1	Biotin	13-0191-85	eBioscience
Sca-1	Ly-6A / E	D7	Biotin	553334	BD Pharmingen
CD5	Ly-1	53-7.3	Biotin	01032D	BD Pharmingen

(B) Antibodies and reagents used to sort donor HSCs/HSPCs and to detect donor-derived cells in multilineage hematopoietic analysis

Antigen	Alternate name	Clone	Conjugation	Catalog #	Vendor
CD34	-	RAM34	Alexa Fluor700	56-0341-82	eBioscience
c-Kit	CD117	2B8	APC	105812B	BioLegend
Sca-1	Ly-6A / E	D7	PE	12-5981-83	eBioscience
CD45.1	Ly5.1	A20	PECy7	25-0453-82	eBioscience
CD45.2	Ly5.2	104	PB	109820	BioLegend

FcγR	CD16 / 32	93	PE	12-0161-83	eBioscience
Sca-1	Ly-6A / E	D7	Alexa Fluor700	56-5981-82	eBioscience
IL-7R	CD127	A7R34	PECy7	25-1271-82	eBioscience
FLK2	CD135	A2F10.1	PE	561068	BD Pharmingen
IgM	-	II/41	APC	17-5790-82	eBioscience
CD43	Ly-48	S7	PE	553271	BD Pharmingen
CD45R (B220)	Ly-5	RA3-6B2	APC-eFluor780	47-0452-82	eBioscience
Gr-1	Ly-6G	RB6-8C5	PE	12-5931-83	eBioscience
Mac-1	CD11b	M1/70	Alexa Fluor750	27-0112-81	eBioscience
CD34	-	RAM34	FITC	110-341-85	eBioscience
CD45.1	SJL	A20	FITC	11-0453-85	eBioscience
CD45.1	SJL	A20	PB	110722	BioLegend
CD45.2	Ly5.2	104	PerCP / Cy5.5	109829	BioLegend
CD45.2	Ly5.2	104	PECy7	109830	BioLegend
CD45R (B220)	Ly-5	RA3-6B2	PE	12-0452-82	eBioscience
Gr-1	Ly-6G / Ly-6C	RB6-8C5	APC	108412	BioLegend
Mac-1	CD11b	M1/70	APC	17-0112-83	eBioscience
CD4	-	RM4-5	Pacific Blue	100531	BioLegend
CD8	-	5H10	Alexa Fluor 405	MCD 0826	Caltag Lab.
Streptavidin	-	-	APC-eFluor780	47-4317-82	eBioscience

Table 2

(A) Transduction efficiency of murine HSCs

Shown are %EGFP-positive cells in transduced HSCs before sorting (~72 hours after transduction). Representative flow cytometry plots in Exp. #1 are shown in Fig 3A. Mock: Mock vector-transduction, WT: WT-*Cxcr4*-transduction, ΔC: ΔC-*Cxcr4*-transduction.

	Mock	WT	ΔC
Experiment #1	88.3	80.8	82.5
Experiment #2	89.2	83.2	84.4
Experiment #3	94.4	84.6	76.8
Experiment #4	87.9	61.3	64.1
Experiment #5	91.9	84.0	82.6

(B) Retention of EGFP reporter expression in donor cells after transplantation

Shown are %EGFP-positive cells (mean ± SD) in donor-type PB leukocytes analyzed in mice that received transduced and $EGFP^+$-sorted HS(P)Cs in a series of competitive repopulation assays. Numbers of mice are shown in parentheses. Times of analysis are indicated as weeks (wks) after transplantation.

	wks	Mock	WT	ΔC
Transplantation #1	16	87.1 ± 21.6 (10)	77.1 ± 18.2 (7)	87.3 ± 13.1 (9)
Transplantation #2	12	94.8 ± 7.0 (7)	69.6 ± 19.0 (7)	75.9 ± 14.0 (8)
Transplantation #3	20	96.4 ± 3.4 (5)	80.4 ± 22.6 (5)	94.5 ± 4.2 (5)

References

1. McCulloch EA, Till JE. Proliferation of Hemopoietic Colony-Forming Cells Transplanted into Irradiated Mice. **Radiat Res** 1964;22:383-397.
2. Schofield R. The relationship between the spleen colony-forming cell and the haemopoietic stem cell. **Blood Cells** 1978;4:7-25.
3. Wilson A, Trumpp A. Bone-marrow haematopoietic-stem-cell niches. **Nature reviews Immunology** 2006;6:93-106.
4. Till JE, Mc CE. A direct measurement of the radiation sensitivity of normal mouse bone marrow cells. **Radiat Res** 1961;14:213-222.
5. Morrison SJ, Wandycz AM, Hemmati HD et al. Identification of a lineage of multipotent hematopoietic progenitors. **Development** 1997;124:1929-1939.
6. Little MT, Storb R. History of haematopoietic stem-cell transplantation. **Nature reviews Cancer** 2002;2:231-238.
7. Spangrude GJ, Heimfeld S, Weissman IL. Purification and characterization of mouse hematopoietic stem cells. **Science** 1988;241:58-62.
8. Osawa M, Hanada K, Hamada H et al. Long-term lymphohematopoietic reconstitution by a single CD34-low/negative hematopoietic stem cell. **Science** 1996;273:242-245.
9. Morrison SJ, Weissman IL. The long-term repopulating subset of hematopoietic stem cells is deterministic and isolatable by phenotype. **Immunity** 1994;1:661-673.
10. Kim M, Cooper DD, Hayes SF et al. Rhodamine-123 staining in hematopoietic stem cells of young mice indicates mitochondrial activation rather than dye efflux. **Blood** 1998;91:4106-4117.
11. Kiel MJ, Yilmaz OH, Iwashita T et al. SLAM family receptors distinguish hematopoietic stem and progenitor cells and reveal endothelial niches for stem cells. **Cell** 2005;121:1109-1121.
12. Majeti R, Park CY, Weissman IL. Identification of a hierarchy of multipotent hematopoietic progenitors in human cord blood. **Cell stem cell** 2007;1:635-645.
13. Notta F, Doulatov S, Laurenti E et al. Isolation of single human hematopoietic stem cells capable of long-term multilineage engraftment. **Science** 2011;333:218-221.
14. Perdomo-Arciniegas AM, Vernot JP. Optimised cord blood sample selection for smallscale CD34+ cell immunomagnetic isolation. **Mol Med Report** 2011.
15. Vose JM, Bierman PJ, Lynch JC et al. Transplantation of highly purified CD34+Thy-1+ hematopoietic stem cells in patients with recurrent indolent non-Hodgkin's lymphoma. **Biology of blood and marrow transplantation** 2001;7:680-687.
16. Michallet M, Philip T, Philip I et al. Transplantation with selected autologous peripheral blood CD34+Thy1+ hematopoietic stem cells (HSCs) in multiple myeloma: impact of HSC dose on engraftment, safety, and immune reconstitution. **Exp Hematol** 2000;28:858-870.

17. Spangrude GJ, Brooks DM. Mouse strain variability in the expression of the hematopoietic stem cell antigen Ly-6A/E by bone marrow cells. **Blood** 1993;82:3327-3332.

18. Weissman IL, Shizuru JA. The origins of the identification and isolation of hematopoietic stem cells, and their capability to induce donor-specific transplantation tolerance and treat autoimmune diseases. **Blood** 2008;112:3543-3553.

19. Randall TD, Weissman IL. Phenotypic and functional changes induced at the clonal level in hematopoietic stem cells after 5-fluorouracil treatment. **Blood** 1997;89:3596-3606.

20. Copelan EA. Hematopoietic stem-cell transplantation. **The New England journal of medicine** 2006;354:1813-1826.

21. Jenq RR, van den Brink MR. Allogeneic haematopoietic stem cell transplantation: individualized stem cell and immune therapy of cancer. **Nature reviews Cancer** 2010;10:213-221.

22. Yoder MC. Generation of HSCs in the embryo and assays to detect them. **Oncogene** 2004;23:7161-7163.

23. Cancelas JA, Jansen M, Williams DA. The role of chemokine activation of Rac GTPases in hematopoietic stem cell marrow homing, retention, and peripheral mobilization. **Exp Hematol** 2006;34:976-985.

24. Selleri C, Maciejewski JP, De Rosa G et al. Long-lasting decrease of marrow and circulating long-term culture initiating cells after allogeneic bone marrow transplant. **Bone Marrow Transplant** 1999;23:1029-1037.

25. Cartier N, Hacein-Bey-Abina S, Bartholomae CC et al. Hematopoietic stem cell gene therapy with a lentiviral vector in X-linked adrenoleukodystrophy. **Science** 2009;326:818-823.

26. Glimm H, Oh IH, Eaves CJ. Human hematopoietic stem cells stimulated to proliferate in vitro lose engraftment potential during their S/G(2)/M transit and do not reenter G(0). **Blood** 2000;96:4185-4193.

27. Zlotnik A, Burkhardt AM, Homey B. Homeostatic chemokine receptors and organ-specific metastasis. **Nature reviews Immunology** 2011;11:597-606.

28. Laing KJ, Secombes CJ. Chemokines. **Dev Comp Immunol** 2004;28:443-460.

29. Fernandez EJ, Lolis E. Structure, function, and inhibition of chemokines. **Annu Rev Pharmacol Toxicol** 2002;42:469-499.

30. Loetscher M, Geiser T, O'Reilly T et al. Cloning of a human seven-transmembrane domain receptor, LESTR, that is highly expressed in leukocytes. **The Journal of biological chemistry** 1994;269:232-237.

31. Moriuchi M, Moriuchi H, Turner W et al. Cloning and analysis of the promoter region of CXCR4, a coreceptor for HIV-1 entry. **J Immunol** 1997;159:4322-4329.

32. Cocchi F, DeVico AL, Garzino-Demo A et al. Identification of RANTES, MIP-1 alpha, and MIP-1 beta as the major HIV-suppressive factors produced by CD8+ T cells. **Science** 1995;270:1811-1815.

33. Saini V, Marchese A, Majetschak M. CXC chemokine receptor 4 is a cell surface receptor for extracellular ubiquitin. **The Journal of biological chemistry** 2010;285:15566-15576.

34. Hernandez PA, Gorlin RJ, Lukens JN et al. Mutations in the chemokine receptor gene CXCR4 are associated with WHIM syndrome, a combined immunodeficiency disease. **Nat Genet** 2003;34:70-74.

35. Balabanian K, Brotin E, Biajoux V et al. Proper desensitization of CXCR4 is required for lymphocyte development and peripheral compartmentalization in mice. **Blood** 2012;119:5722-5730.

36. Kawai T, Malech HL. WHIM syndrome: congenital immune deficiency disease. **Curr Opin Hematol** 2009;16:20-26.

37. Huang X, Shen J, Cui M et al. Molecular dynamics simulations on SDF-1alpha: binding with CXCR4 receptor. **Biophys J** 2003;84:171-184.

38. Lagane B, Chow KY, Balabanian K et al. CXCR4 dimerization and beta-arrestin-mediated signaling account for the enhanced chemotaxis to CXCL12 in WHIM syndrome. **Blood** 2008;112:34-44.

39. Dotta L, Tassone L, Badolato R. Clinical and genetic features of Warts, Hypogammaglobulinemia, Infections and Myelokathexis (WHIM) syndrome. **Curr Mol Med** 2011;11:317-325.

40. Sugiyama T, Kohara H, Noda M et al. Maintenance of the hematopoietic stem cell pool by CXCL12-CXCR4 chemokine signaling in bone marrow stromal cell niches. **Immunity** 2006;25:977-988.

41. Trumpp A, Essers M, Wilson A. Awakening dormant haematopoietic stem cells. **Nature reviews Immunology** 2010;10:201-209.

42. Nagasawa T, Kikutani H, Kishimoto T. Molecular cloning and structure of a pre-B-cell growth-stimulating factor. **Proc Natl Acad Sci U S A** 1994;91:2305-2309.

43. Peled A, Petit I, Kollet O et al. Dependence of human stem cell engraftment and repopulation of NOD/SCID mice on CXCR4. **Science** 1999;283:845-848.

44. Nagasawa T, Hirota S, Tachibana K et al. Defects of B-cell lymphopoiesis and bone-marrow myelopoiesis in mice lacking the CXC chemokine PBSF/SDF-1. **Nature** 1996;382:635-638.

45. Zou YR, Kottmann AH, Kuroda M et al. Function of the chemokine receptor CXCR4 in haematopoiesis and in cerebellar development. **Nature** 1998;393:595-599.

46. Tachibana K, Hirota S, Iizasa H et al. The chemokine receptor CXCR4 is essential for vascularization of the gastrointestinal tract. **Nature** 1998;393:591-594.

47. Nie Y, Han YC, Zou YR. CXCR4 is required for the quiescence of primitive hematopoietic cells. **The Journal of experimental medicine** 2008;205:777-783.

48. Tzeng YS, Li H, Kang YL et al. Loss of Cxcl12/Sdf-1 in adult mice decreases the quiescent state of hematopoietic stem/progenitor cells and alters the pattern of hematopoietic regeneration after myelosuppression. **Blood** 2011;117:429-439.

49. Sharma M, Afrin F, Satija N et al. Stromal-derived factor-1/CXCR4 signaling: indispensable role in homing and engraftment of hematopoietic stem cells in bone marrow. **Stem cells and development** 2011;20:933-946.

50. Kahn J, Byk T, Jansson-Sjostrand L et al. Overexpression of CXCR4 on human CD34+ progenitors increases their proliferation, migration, and NOD/SCID repopulation. **Blood** 2004;103:2942-2949.

51. Kawai T, Choi U, Cardwell L et al. WHIM syndrome myelokathexis reproduced in the NOD/SCID mouse xenotransplant model engrafted with healthy human stem cells transduced with C-terminus-truncated CXCR4. **Blood** 2007;109:78-84.

52. Brenner S, Whiting-Theobald N, Kawai T et al. CXCR4-transgene expression significantly improves marrow engraftment of cultured hematopoietic stem cells. **Stem Cells** 2004;22:1128-1133.

53. McDermott DH, Lopez J, Deng F et al. AMD3100 is a potent antagonist at CXCR4(R334X) , a hyperfunctional mutant chemokine receptor and cause of WHIM syndrome. **J Cell Mol Med** 2011;15:2071-2081.

54. Diaz GA, Gulino AV. WHIM syndrome: a defect in CXCR4 signaling. **Curr Allergy Asthma Rep** 2005;5:350-355.

55. Chung SH, Seki K, Choi BI et al. CXC chemokine receptor 4 expressed in T cells plays an important role in the development of collagen-induced arthritis. **Arthritis Res Ther** 2010;12:R188.

56. Kuhn R, Schwenk F, Aguet M et al. Inducible gene targeting in mice. **Science** 1995;269:1427-1429.

57. Hamanaka S, Ooehara J, Morita Y et al. Generation of transgenic mouse line expressing Kusabira Orange throughout body, including erythrocytes, by random segregation of provirus method. **Biochem Biophys Res Commun** 2013;435:586-591.

58. Yamamoto R, Morita Y, Ooehara J et al. Clonal analysis unveils self-renewing lineage-restricted progenitors generated directly from hematopoietic stem cells. **Cell** 2013;154:1112-1126.

59. Hamanaka S, Nabekura T, Otsu M et al. Stable transgene expression in mice generated from retrovirally transduced embryonic stem cells. **Mol Ther** 2007;15:560-565.

60. Sanuki S, Hamanaka S, Kaneko S et al. A new red fluorescent protein that allows efficient marking of murine hematopoietic stem cells. **The journal of gene medicine** 2008;10:965-971.

61. Ema H, Morita Y, Yamazaki S et al. Adult mouse hematopoietic stem cells: purification and single-cell assays. **Nat Protoc** 2006;1:2979-2987.

62. Nabekura T, Otsu M, Nagasawa T et al. Potent vaccine therapy with dendritic cells genetically modified by the gene-silencing-resistant retroviral vector GCDNsap. **Mol Ther** 2006;13:301-309.

63. Ory DS, Neugeboren BA, Mulligan RC. A stable human-derived packaging cell line for production of high titer retrovirus/vesicular stomatitis virus G pseudotypes. **Proc Natl Acad Sci U S A** 1996;93:11400-11406.

64. Kawai T, Choi U, Whiting-Theobald NL et al. Enhanced function with decreased internalization of carboxy-terminus truncated CXCR4 responsible for WHIM syndrome. **Exp Hematol** 2005;33:460-468.

65. Janda E, Palmieri C, Pisano A et al. Btk regulation in human and mouse B cells via protein kinase C phosphorylation of IBtkgamma. **Blood** 2011;117:6520-6531.

66. Takano H, Ema H, Sudo K et al. Asymmetric division and lineage commitment at the level of hematopoietic stem cells: inference from differentiation in daughter cell and granddaughter cell pairs. **J Exp Med** 2004;199:295-302.

67. Ogaeri T, Eto K, Otsu M et al. The actin polymerization regulator WAVE2 is required for early bone marrow repopulation by hematopoietic stem cells. **Stem Cells** 2009;27:1120-1129.

68. Ploemacher RE, van der Sluijs JP, van Beurden CA et al. Use of limiting-dilution type long-term marrow cultures in frequency analysis of marrow-repopulating and spleen colony-forming hematopoietic stem cells in the mouse. **Blood** 1991;78:2527-2533.

69. Neben S, Anklesaria P, Greenberger J et al. Quantitation of murine hematopoietic stem cells in vitro by limiting dilution analysis of cobblestone area formation on a clonal stromal cell line. **Exp Hematol** 1993;21:438-443.

70. Dykstra B, Olthof S, Schreuder J et al. Clonal analysis reveals multiple functional defects of aged murine hematopoietic stem cells. **J Exp Med** 2011;208:2691-2703.

71. Signoret N, Oldridge J, Pelchen-Matthews A et al. Phorbol esters and SDF-1 induce rapid endocytosis and down modulation of the chemokine receptor CXCR4. **The Journal of cell biology** 1997;139:651-664.

72. Hoggatt J, Singh P, Sampath J et al. Prostaglandin E2 enhances hematopoietic stem cell homing, survival, and proliferation. **Blood** 2009;113:5444-5455.

73. McCormick PJ, Segarra M, Gasperini P et al. Impaired recruitment of Grk6 and beta-Arrestin 2 causes delayed internalization and desensitization of a WHIM syndrome-associated CXCR4 mutant receptor. **PLoS One** 2009;4:e8102.

74. Bachelerie F. CXCL12/CXCR4-axis dysfunctions: Markers of the rare immunodeficiency disorder WHIM syndrome. **Dis Markers** 2010;29:189-198.

75. Levesque JP, Helwani FM, Winkler IG. The endosteal 'osteoblastic' niche and its role in hematopoietic stem cell homing and mobilization. **Leukemia** 2010;24:1979-1992.

76. Ema H, Takano H, Sudo K et al. In vitro self-renewal division of hematopoietic stem cells. **J Exp Med** 2000;192:1281-1288.

77. Umemoto T, Yamato M, Ishihara J et al. Integrin-alphavbeta3 regulates thrombopoietin-mediated maintenance of hematopoietic stem cells. **Blood** 2012;119:83-94.

78. Dar A, Kollet O, Lapidot T. Mutual, reciprocal SDF-1/CXCR4 interactions between hematopoietic and bone marrow stromal cells regulate human stem cell migration and development in NOD/SCID chimeric mice. **Exp Hematol** 2006;34:967-975.

79. Haribabu B, Richardson R, Fisher I et al. Regulation of human chemokine receptors CXCR4. Role of phosphorylation in desensitization and internalization. **The Journal of biological chemistry** 1997;272:28726-28731.

80. Bonig H, Priestley GV, Papayannopoulou T. Hierarchy of molecular-pathway usage in bone marrow homing and its shift by cytokines. **Blood** 2006;107:79-86.

81. Christopherson KW, 2nd, Hangoc G, Mantel CR et al. Modulation of hematopoietic stem cell homing and engraftment by CD26. **Science** 2004;305:1000-1003.

82. Lapidot T, Kollet O. The essential roles of the chemokine SDF-1 and its receptor CXCR4 in human stem cell homing and repopulation of transplanted immune-deficient NOD/SCID and NOD/SCID/B2m(null) mice. **Leukemia** 2002;16:1992-2003.

83. Kollet O, Spiegel A, Peled A et al. Rapid and efficient homing of human CD34(+)CD38(-/low)CXCR4(+) stem and progenitor cells to the bone marrow and spleen of NOD/SCID and NOD/SCID/B2m(null) mice. **Blood** 2001;97:3283-3291.

84. Cavazzana-Calvo M, Fischer A, Bushman FD et al. Is normal hematopoiesis maintained solely by long-term multipotent stem cells? **Blood** 2011;117:4420-4424.

85. Broxmeyer HE, Cooper S, Kohli L et al. Transgenic expression of stromal cell-derived factor-1/CXC chemokine ligand 12 enhances myeloid progenitor cell survival/antiapoptosis in vitro in response to growth factor withdrawal and enhances myelopoiesis in vivo. **J Immunol** 2003;170:421-429.

86. Porecha NK, English K, Hangoc G et al. Enhanced functional response to CXCL12/SDF-1 through retroviral overexpression of CXCR4 on M07e cells: implications for hematopoietic stem cell transplantation. **Stem cells and development** 2006;15:325-333.

87. Lapidot T, Dar A, Kollet O. How do stem cells find their way home? **Blood** 2005;106:1901-1910.

Copyright Statement

Most of work described has recently been published in *Stem Cells* as of:

- Lai, C. Y., Yamazaki, S., Okabe, M., Suzuki, S., Maeyama, Y., Iimura, Y., Onodera M, Kakuta S, Iwakura Y, Nojima M, Otsu M, Nakauchi, H. (2014). Stage-specific roles for Cxcr4 signaling in murine hematopoietic stem/progenitor cells in the process of bone marrow repopulation. ***Stem Cells.*** doi: 10.1002/stem.1670. The copyright in the article is now assigned to *AlphaMed Press*.

The author of this thesis has included the copyrighted materials as per Journal's guidelines stating "*As an author, you are granted rights for a large number of author uses, including use by your employer (institution or company). These rights are granted and permitted without the need to obtain specific permission from the copyright holder, AlphaMed Press, provided a full credit line is prominently placed [i.e., author name(s), journal name, copyright year, volume number, inclusive pages, and copyright holder]. These author rights are granted and apply only to articles for which you are named as the author or co-author. The author rights include: the right to include the article in full or in part in a thesis or dissertation (provided that this is not to be published commercially);* ".

In addition, the corresponding author of the article has received written permission to use part or all of the article in a dissertation or thesis by the Editorial Manager of *Stem Cells* (Feb 4, 2014).

Acknowledgements

I would like to take this special opportunity to express my gratitude to Prof. Hiromitsu Nakauchi for his critical instruction and guidance. I am also deeply appreciative of Dr. Makoto Otsu, whose mentoring has taught me how to become a researcher by providing direct supervision and constructive criticism. My work could not have been accomplished without his great encouragement. I also thank our laboratory members for their kind help and input; I thank Yuji Yamazaki, Jun Ooehara, R. Yamamoto, and Syoichi. Iriguchi for their technical assistance, Sanae Hamanaka for Kusabira Orange Tg mice, Takunori Ogaeri for his advice on the C3H10T1/2-cocluture assay, and Huan-Ting Lin for his critical comments.

In addition, I am grateful to my collaborators Prof. Iwakura Yoichiro and Dr. Kakuta Shigeru who kindly provided the gene targeting mice of CXC chemokine receptor type 4. My gratitude also extends to Dr. Onodera for providing the vector used for the gain-of-function study.

My appreciation goes to Prof. Miyajima Atsushi, Prof. Watanabe Toshiki, Prof. Kitamura Toshio, and Dr. Takahashi Satoshi for their critical comments and suggestions for this thesis. Finally, I would like to express my heartfelt thanks to my family for their endless love, understanding, encouragement and supports.

This work was supported by grants from the Ministry of Education, Culture, Sport, Science and Technology, Japan and the Ministry of Health, Labour and Welfare, Japan.

I would like to express my gratitude again to all people mentioned above. This dissertation would not have been possible without the help of them.